TECHNISCHE UNIVERSITÄT MÜNCHEN

TUM School of Life Sciences

Mechanisms of Notch signaling in pancreatic development and carcinogenesis

Roxanne Leontine Brodylo

Vollständiger Abdruck der von der TUM School of Life Sciences der Technischen Universität München zur Erlangung des akademischen Grades einer

Doktorin der Naturwissenschaften

genehmigten Dissertation.

Vorsitz: Prof. Dr. Heiko Witt

Prüfer der Dissertation:

1. Prof. Dr. Martin Klingenspor
2. Prof. Dr. Jens Siveke

Die Dissertation wurde am 07.02.2022 bei der Technischen Universität München eingereicht und durch die TUM School of Life Sciences am 31.05.2022 angenommen.

„When you learn, teach. When you get, give.“

Maya Angelou

Zusammenfassung

Das pankreatische duktale Adenokarzinom (PDAC) ist die vierthäufigste Ursache für tumorassoziierte Sterblichkeit in der westlichen Welt. Die schlechte Prognose dieser Erkrankung liegt unter anderem am Fehlen effektiver therapeutischer Strategien. Zur Identifizierung neuer Therapieansätze ist ein umfassendes Verständnis der genetischen und morphologischen Prozesse innerhalb der Entstehung und Entwicklung des PDACs unabdingbar. Genetisch modifizierte Mausmodelle mit einer pankreas-spezifischen konstitutiven Aktivierung des KRAS-Onkogens (*Kras*^{G12D}), die den Verlauf von frühen präneoplastischen Läsionen bis hin zum PDAC gut abbilden, haben bereits zu großen Forstschritten bezüglich der Charakterisierung der PDAC-Entstehung und -Entwicklung beigetragen.

Der Notch Signalweg ist ein evolutorisch konservierter Signalweg, der eine wichtige Rolle in der Organogenese des Pankreas, bei regenerativen Prozessen der exokrinen Funktionalität nach akuter Pankreatitis sowie in der *Kras*^{G12D} getriebenen onkogenen Transformation, spielt. Ziel dieser Arbeit war es, mittels eines Mausmodells mit pankreas-spezifischer Deletion von *Hes1*, die Rolle des Notch Signalweg nachgeschalteten Schlüsseltargets HES1 zu untersuchen. Hierbei wurden die azinären Plastizität, die regenerativen Fähigkeit des Pankreas nach akuter Pankreatitis sowie die Entstehung und Progression des pankreatischen duktalen Adenokarzinomsim im Kontext des *Kras*^{G12D}-Mausmodells betrachtet.

In der vorliegenden Arbeit wurde gezeigt, dass HES1 zur vollständigen Differenzierung und Aufrechterhaltung der azinären Zellidentität erforderlich ist. Während der Regeneration des exokrinen Kompartments nach akuter Pankreatitis führt der Verlust von HES1 zu eingeschränkter Regenerationsfähigkeit, azinär-duktaler Metaplasie (ADM) und Lipomatose. Im Kontext der *Kras*^{G12D}-initiierten PDAC Entwicklung kommt es zu erhöhter Inzidenz von ADM bei gleichzeitig geringer-gradigen pankreatischen intraepithelialen Neoplasien (PanIN) und erhöhter Mortalität. Diese Ergebnisse sprechen für einen Rolle von HES1 hinsichtlich der *Kras*^{G12D}-getriebenen Karzinogenese im Bereich der klassischen PanIN-zu-PDAC Progression.

Abstract

Pancreatic ductal adenocarcinoma (PDAC) is one of the most devastating malignancies and the fourth leading cause of cancer-related mortality in the western world. The dismal outcome of the disease is due to its late detection concomitant with metastasis at the point of diagnosis as well as a lack of effective therapeutic strategies. Even though the development of genetically engineered mouse models (GEMMs), which recapitulate the human disease, have led to great advancements concerning the identification and characterization of genetic and morphological processes in the initiation of this disease a lot remains unknown.

Developmental pathways are believed to play a crucial role in influencing cellular plasticity and oncogenic transformation therefore a thorough understanding of these processes is crucial. The Notch pathway is an evolutionary conserved pathway that plays an important role in pancreatic development, during exocrine regeneration as well as *Kras*^{G12D}-driven PDAC development. To analyse the role of HES1, a key downstream target of the Notch signaling pathway, mice with a pancreas-specific deletion of *Hes1* in a GEMM of endogenous PDAC were generated. Using this model, the role of HES1 in murine acinar cell plasticity and pancreatic regeneration after caerulein-induced pancreatitis as well as in *Kras*^{G12D}-driven PDAC development was analysed within the scope of this thesis.

Loss of HES1 did not interfere with pancreatic development but lead to impaired acinar differentiation and maintenance associated with fatty metaplasia with age. During exocrine compartment regeneration in relation to acute pancreatitis, loss of HES1 lead to impaired exocrine regeneration, fatty metaplasia and sustained acinar-to-ductal metaplasia. In the context of *Kras*^{G12D}-initiated PDAC development *Hes1* ablation resulted in an increase of ADM. While the PanIN lesions present were of lower grade, loss of HES1 lead to accelerated progression to PDAC and shortened survival. In conclusion, this loss of *Hes1* GEMM demonstrated a key role of HES1 in acinar cell integrity and plasticity during cell maturation as well as in regenerative processes after acute pancreatitis. In *Kras*^{G12D}-driven carcinogenesis HES1 appears to promote a PanIN to PDAC route.

Parts of this thesis were presented on national and international symposia and publication.

Publication

***Hes1* Controls Exocrine Cell Plasticity and Restricts Development of Pancreatic Ductal Adenocarcinoma in a Mouse Model**
Ana Hidalgo-Sastre*, **Roxanne L. Brodylo***, Clara Lubeseder-Martellato, Bence Sipos, Katja Steiger, Marcel Lee, Guido von Figura, Barbara Grünwald, Suyang Zhong, MarijaTrajkovic-Arsic, Florian Neff, Roland M. Schmid, Jens T. Siveke
(* authors contributed equally)
Am J Pathol. 2016 Sep 14. pii: S0002-9440(16)30310-8. doi: 10.1016/j.ajpath.2016.07.025.

Oral presentation

The role of Hes1 in exocrine cell maturation, homeostasis and malignant transdifferentiation
(EMBO Workshop on Liver and pancreas development, function and disease, May 26-30, 2013, Athens, Greece)

Poster presentation

Notch pathway regulates pancreatic acinar-to-ductal metaplasia
Roxanne L. Brodylo, M. Lee, C. Lubeseder-Martellato, P.K. Mazur, F. Hampel, U. Zimber-Strobel, L.J. Strobel, Roland M. Schmid and Jens T. Siveke
(Second AACR International Conference on Frontiers in Basic Cancer Research--Sep 14-18, 2011; San Francisco, USA)

The role of Hes1 in Pancreatic Ductal Adenocarcinoma (PDAC) development
Roxanne L. Brodylo, C. Lubeseder-Martellato, A. Herner, E. Kalideris, B. Sipos, P. K. Mazur, R. Kageyama, R. M. Schmid and J. T. Siveke
(AACR conference: Pancreatic Cancer: Progress and Challenges, June 18-21, 2012, Lake Tahoe, USA)

Table of Contents

List of figures

List of tables

1. Introduction

Due to a steady increase in the global population and an overall increased life expectancy, cancer has become an ever growing cause of mortality [1]. While pancreatic cancer only poses as the 10th leading cancer type in both sexes, it is ranked 4th in cancer related death. As mortality rates for other cancers, including the four most common cancers (prostate, lung/bronchus, colon/rectum, urinary bladder in males and breast, lung/bronchus, colon/rectum and urinary corpus in females) have been declining in high-income countries in the past decade due to improvements in detection and therapy, this cannot be observed for pancreatic cancer [2]. Pancreatic ductal adenocarcinoma (PDAC), the most common form of pancreatic cancer, has a 5-year overall survival rate of at most 8 % and a median overall survival of 6-11 months at metastatic stage [3], [4], [5].

Recent studies, mainly from genetically engineered mouse models (GEMM), suggest that even though PDAC displays ductal morphology it may arise from acinar cells. This morphological switch is proposed to be caused by a process called acinar-to-ductal metaplasia (ADM) in which acinar cell identity is impaired concomitant with activation of ductal markers and reactivation of key signaling pathways involved in the development of the pancreas such as the Notch signaling pathway[6], [7], [8]. In order to improve therapeutic strategies to treat this devastating disease it is crucial to gain further insight into the processes of cellular plasticity involved in the initiation of PDAC [9],[10, 11], [12].

To this end a loss of function GEMM was used to examine the role of HES1 in murine acinar cell plasticity and pancreatic regeneration after caerulein-induced pancreatitis and in *Kras*^{G12D}-driven PDAC development.

1.1. The Pancreas

1.1.1. Pancreatic anatomy and physiology

The pancreas is located in the abdominal cavity and is morphologically divided into pancreatic head, body and tail. The pancreatic head rests in the duodenal loop with the pancreatic body extending to the pyloric region of the stomach, the pancreatic tail is connected to the spleen (Figure 1 -1A).

In mammals the pancreas is a gland organ comprising two functionally distinct compartments, the exocrine and endocrine compartments that have separate specific roles in food digestion, nutrition uptake and homeostasis.

The exocrine compartment comprises up to 90 % of the pancreas and consists of acini appearing as berry shaped cell clusters and ductal cells forming an elaborate network of larger and smaller inter- and intralobular ducts (Figure 1 -1B, C). Acinar cells produce and secrete digestive enzyme precursors called zymogens, which are drained into the ductal system. The ductal system transports these digestive enzymes and secretes bicarbonate and mucins [13], [14].

The endocrine compartment is organized in cell clusters called Islets of Langerhans scattered within the exocrine parenchyma (Figure 1 -1D). Islets of Langerhans are composed of five different cell types, which produce specific peptide hormones which participate in the regulation of glucose homeostasis and nutrient metabolism: glucagon-secreting α-cells, insulin-secreting β-cells, somatostatin-releasing δ-cells, ghrelin-producing ε-cells, and the pancreatic polypeptide-secreting PP-cells [15].

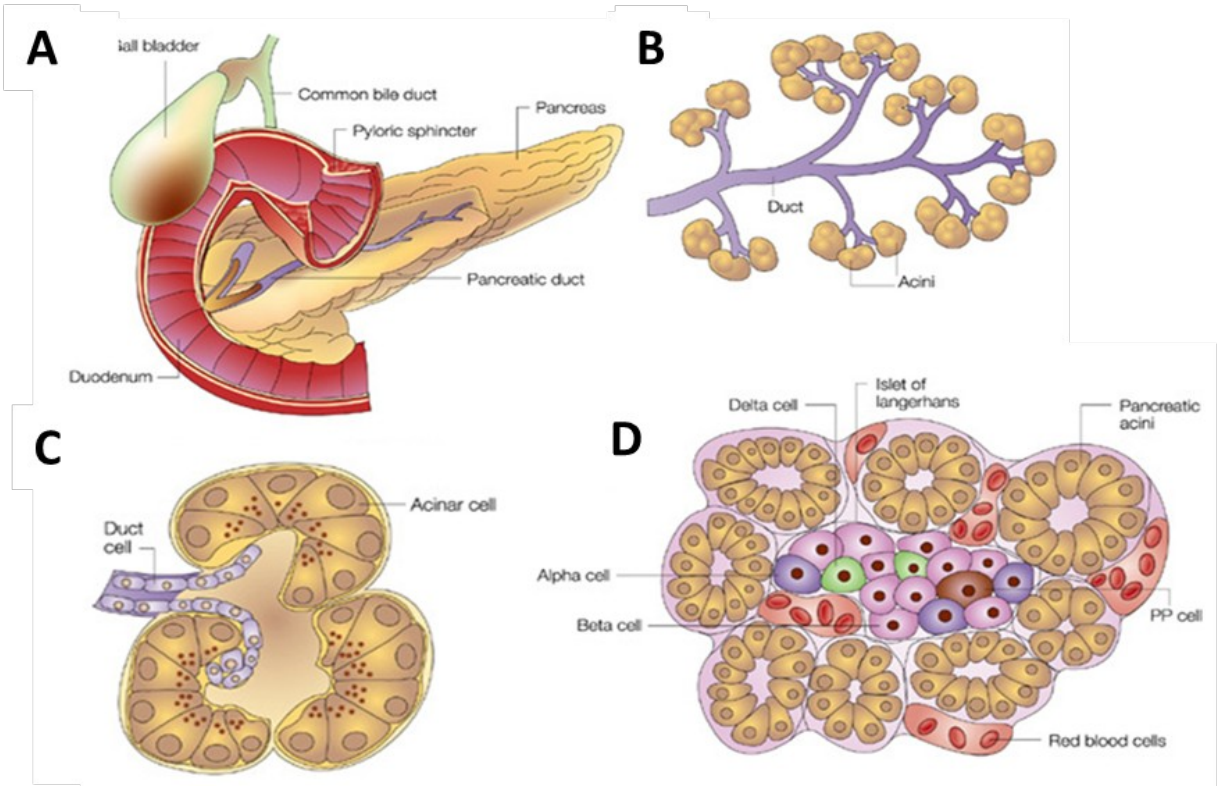

Figure 1-1: Anatomy and histology of the pancreas
From Bardeesy and DePinho [16]
Schematic of the **A**: gross morphology and **B**: structural elements of the pancreas; arrangement of the berry shaped acinar units ending into the ductal tree. **C**: Histology of the acinar and adjacent ductal cells. **D**: Histology of Islet of Langerhans embedded in acinar cells.

Centroacinar cells (CAC) are located at the interface between acinar cells and bordering duct cells [17] with a distinct expression pattern (Figure 1 -2 A, B), including active Notch signaling and expression of Sox9, both of which are markers of progenitor cells in the developing pancreas [18], [19], [20]. To date is not fully understood whether centroacinar and terminal ductal cells are two distinct cell types. Several studies have proposed the centroacinar cell as a type of multipotent progenitor cell in adult pancreas [11], [21], [22], [23].

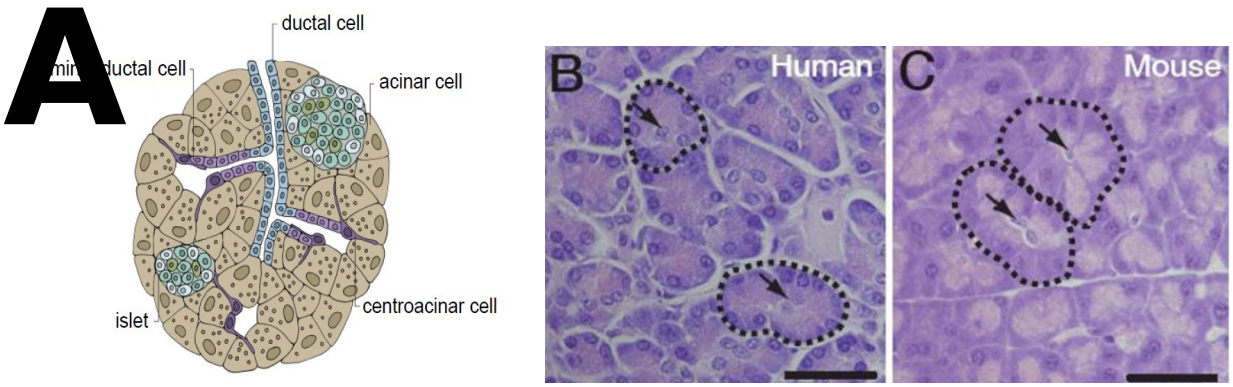

Figure 1-2: Location and histology of centroacinar cells
From Beer et al. 2016 [24]
Schematic of the **A**: structural elements of pancreatic histology including centroacinar/terminal duct cells (dark purple). H&E staining of **B**: human and **C**: mouse pancreas, dashed outlines mark acinar cell unit with centroacinar cells (arrows). Scale bar = 40 µm

1.1.2. Anatomical and morphological development of the pancreas

Murine pancreatic organogenesis starts at embryonic day 8.5 (E8.5). Two pancreatic buds, dorsal and ventral, evaginate from endodermal foregut epithelium [25], [26], [13] in response to signals from adjacent mesodermal tissue (reviewed in [27] and [28]). This stage is termed the **First Transition**. At around E10.5 branching morphogenesis of partially differentiated ductal progenitors begins, leading to two highly branched ductal trees. The dorsal and ventral pancreatic buds get into close proximity at around E13 due to rotation of the gut tube [29], [30]. The ducts of the ventral and dorsal pancreatic buds fuse to form the main pancreatic duct (**Figure 1 -3**A) [27].

Starting at E13.5 the pancreatic epithelium undergoes a massive differentiation wave termed the **Secondary Transition** which entails cellular and architectural changes. Even though the epithelial cells of both the exocrine and endocrine pancreas arise from a common field of cells in the primitive gut tube of the embryo, compartmentalization into “tip” and “trunk” domains results in lineage restriction. Between E14.5 and E18.5 the tip progenitors acquire acinar fate while trunk progenitors acquire endocrine/ductal fate. Endocrine cells aggregate but formation of mature Islets of Langerhans takes place only shortly after birth (**Figure 1 -3**B) [27], [31], [32, 33].

Exocrine differentiation is dependent on the PTF1 (pancreas transcription factor 1) transcription complex which is comprised of Ptf1/p48 (Ptf1a, pancreas specific transcription factor 1a) and a class I E-box binding partner. Active Notch signaling inhibits Ptf1a/p48 function but not its expression, and acinar cell differentiation only occurs upon loss of Notch signaling (Figure 1 -3C) [34], [35]. Inhibition of the PTF1 complex is mediated by direct interaction between HES1 and Ptf1a/p48 [36]. The onset of the secondary transition and progressive restriction of Notch signaling coincides with endocrine differentiation and NGN3 activation [37].

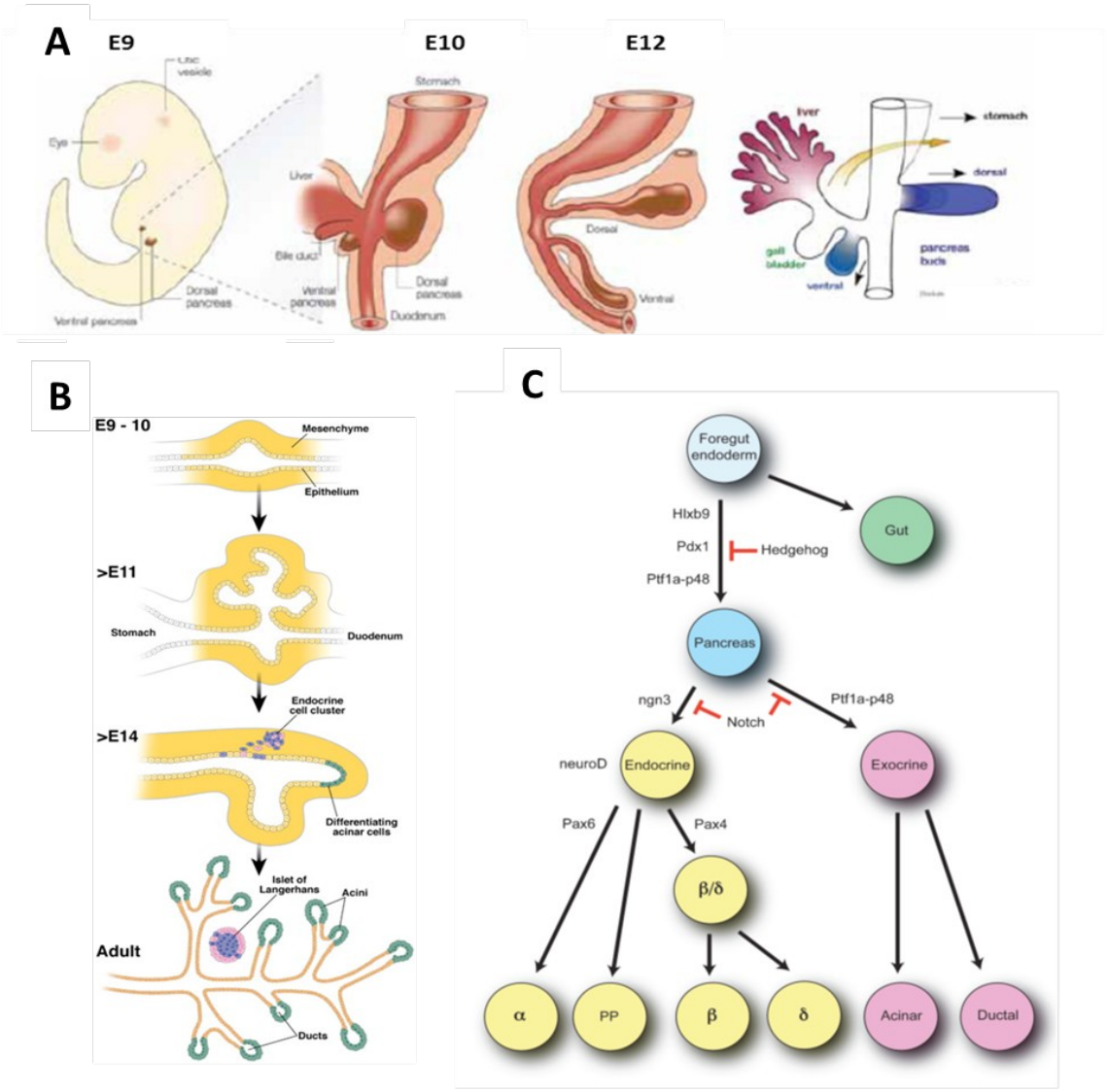

Figure 1-3: Overview of pancreatic development and its transcriptional control in the mouse.
A: Formation of dorsal and ventral pancreatic buds is followed by gut rotation. Adapted from [38]. **B**: First and second transition of pancreatic organogenesis. Adapted from [14]. **C:** Depiction of selected transcription factors relevant for pancreatic lineage differentiation. From Von Hoff et al., 2005.

1.1.3. Notch signaling during pancreatic organogenesis

The Notch signaling pathway is an evolutionary conserved developmental pathway. It is a key regulator of cell-fate decision, tissue patterning as well as cell differentiation and proliferation in various organs [39], [26]. It plays a major role during pancreatic development by maintaining an undifferentiated precursor cell pool (as mentioned in 1.1.2., Figure 1 -5) [34], [40].

The significance of the Notch receptor was first observed in *Drosophila melanogaster* in which partial loss of function was discovered to lead to “notches” at the wing margins (Dexter et al., 1914, Morgan et al., 1917; Mohr et al., 1919).

There are four mammalian Notch receptors, Notch 1-4 [41], [42], [43], [44], [45] and five transmembrane ligands, namely Jagged1, Jagged2, Delta-like1, Delta-like3 and Delta-like4[46] (Figure 1 -4A, B). Notch signaling is initiated upon ligand-receptor interaction of adjacent cells. The receptor subsequently undergoes two proteolytic cleavages. The **first cleavage** is catalyzed by ADAM (A Disintegrin And Metalloproteinase) family members ADAM17/TACE, and the **second cleavage** is mediated by a multiprotein complex named gamma-secretase [47], [48]. The second cleavage leads to the release of the NOTCH intracellular domain (NIC) which then translocates to the nucleus. Mammalian RBP-J belongs to the CSL protein family(CSL= CBF1 [C-promoter binding factor] in human, RBP-J [recombination signal binding protein] in mouse, Su(H) [Suppressorof hairless] in Drosophila melanogaster, Lag-1 in *C.elegans*) [26], [46], [49], [50] and acts as a constitutive transcriptional repressor in conjunction with co-repressors forming a histone deacetylase co-repressor complex [51], [52], [53]. Through binding to RBP-J, NIC replaces the SMRT co-repressor complex with a co-activator complex including SKIP, MAML1 (Mastermind-like 1), the histone acetyltransferase p300, and other factors, leading to the initiation of target gene expression including members of the Hes (Hairy and Enhancer of Split) and Her (Hes-related repressor protein) family of bHLH (basic helix-loop-helix) transcriptional repressors[39], [54], [55, 56], (reviewed in [50]) (Figure 1 -4C, D).

Hes (Hairy and Enhancer of split) genes encode bHLH transcription factors which control developmental processes such as segmentation, myogenesis and neurogenesis in *Drosophila melanogaster* [57]. The DNA-binding basic domain (b) lies adjacent to the helix-loop-helix region (HLH) and is followed by the Orange domain (Or) which consists of two alpha-helices and the C-terminal WRPW motif [58] (Figure 1 -4D). Seven *Hes* (*Hes1-7*) [59], [60], [61], [62], [63] and three *Hey* (*Hey1,2,L*) [64], [65], [66]genes have been determined. Murine HES proteins are very similar to their Drosophila counterparts in terms of domain arrangement. HES proteins bind to N- and E-box DNA sequences and are able to recruit TLE1-4 co-repressors [56]. The Notch signaling pathway can induce activation of *Hes1*, *Hes5* and *Hes7* [39], [67], [63] as well as all *Hey* gene family members [65] while *Hes2*, *Hes3* and *Hes6* seem to act independent of Notch signaling and data on *Hes4* are insufficient [68], [69].

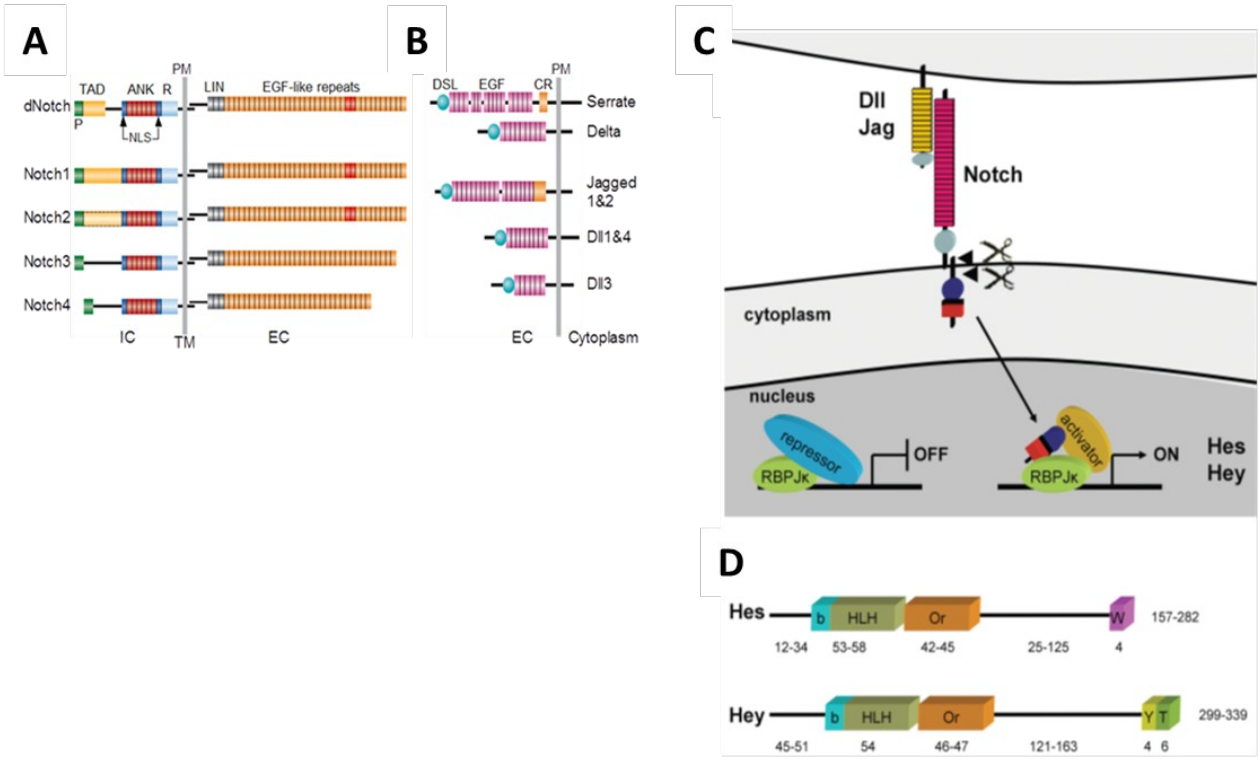

Figure 1-4: Notch family members and signaling pathway.
A: Overview of Notch receptors and **B**: ligands. The extracellular (EC) domain of Notch receptors contain epidermal growth factor (EGF)-like repeats essential for ligand binding. The intracellular (IC) domain contains different conserved protein domains.Adapted from Radtke et al., 2005. **C:** Schematic of Notch signaling cascade. Upon interaction of adjacent cells the Notch receptors (Notch 1-4) are activated by ligands of the Jagged (Jag) and Delta-like (Dll) families. Ligand-receptor interaction leads to two successive proteolytic cleavages resulting in the liberation of the Notch Intracellular domain and its

translocation to the nucleus. NIC replaces the co-repressors and forms a complex with RBPjk and co-activatorsin order to transcriptionally activate Notch target genes of the Hes and Hey families. **D:** Organisation of Hes and Hey protein domains. **C** and **D** adapted from[70].

The Notch signaling pathway has been shown to be of relevance in pancreatic cell fate decision by means of maintenance and expansion of an undifferentiated progenitor pool as well as by blocking premature endocrine and exocrine differentiation (Figure 1 -3C, Figure 1 -5)[34], [71], [72], [73], [74], [35], [75]. Expression of the Notch receptor genes *Notch1*, *Notch2* and *Notch3* as well as Notch ligands *Jag1*,*2* and *Dll1* and *Dll3* and the Notch effector *Hes1* gene could be detected in embryonic pancreas[40], [76].

Several developmental loss-of-function mouse models have elucidated the role of members of the Notch signaling pathway in pancreatic development and its role in pancreatic cell differentiation. The role of Notch signaling in exocrine pancreas development was validated by *Notch1/2* double knock-out mice and *Rbpj* deficient mice[77]. Loss of NOTCH 1/2 leads to only minor phenotypic effects while the loss of RBPJ leads to diminished differentiation of acinar cells, disturbance of ductal branching and premature endocrine differentiation [77].

The essential role of HES1 in pancreatic development was established by loss of function GEMM. *Hes1* deficient mice present with pancreatic hypoplasia due to depletion of pancreatic precursors and accelerated endocrine differentiation in which pancreatic defects and defective endocrine differentiation were documented. These results show a role for HES1 as negative regulator of endocrine differentiation. A loss of other HES family members lead to less severe phenotypes but in combination with HES1 deficiency lead to more comprehensive phenotypes due to partial redundancy among gene family members [40].

Notch signaling retains pancreatic cells in a progenitor state by restricting endocrine differentiation in the trunk domain. High levels of Notch lead to expression of Hes1, which in turn promotes expression of Sox9 and Nkx6.1 while inhibiting expression of the endocrine determinant Ngn3 [34], [78], [79]. HES1 is increasingly diminished and at E14.5 limited to Ngn3-negative, CPA-negative trunk epithelium [76]. At birth HES1 expression is limited to CAC and terminal duct cells which for the most part also express SOX9 [21], [35]. Some studies have suggested that since the transcription factors Hes1, Sox9 become restricted to the cells that are located at the tip-trunk junction, they are supposed to give rise to adult centroacinar cells / terminal duct cells [24].

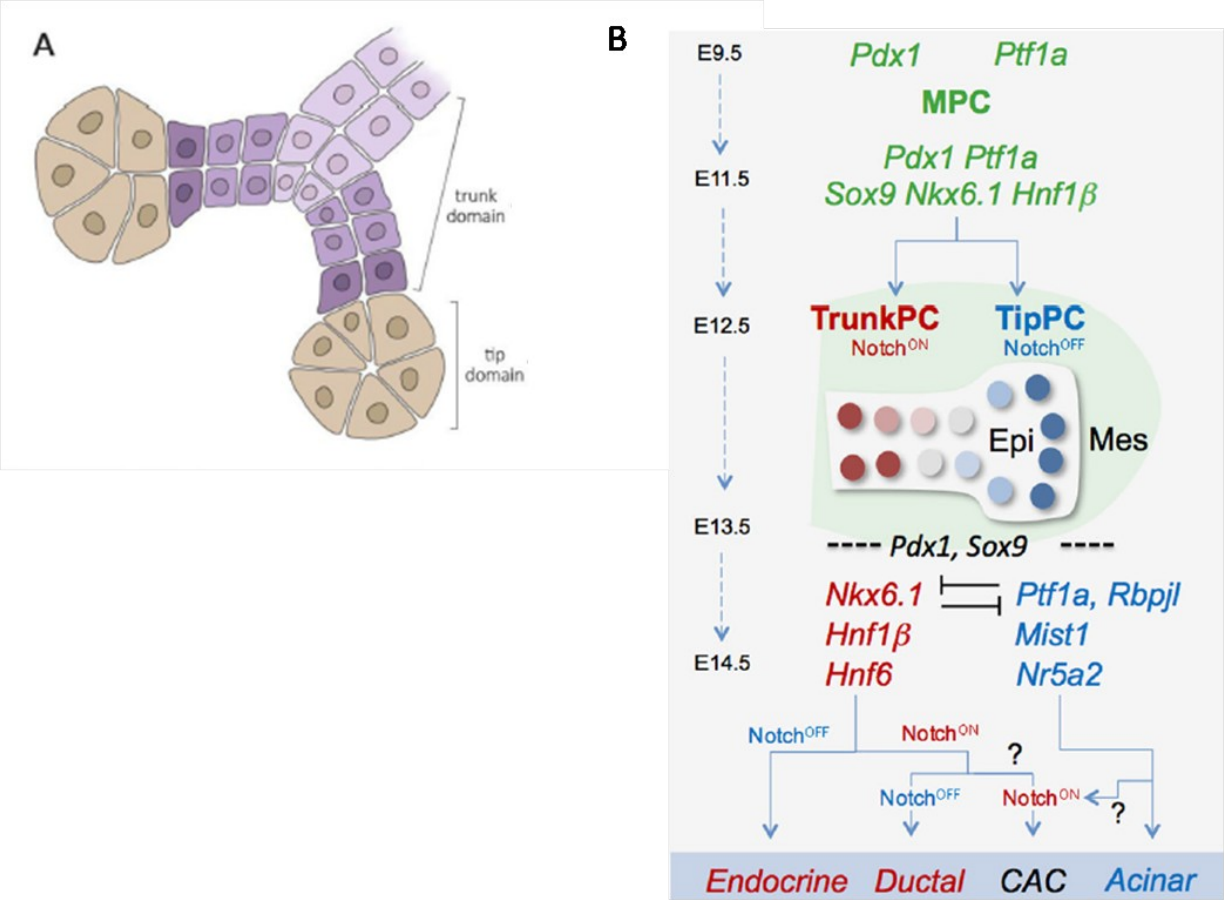

Figure 1-5: Notch signaling in pancreatic cell fate decision.
A: Representation of tip/trunk formation during pancreatic development. Acinar progenitors (brown) in the tip domain and ductal and endocrine progenitors in the trunk domain (purple). **B:** Involvement of Notch signaling in pancreatic cell identity formation. From Beer et al. and Cleveland et. al. [24], [23].

Figure 1 -6 shows HES1 immunostaining at different embryonic stages in pancreatic epithelium, demonstrating a widespread expression of HES1 at E11.5 throughout pancreatic epithelium and its subsequent downregulation at E13.5. This downregulation and restriction to “trunk” progenitors underlines the role of HES1 as marker of early pancreatic progenitor cells.

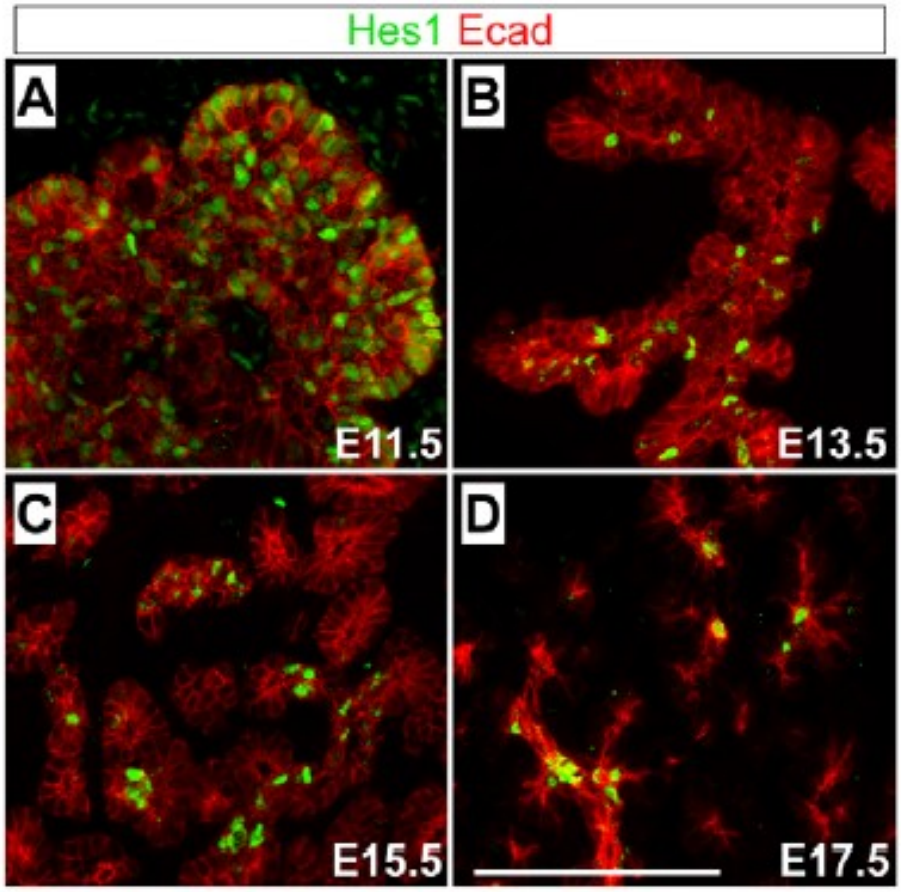

Figure 1-6: Hes1 expression in the developing pancreas (from [76]**).**
Hes1 immunofluorescence staining (green) and epithelial marker E-Cadherin (red) in embryonic pancreata show decreased Hes1 expression with progressing pancreatic development underscoring its role as marker of early undifferentiated pancreatic progenitors. Scale bar: 100 µm

1.2. Pancreatitis and pancreatic cancer

1.2.1. Acute and chronic Pancreatitis

It has been shown previously that acute [80] as well as chronic [81] pancreatitis can contribute to and enhance the development of pancreatic cancer. Acute pancreatitis is a sudden inflammation of the pancreas, in most cases triggered by alcohol or gallstones. Patients present with symptoms such as severe epigastric pain, nausea and vomiting, significantly elevated levels of digestive enzymes, diarrhea and fever [82]. Acute pancreatitis leads to acinar cell damage, liberation of digestive enzymes and inflammatory events such as migration of neutrophils into damaged tissue[83]. Chronic pancreatitis is characterised by chronic inflammation, progressive fibrosis, pain and the loss of exocrine and endocrine function. In the context of chronic pancreatitis an activation of Notch signaling pathway in ectatic ducts was shown [84].

1.2.2. Acinar-to-ductal metaplasia

Metaplasia refers to the replacement of one cell type by another without implications to the nature of this change. During acinar-to-ductal metaplasia (ADM), pancreatic acinar cells undergo genetic reprogramming and transdifferentiate to pancreatic duct cells. As mentioned in 1.2.1. the pancreas activates regenerative processes in response to injury. It is proposed that upon insult acinar cells dedifferentiate into a ductal cell state with activation of early developmental signaling pathways such as Notch and Hedghog signaling [10], [85]. Upon regeneration cells redifferentiate into mature acinar cells. Through genetically engineered mouse models (GEMMs) as well as through observation of cases of patients with familial pancreatic cancer, ADM lesions have been stipulated to be an alternate-route origin of PDAC through a metaplasia-displasia sequence. In most cases ADM is correlated with fibrosis and inflammation; a loss of acinar markers coincides with an increase of ductal markers (such as CK7, CK19, Sox9 and Clusterin) and goes along with the formation of tubular complexes [86]. Transdifferentiation can be

transient as observed during acute pancreatitis or permanent (Figure 1 -7). Persistent metaplasia is associated with an increased risk of subsequent neoplasia [87], [88], [6].Genetic mutations as well as acute and chronic pancreatitis can be initiating factors for ADM [89] and recent studies have suggested that ADM can both serve as PDAC precursors along a metaplasia-dysplasia sequence but also result in pancreatic intraepithelial neoplasia [7], [90].

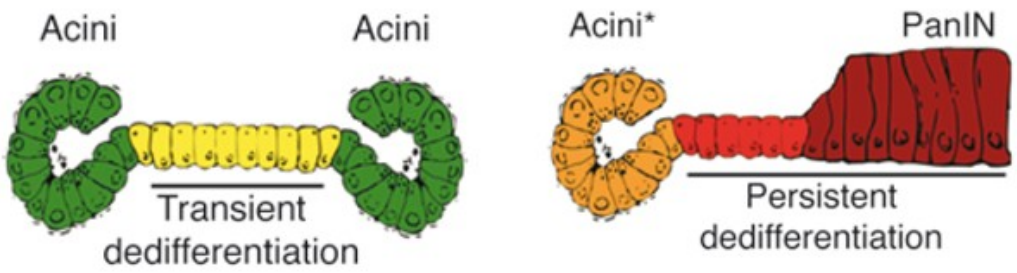

Figure 1-7: Schematic of transient and persistent acinar metaplasia.
Transient metaplasia (left) occurs during acute pancreatitis in which acinar architecture and function are restored. Persistent acinar metaplasia (right) can result in subsequent neoplasia and thus reprogramming of acini into ductal PanIN. From [6].

In Figure 1 -8 possible transdifferentiation patterns of acinar cells are depicted. Adult acinar cells have the potential to transdifferentiate into different cell types. A loss of function GEMM with conditionally inactivated c-Myc demonstrated transdifferentiation of acinar cells to adipocytes. This epithelial-to-mesenchymal transdifferentiation was observed after cearulein-induced insult [91]. Studies showed that acinar cells can transdifferentiate into malignant precursor lesions. De la O et al. have found, that Notch/ Kras co-activation promotes rapid reprogramming of acinar cells to a duct-like phenotype and therefore provide an explanation of a possible acinar cell of origin of PDAC [92].

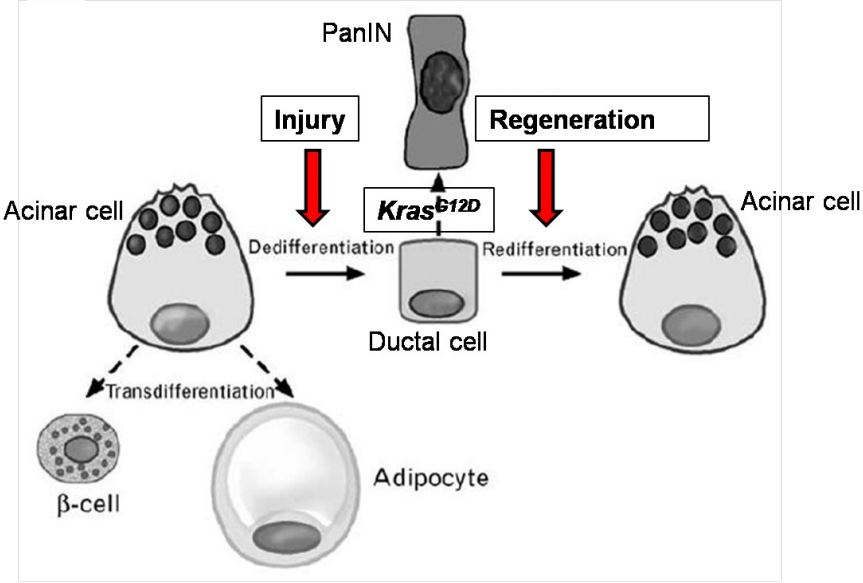

Figure 1-8: Possible transdifferentiation patterns of acinar cells
Acinar cells can regenerate after injury undergoing a dedifferentiation to a ductal phenotype and subsequent redifferentation to an acinar state. Under certain circumstances, like specific genetic or environmental cues, acinar cells can transdifferentiate to adipocytes or ß-cells. In the context of activating oncogenic *Kras,* the dedifferentiated ductal state is susceptible to malignant neoplastic transformation. From Husain et al. 2009, [93].

ADM present as intralobular change characterised by progressive replacement of acinar structures by a ductal phenotype with intracytoplasmic mucin and accompaniment of fibrosis and inflammation. Whereas atypical flat lesions have been described as “mostly non-mucinous, intralobular aggregates of small ducts usually measuring less than 0,5 cm, lined by cuboidal cells with cytological atypia and surrounded by cellular stroma, often with whorls of spindle cells in a myxomatous matrix” [86]. As ADM are proposed to be a possible precursor to PanIN it is important to investigate the molecular mechanisms underlying their formation and the role of HES1 here within [89].

1.2.3. Pancreatic precursor lesions

Clinical and histological studies have identified three major types of pancreatic precursor lesions of PDAC: Pancreatic Intraepithelial Neoplasias (PanIN), intraductal mucinous cystic neoplasms (IPMN) and mucinous cystic neoplasms (MCN). IPMNs and MCNs are both cystic lesions, less frequent and therefore less well characterised than PanINs.

IPMNs arise within the main pancreatic duct or one of its branches[94]. MCNs consist of multiocular mucin filled cysts encircled by columnar epithelial cells, which are surrounded by an ovarian-like stroma, which expresses progesterone and estrogen receptors[95], [96], [97].

PanINs are the most common and best studied precursor lesion type and are proposed to originate from acinar cells that have undergone permanent dedifferentiation (Figure 1 -7), [6], [8]. They are graded into four different stages, depending on the grade of architectural and nuclear atypia culminating in invasive neoplasia. PanIN1A and PanIN1B are low grade, PanIN2 are considered intermediate grade and PanIN 3 are considered high-grade lesions with increasing morphological and genetic abnormalities (Figure 1 -9) [98], [99]. The earliest preneoplastic lesions possess constitutive activation of RAS signaling marked by activating *Kras* mutations, which is considered to be necessary and sufficient for pancreatic cancer initiation and is also required for pancreatic cancer maintenance [100], [101], [102, 103]. During PanIN progression inactivating mutations of tumor suppressor genes p16 [104], [105] and p53 [106], [102] occur as well as inactivation of DPC4/SMAD4 resulting in decreased growth inhibition Figure 1 -9[107].

It should be noted that the three-tiered classification for PanINS, IPMNs and MCNs depicted in Figure 1 -9 was reviewed and revised in order to accommodate clinical management rendering the old nomenclature outdated. In the new two-tiered approach only the most advanced dysplasia is to be considered high-grade lesions whereas PanIN-2 and intermediate-grade dysplasia of IPMN and MCN categories are

considered low grade. For details and overview on re-classification of lesions please refer to [86], [108].

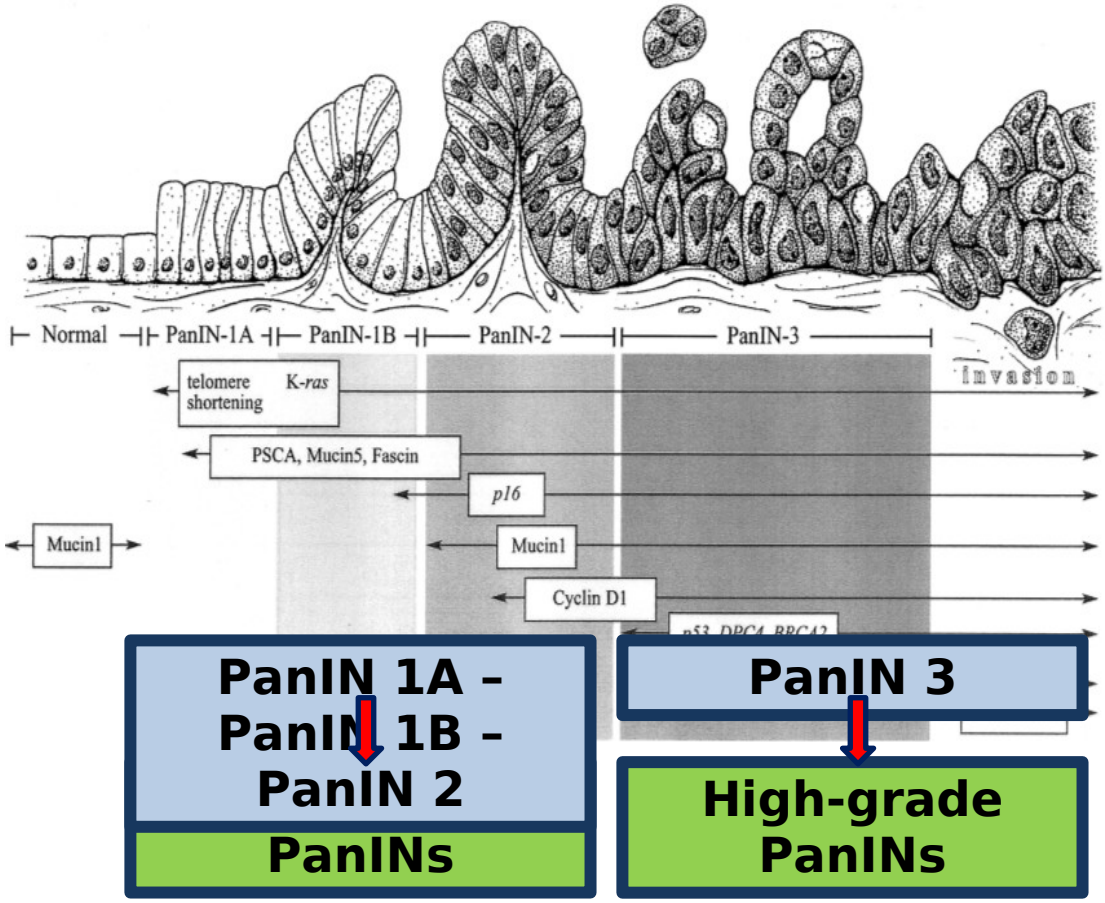

Figure 1-9: "PanINgram" adapted from [109]
Histological and genetic progression model of PanIN lesions.
PanIN1A – flat, absence of nuclear atypia, retained nuclear polarity
PanIN1B –papillary, absence of nuclear atypia, retained nuclear polarity
PanIN2- increased architectual complexity, loss of nulear polarity, nulear crowding, and variation in nuclear size (pleomorphism), nuclear hyperchromasia, nuclear pseudostratification and rare mitoses
PanIN3 – carcinoma in situ, widespread loss of polarity, nuclear atypia, frequent mitoses, still contained within the basement membrane [109]. Revised nomenclature of lesions [86]

1.2.4. Pancreatic cancer

Pancreatic neoplasia can arise from all cell compartments of the pancreas and are classified upon cellular lineage and the histology they recapitulate. In addition to pancreatic ductal adenocarcinoma (PDAC), the most common pancreatic cancer, endocrine neoplasms, acinar cell carcinoma, cystic serous and mucinous neoplasms, solid pseudopapillary tumors, squamous cell carcinoma, pancreatic lymphoma and metastatic lesions of the pancreas exist[110].

Pancreatic cancers emerge from a sequence of histological and genetic aberrations in gradual precursor lesion stages which culminate in invasive neoplasia[111]. The analysis of the molecular pathogenesis has shown that certain genetic aberrations are associated with defined histopathological stages in the progression of PDAC (Figure 1 -9). Key mutations occurring during pancreatic tumorigenesis involve oncogenes and tumor suppressors as well as genes encoding critical regulators of signal transduction networks that regulate cell cycle, differentiation and survival (for review refer to [112]).

Activating oncogenic *Kras* mutations are the key genetic alterations in most PDACs [113]. Given that the cell of origin of PDAC is still speculated upon, the use of genetically engineered mouse models (GEMMs) has provided an increasing amount of evidence suggesting that pancreatic acinar cells, undergoing SOX9-dependent ADM, are likely candidates of cellular origin of the precursor lesions of PDAC (Figure 1 -10)[114-116], [117], [118].

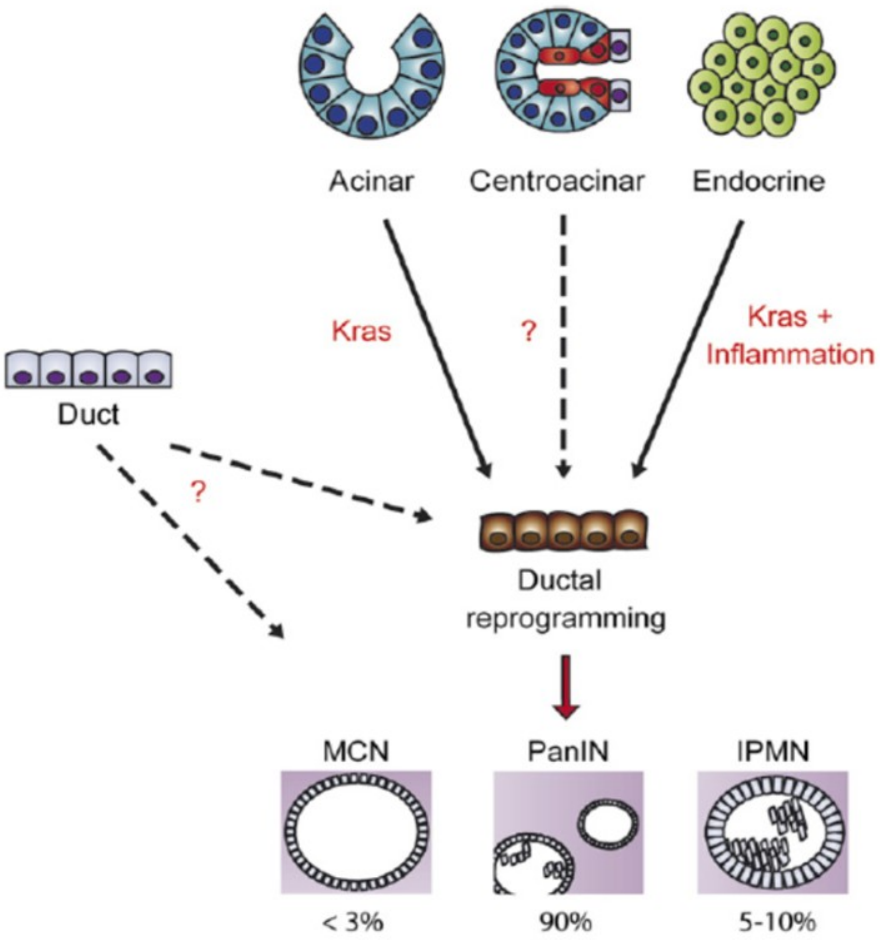

Figure 1-10: Putative cells of origin of PDAC.
Schematic of possible cells of origin of PDAC. Adapted from Mazur and Siveke 2011 [115].
Activating oncogenic *Kras* mutations in specific cell types has shown that acinar cells, centroacinar cells as well as endocrine cells can give rise to PanINs. Ductal reprogramming needs to occur in order for these cell types to assume the PanIN-to-PDAC route.

1.2.5. Models of pancreatitis and pancreatic cancer

Caerulein-Induced Pancreatitis as model of regeneration

The pancreas possesses a great regenerative capacity after acute pancreatitis. These regenerative processes include the activation and proliferation of progenitor cell programs as well as de- and subsequent re-differentiation of pre-existing cells. The underlying mechanisms responsible are still poorly understood. To study the disease and the mechanisms involved in pancreatic recovery the caerulein-hyperstimulation animal model which mimics the human condition is routinely used. In this model acute pancreatitis is induced upon repeated intraperitoneal injections of the synthetic cholecystokinin analogue caerulein that induces secretion of pancreatic enzymes. Over the course of this treatment, pancreatic damage can be observed, including edema, increased serum levels of pancreatic enzymes, invasion of inflammatory cells, formation of metaplastic ductal lesions, apoptosis and necrosis [119-121].Several days after the induction of pancreatitis the pancreas is completely regenerated [122, 123]. In the context of this model of acute pancreatitis it could be shown that processes of cellular de-differentiation and re-differentiation are activated. This aspect lends the murine pancreatitis model as a means to study cellular integrity and the development of early precursor lesions such as ADM [80], [6], [124], [125].

During the course of this process embryonic pathways, including the Notch signaling pathway which is down-regulated in the adult pancreas [126], have been identified as being reactivated, indicative of a shift in differentiation status during regenerative processes [127]. Siveke and colleagues could demonstrate that cellular regeneration was impaired in *Notch* compromised animals suggesting that Notch signaling plays a functional role during the regeneration of exocrine pancreatic tissue and is a key factor in the restoration of pancreatic homeostasis[128].

Genetically engineered mouse models

Most conditional GEMMs are based on the *Cre/loxP* system, where the bacteriophage P1 derived *Cre* recombinase is expressed in a cell lineage restricted fashion under the

control of a specific promotor. The CRE enzyme can specifically excise DNA sequences that are flanked by *loxP* sites, which are short DNA (34 bp) repeats. In the *Ptf1a*$^{+/Cre}$ model, one allele of the endogenous *Ptf1a* gene is replaced by the *Cre* gene sequence that is expressed under the control of the endogenous *Ptf1a* promoter making these mice haploinsufficient for *Ptf1a*. In this model CRE is active in almost all cells of the developing pancreas. It should be mentioned that *Ptf1a* is also expressed in the nervous system including brain, spine and retina [129].

The *Kras*$^{+/LSL\text{-}G12D}$ model developed by Hingorani and colleagues [113] was a breakthrough in the development of GEMM for PDAC. This model was based on the rationale that over 90 % of invasive PDAC harbor activating mutations in the KRAS protooncogene representative of an initiating event [113]. One endogenous *Kras* allele is replaced with a mutated knock-in construct silenced by a *STOP* cassette flanked by *loxP* sites. The mutated constitutively active KRAS^{G12D} is therefore only expressed in cells when CRE recombinase has excised the *Lox-Stop-Lox (LSL)* sequence.

These mice recapitulate the full spectrum of human PanIN lesions, desmoplasia and progress sporadically to invasive and metastatic PDAC.It has to be noted, that due to CRE activation mutant KRAS^{G12D} is activated in the developing pancreas which does not reflect sporadic mutations as in the human condition. Although pancreatic carcinogenesis requires 12 to 15 months in this GEMM, first PanIN lesions can already be detected at 4 to 6 weeks of age. This suggests that additional genetic and non-genetic factors are needed to be acquired in the cells on their route to PDAC.

1.2.6. Notch signaling in pancreatic cancer

In recent years the assumption that PDAC arises from ductal cells [104] has been questioned due to evidence from several new GEMMs [130], [131], [81] that instead suggest trans-differentiated acinar cells as the cell of origin [81], [7], [90]. It has been suggested that Notch signaling is a player in these trans-differentiation processes since a reactivation of Notch signaling in PanIN lesions was demonstrated in the aforementioned *Kras*$^{+/LSL\text{-}G12D}$ GEMM. Notch signaling activity was evidenced by strong

nuclear expression of HES1 [92]. In pancreatic cancer aberrant Notch signaling components can function as oncogene or tumor suppressor depending on temporal and spatial context of tumor development [132], [133].

NOTCH1 is expressed in acinar cells, NOTCH2 is expressed in ductal and centroacinar cells in wild type mice. Recent studies have shown that NOTCH1 may be a tumor suppressor whereas NOTCH2 has a pro-tumorigenic role in PDAC development. Loss of *Notch1* leads to increased PanIN occurrence and progression in the context of oncogenic *Kras* and therefore has been suggested to be a tumor suppressor [132]. Deletion of NOTCH1 and concomitant *Kras* activation in adult mouse suggests that NOTCH1 is not required for *Kras*-driven PanIN development. Pancreatic insult in form of acute pancreatits does not lead to earlier onset of PanIN or similar grade of pancreatic pathology but leads to a greater number of PanIN suggesting a role for NOTCH1 in making acinar cells more vulnerable to formation of *Kras*-driven PanIN lesion [134]. Deletion of *Notch2* leads to prolonged survival and late cancer onset. Reason for this is inhibition of NOTCH2 activated MYC signaling that seems to be important for *Kras*-driven PDAC development. In *Kras* mice NOTCH2 is expressed in PanIN and surrounding stroma, a lack of NOTCH1 expression in PanIN suggests a predominant role of NOTCH2 in PDAC [9].

1.3. Aim of this thesis

The Notch pathway is reactivated and target gene HES1 is upregulated upon pancreatic injury or oncogene activity and coincides with the development of duct-like lesions indicating a requirement of Notch signaling and HES1 expression for PanIN-to-PDAC progression [90], [126], [135], [7], [136], [137]. In order to get definitive evidence of the involvement of HES1 in disease pathogenesis we generated a mouse model with pancreas-specific*Hes1* deletion in the context of established mouse models of pancreatic cancer. This approach will determine the role of this developmental pathway target in malignant processes and help gain further insight into the cell of origin of PDAC.

In this thesis the role of the Notch signaling effector HES1 in pancreatic organogenesis, maintenance and carcinogenesis was characterised.

The specific aims of this thesis are as follows.

- Crossing of *Ptf1a*$^{+/Cre}$ mice with *Hes1*$^{fl/fl}$ mice for histomorphological characterization of the *Hes1*$^{\Delta/\Delta}$ phenotype in order to determine the role of Notch signaling and specifically HES1 in pancreatic organogenesis and organ homeostasis.
- Performing acute pancreatitis experiments with *Hes1*$^{\Delta/\Delta}$ mice in order to gain further insight into the role of Notch signaling and HES1 in particular in regenerative processes of the murine pancreas.
- Crossing of *Ptf1a*$^{+/Cre}$;*Kras*$^{+/LSL-G12D}$ mice with *Hes1*$^{fl/fl}$ mice to further investigate the role of HES1 in ADM as putative earliest pancreatic lesion as suggested by[138], [139]. Histomorphological characterization of preneoplastic lesion formation at defined time points and investigation of the incidence of invasive pancreatic cancer and survival.

2. Materials and Methods

2.1. Materials

2.1.1. Technical equipment

Technical Equipment	Source
ASP300 Tissue Processor	Leica Mikrosysteme Vertrieb GmbH,Wetzlar
Centrifuge	Zentrifuge 5415R, Eppendorf
Digital camera	AxioCamHRc, Zeiss
Digital Imaging software	AxioVision, Zeiss
Film developer	AmershamHyperprocessor, GE Healthcare
FluorescenceMicroscope	Axiovert 200M, Zeiss
Homogenizer	HeidolphDiax 900, Heidolph Instruments
Glucose meter	AccuCheck, Roche
Light Microscope	Axio Imager.A1, Zeiss, 490801-0001-000
Microtome	Microm International, HM 355S
Microplate reader	Bio-Rad Laboratories GmbH, München
Mini Protein Gel System chambers	Bio-Rad Laboratories GmbH, München
MolecularImager Gel Doc XR System	Bio-Rad Laboratories GmbH, München
Nano-Drop 2000 spectrophotometer	Thermo Scientific
pH-meter	MP220 pH-meter, Mettler-Toledo
Pipettes	Eppendorf Research (Variable), Eppendorf
Sonicator	Sonopuls, Bandelin
Thermocycler	Primus 96 plus; MWG Biotech

2.1.2. Disposables

Disposable	Source
Cell culture plastics	BD Bioscience, Franklin Lakes, NJ, USA
Cell scrapers	TPP Tissue Culture Labware, Trasadingen, CH
Chromatography paper 3 mm	Whatman plc, Kent, UK
Cover slips	Carl Roth GmbH, Karlsruhe, H877; 1871
Cryotubes™	Nunc™ Brand Products, Napeville, IL, USA
Feather disposable scalpel	Feather Safety Razor Co., Ltd, Osaka
Immobilon transfer membrane	Millipore Corporate, Billerica, MA, USA
MicroAmp® optical 96-well reaction plate	Applied Biosystems Inc., Carlsbad, CA,USA
Microtome blades S35	Feather Safety Razor Co, Ltd., Osaka, Japan
Nanodrop	Thermo Fisher Scientific GmbH, Henningsdorf
PCR reactiontubes	Eppendorf AG, Hamburg
Petri dishes	Sarstedt AG&Co., Nümbrecht
Reaction tubes 1.5 and 2 mL	Eppendorf AG, Hamburg
Serological pipettes	BD Bioscience, Franklin Lakes, NJ, USA
Single usesyringe	CODAN Medizinische Geräte GmbH, Lensahn
Sterile pipet tips	Biozym Scientific GmbH, Hessisch Oldendorf
Superfrost® Plus glassslides	Menzel-Gläser, Braunschweig
X-ray film	AmershamHyperfilm ECL, GE Healthcare

2.1.3. Reagents

Reagent	Source
Acrylamide	Rotiphorese gel 30 Roth, 3029.2
Acetic acid 100%	MerckKgaA, Darmstadt, 100063
Caerulein	Sigma-Aldrich Chemie GmbH, Steinheim
Eosin	Croma-PharmaGmbH,Leobendorf, 2C-140
Goatserum	Sigma-Aldrich Chemie GmbH, Steinheim
Haematoxilin	Merck KgaA, Darmstadt, 105174
1,4-Dithiothreitol (DTT	Carl Roth GmbH, Karlsruhe
1 kbextensionladder	Invitrogen GmbH, Karlsruhe
5-Bromo-2´-deoxyuridine (BrdU)	Sigma-Aldrich Chemie GmbH, Steinheim
Agarose	PEQLAB Biotechnologie GmbH, Erlangen
Ampicillin (100 mg/mL)	Carl Roth GmbH, Karlsruhe
Bio-Rad Precision Plus protein standard	Bio-Rad Laboratories GmbH, München
Bromphenol blue	Sigma-Aldrich Chemie GmbH, Steinheim
Chloramphenicol (30 mg/mL)	Applichem, Darmstadt
Dimethylsulfoxide (DMSO)	Carl Roth GmbH, Karlsruhe
Ethanol 100%	Carl Roth GmbH, Karlsruhe
Ethidium bromide (10 mg/mL)	Carl Roth GmbH, Karlsruhe
Glycerol	Sigma-Aldrich Chemie GmbH, Steinheim
Glycin	Carl Roth GmbH, Karlsruhe
HCl	Carl Roth GmbH, Karlsruhe
HEPES	Sigma-Aldrich Chemie GmbH, Steinheim

Reagent	Source
IsofluranForene	Abbott GmbH, Wiesbaden
Isopropanol	Carl Roth GmbH, Karlsruhe
ß-Mercaptoethanol	Sigma-Aldrich Chemie GmbH, Steinheim
Methanol	Carl Roth GmbH, Karlsruhe
NaOH	Carl Roth GmbH, Karlsruhe
Nonidet NP-40	Sigma-Aldrich Chemie GmbH, Steinheim
Phosphatase inhibitorset	Roche Diagnostics Deutschland GmbH, Mannheim
Protease inhibitorset	Roche Diagnostics Deutschland GmbH, Mannheim
Proteinase K	Roche Diagnostics Deutschland GmbH, Mannheim
REDTaq® ReadyMix™PCR reaction mix	Sigma-Aldrich Chemie GmbH, Steinheim
Rotiphorese® Gel 30	Carl Roth GmbH, Karlsruhe
Sodium dodecyl sulphate (SDS)	Carl Roth GmbH, Karlsruhe
5-Bromo-2´-deoxyuridine (BrdU)	Sigma-Aldrich Chemie GmbH, Steinheim
SuperScript II reverse transcriptase	Invitrogen GmbH, Karlsruhe
SYBR® Green PCR master mix	Applied Biosystems
TEMED	Carl Roth GmbH, Karlsruhe
TrisHCl	Carl Roth GmbH, Karlsruhe
Tween-20	Carl Roth GmbH, Karlsruhe
Vectashield® mounting medium with DAPI	Vector Laboratories, Burlingame, CA, USA
Tamoxifen	Sigma-Aldrich Chemie GmbH, Steinheim

Reagent	Source
TritonX-100	Sigma-Aldrich Chemie GmbH, Steinheim
Histoclear	BiozymDiagnostic GmbH
Hydrogenperoxide 30%	Sigma-Aldrich Chemie GmbH, Steinheim
LE Agarose	Biozym Scientific GmbH
Mounting medium	Medite GmbH, Burgdorf, PER 20000
PFA	Carl Roth GmbH, Karlsruhe
PBS	Biochrom GmbH, Berlin,L182-50
Ponceau red	Sigma-Aldrich Chemie GmbH, Steinheim
Rabbit serum	Sigma-Aldrich Chemie GmbH, Steinheim
Skim milk powder	Sigma-Aldrich Chemie GmbH, Steinheim
Tissue Freezing Medium	Tissue-Tec, Sakura, 4583
Tris-Base	Carl Roth GmbH, Karlsruhe,5429.2
X-gal	Croma-Pharma GmbH, Leobendorf, 2C-140
SuperScript™ II Reverse Transcriptase	Invitrogen GmbH, Karlsruhe, 18064-022
dNTP	Sigma-Aldrich Chemie GmbH, Steinheim
Random primer	PromegaGmbH, Mannheim, C1181
RNAse Inhibitor	Ambion, SUPERase In, AM2694
5x buffer	PromegaGmbH, Mannheim, G3311
Tris HCl	Sigma-Aldrich Chemie GmbH, Steinheim
NaCl	Sigma-Aldrich Chemie GmbH, Steinheim
Glycerol	Sigma-Aldrich Chemie GmbH, Steinheim
NP-40	Sigma-Aldrich Chemie GmbH, Steinheim
EDTA	Sigma-Aldrich Chemie GmbH, Steinheim

2.1.4. Buffers and solutions

Buffers and solutions	Ingredients
NDLB	20 mMTris HCl pH 8, 137 mM NaCl 10 % Glycerol 1 % NP-40 2 mM EDTA pH 8
10x PBS	10 M PBS
PBS-T	1x PBS 0.1 % v/v Tween-20
50x TAE	2 M Tris-acetate 50 mM EDTA, pH 8.3
TBE	0.89 M Tris-Base 0.89 M Boric Acid 0.02 M EDTA
10x TBS	80 g NaCl 31.5 g Tris-HCl add 1 l H_2Odd., pH 7.6
TBS	10 mM Tris-Base 150 mMNaCl
TBS-T	1x TBS, 0.1 % v/v Tween-20
HEPES	1 M HEPES, pH adjusted to 7.9 with 1 M NaOH
Separating Gel Buffer	1,5 M Tris-Base, pH 8,9 adjusted with HCl
Assemble Gel Buffer	0,5 M Tris-Base, pH 8,9 adjusted with HCl
SDS RunningBuffer	25 mM Tris base 192 mM Glycine 0.1 % w/v SDS
LaemmliLoadingBuffer	0.35 M Tris-Base pH 6.8 36 % Glycerin 10.28 % SDS 0.6 M DTT 0.012 % bromphenol blue
Transfer Buffer	25 mM Tris-Base pH 8.3 150 mMGlycin 10 % Methanol
BlockingBuffer	Skim milk 5 % w/v in TBS-T

2.1.5. Kits

Kit	Source
ABC Kit	Vector Labortatories, Vectastain
DAB Kit	Vector Labortatories, Vectastain
DNA blood and tissue kit	Qiagen GmbH, Hilden
BCA kit	Thermo Fisher Scientific GmbH, Henningsdorf
RNeasy Mini Kit	Qiagen GmbH, Hilden, 74106

2.1.6. Antibodies

Table 2-1: Antibodies IHC/IF

Primary Antibody	Species	Dilution	Source
Amylase	rabbit	1:1000	Sigma
BrdU	rat	1:250	Serotec
CK19	rat	1:200	DSHB
Cleaved Caspase-3	rabbit	1:500	CellSignaling
Clusterin	goat	1:500	Santa Cruz
Claudin18	rabbit	1:500	Invitrogen
E-Cadherin	rabbit	1:500	Cell Signaling
Glucagon	rabbit	1:750	Dako
Hes1	rat	1:250	Biozol
Insulin	rabbit	1:500	Dako
Ki67	rabbit	1:5000	Abcam
Muc5AC	mouse	1:500	Neomarkers
N2-IC	rat	1:1000	DSHB
Pdx1	goat	1:10000	Gift from C.V. Wright
Sox9	rabbit	1:2000	Millipore
Western Blot			
Hes1	rabbit	1:1000	Abcam
Hsp90	rabbit	1:3000	Santa Cruz

Secondary Antibody	Species	Dilution	Source
IHC			
Anti-rabbit Biotin conjugate	goat	1:500	VectorLaboratories
Anti-goat Biotin conjugate	rabbit	1:500	Vector Laboratories
Anti-Rat Biotin conjugate	rabbit	1:500	Vector Laboratories
Anti-Guinea-pig	goat	1:500	Dianova
IF			
AlexaFluor 488		1:500	Abcam
AlexaFluor 568		1:500	Abcam
Western Blot			
Anti-rabbit IgG HRP conjugate	goat	1:1000	GE Healthcare
Anti-mouse IgG HRP conjugate	rabbit	1:1000	GE Healthcare
Anti-goat IgG HRP conjugate	donkey	1:1000	Santa Cruz

2.1.7. Primers

Table 2-2: Genotyping primers

Primer	Sequence 5' – 3'		Size in bp wt / lox
Ptf1a$^{+/Cre(ex1)}$	**Forward**	**GTC CAA TTT ACT GAC CGT ACA CCA A**	**1155**
	Reverse	**CCT CGA AGG CGT CGT TGA TGG ACT GCA**	
Cre recombinase	**Forward 1**	**ACC AGC CAG CTA TCA ACT CG**	**324 199**
	Reverse 1	**TTA CAT TGG TCC AGC CACC**	
	Forward 2	**CTA GGC CAC AGA ATT GAA AGA TCT**	
	Reverse 2	**GTA GGT GGA AAT TCT AGC ATC ATC C**	
	Reverse	**AGGGTGCTGGACAGAAATGTGTA**	
Hes1	**Forward**	**CAG CCA GTG TCA ACA CGA CAC CGG ACA AAC**	**200 250**
	Reverse	**TGC CCT TCG CCT CTT CTC CAT GAT A**	
Kras	**Forward**	**CAC CAG CTT CGG CTT CCT ATT**	**280 180**
	Reverse	**AGC TAA TGG CTC TCA AAG GAA TGT A**	
		CCA TGG CTT GAG TAA GTC TGC	

Table 2-3: PCR Primers used for RT-PCR

Forward primer	Sequence(5'-3')	Reverse primer	Sequence(5'-3')
*Notch1*_Fw	5'-ACATCCGTGGCTCCATTGTCTA-3'	*Notch1*_Rw	5'-TCTTGTAAGGAATATTGAGGCTGC-3'
*Notch2*_Fw	5'-GCCTCCCATCGTGACTTTCC-3'	*Notch2*_Rw	5'-GGGCAACTGGACTGCGTC-3'
*Delta-like1*_Fw	5'-CCTGGCTGTGTCAATGGAGT-3'	*Delta-like1*_Rw	5'-TGGCAGTCCTTTCCAGAGAA-3'
*Rbpj*_Fw	5'-TGGATGCAGACGACCCTGTAT-3'	*Rbpj*_Rw	5'-TGGAGTGGCCTGAAATTGG-3'
*Rbpl*_Fw	5'-ATGCCTTGCCACAGAGAAGGT-3'	*Rbpl*_Rw	5'-TGCCAATGATGGTCCAGCA-3'
*Pdx1*_Fw	5'-TGCCACCATGAACAGTGAGG-3'	*Pdx1*_Rw	5'-GGAATGCGCACGGGTC-3'
*Hes1*_Fw	5'-AAAGCCTATCATGGAGAAGAGGCG-3'	*Hes1*_Rw	5'-GGAATGCCGGGAGCTATCTTTCTT-3'
*Hes3*_Fw	5'-CCCTGCTTAGCACTGCTGAGA-3'	*Hes3*_Rw	5'-CAGGGCTCAGAAGGCACTAAA-3'
*Hes5*_Fw	5'-AGATGCTCAGTCCCAAGGAG-3'	*Hes5*_Rw	5'-TAGCCCTCGCTGTAGTCCTG-3'
*Hes7*_Fw	5'-ATCAACCGCAGCCTAGAAGA-3'	*Hes7*_Rw	5'-CACGGCGAACTCCAGTATCT-3'
*Hey1*_Fw	5'-CACTGCAGGAGGGAAAGGTTATT-3'	*Hey1*_Rw	5'-GCCAGGCATTCCCGAAAC-3'
*HeyL*_Fw	5'-TGCCAGGAGCATAGTCCCAA-3'	*HeyL*_Rw	5'-TGGTAGAACACTGCTCCCGC-3'
*Cyclophillin*_Fw	5'-ATGGTCAACCCCACCGTGT-3'	*Cyclophillin*_Rw	5'-TTCTGCTGTCTTTGGAACTTTGTC-3'

2.2. Animal Model

2.2.1. Animals

All mouse experiments were performed according to the German Federal Animal Protection Laws and were approved by the Institutional Animal Care and Use Committees of the government of Bavaria and the Technical University of Munich. Mice were maintained in the animal facility of the II. Medizinische Klinik, Klinikum rechts der Isar, Technical University Munich, and kept on constant 12-hour light-dark cycles. Mice had access to standard rodent chow diet and water *ad libitum*. Mice were intercrossed to obtain the indicated genotypes.

Littermates without *Ptf1a*$^{+/Cre(ex1)}$ and *Ptf1a*$^{+/Cre}$;*Kras*$^{+/LSL\ G12D}$ served as controls. For genotyping purposes, mice were tailed at three weeks of age, DNA isolation and genotyping PCR was performed as described in 2.4.1.and2.4.2. and subsequently weaned at four weeks of age.

Ptf1a$^{+/Cre(ex1)}$[140] mice express Cre-recombinase under Ptf1a promoter which is active in pancreatic progenitor cells as well as in the exocrine and endocrine pancreas. This Cre-recombinase is also expressed in the neurons of the retina, in the cerebellum and the dorsal neural tube. One allele of the pancreas-specific transcription factor Ptf1a is heterozygously substituted with Cre recombinase

Kras$^{+/LSL-G12D}$[113] knock-in mice have a mutation in the Kras gene that is prevalent in human PDAC. In codon 12 of the first coding exon glycin is changed to aspartic acid which leaves Kras constitutively active after deletion of the Stop cassette (Lox-STOP-Lox, LSL) and thereby leads to constant activation of the Kras signaling pathway.

In the *Hes1*$^{f/lf}$[141] mice, a construct is employed in which exons 2 to 4 are flanked by *loxP* sites Upon *Cre*-mediated recombination these parts of the *Hes1* gene are deleted resulting in a total knockout of the gene.

Construct	***Name***

Ptf1a$^{+/Cre}$;Hes1$^{fl/fl}$	*Hes1$^{\Delta/\Delta}$*
Ptf1a$^{+/Cre}$;Kras$^{+/LSL-G12D}$	*Kras^{G12D}*
Ptf1a$^{+/Cre}$;Kras$^{+/LSL-G12D}$;Hes1$^{fl/fl}$	*Kras^{G12D};Hes1$^{\Delta/\Delta}$*

2.2.2. Organ preparation and pancreatic weight analysis

Both upon indicated time points and upon tumor development with notable symptoms of disease such as cachexia and pain the mice were anesthetized using isoflurane and killed by cervical dislocation. The abdomen was opened to examine the organs for macroscopic alterations. Tissue samples for subsequent RNA and protein isolation (2.5.1. and 2.6.1.) were taken from three different regions of the pancreas immediately after exposure of the organ to keep the effect of autodigestive and degrading processes at a minimum. Samples for RNA preparation were transferred into a cryo tube containing RLT buffer (supplemented with 1 % v/v -mercaptoethanol), homogenized and snap frozen in liquid nitrogen. Samples for protein preparation were directly transferred into a cryotube and snap frozen in liquid nitrogen.

The pancreas was either dissected from the surrounding tissue and pancreatic weight was measured immediately in a precision scale under sterile technique or taken with part of duodenum and spleen to preserve the orientation of the organ. Additionally, parts of the lung, liver, the upper duodenum, and the spleen were resected. Tissue was either put to 4 % paraformaldehyde overnight for FFPE (2.3.1.) or directly embedded in tissue freezing medium (TissueTek) and snap frozen in liquid nitrogen for cryo sectioning.

2.2.3. Intra Peritoneal Glucose tolerance test (IPGTT)

Age and sex matched mice (6-12 weeks of age) were fasted overnight prior to initial measurement of serum glucose levels. Glucose levels were determined using blood from the tail vein. After initial measurement of glucose levels, 2 g glucose/kg body weight was injected i.p., using 20% glucose solution. Glucose levels were subsequently measured and blood was drawn from tail vein to measure blood glucose levels at indicated time points after initial glucose injection.

2.2.4. Induction of Pancreatitis

Pancreatitis was induced in mice by repeated i.p. injections of caerulein according to the protocol described in[135]: 8 hourly injections of 200 µl of caerulein (10µg/ml) were administered on two consecutive days. Mice were sacrificed 24 h, 72 h and 5 days after the final caerulein injection (n = at least 4 mice per group).

2.2.5. Blood analysis

Blood extracted from the tail vain of individual mice was treated with EDTA and centrifuged at 5000 rpm for 5 min. Blood serum was sent to the clinical chemistry facility in order to determine amylase and lipase levels to confirm mice in which pancreatitis was induced.

2.3. Histological methods

2.3.1. Production of FFPE-tissue samples

Prior to paraffin embedding, freshly harvested organs were put into a histological cassette and fixed overnight in 4 % paraformaldehyde at 4°C and then dehydrated with increasing concentrations of ethanol, xylol and paraffin in a Leica S300 tissue processing unit and embedded in paraffin. The formalin-fixed, paraffin-embedded (FFPE) blocks were stored at room temperature.

2.3.2. Paraffin sections

For histological analysis FFPE-blocks were cooled to -20 °C and cut into 3 µm slides on a microtome, transferred to a 50 °C water bath for stretching and collected on glass slides. Sections were allowed to dry at RT overnight before further use.

2.3.3. H&E Staining

For hematoxylin and eosin (H&E) staining paraffin sections were deparaffinized in Histoclear followed by rehydration in a graded series of ethanol (100, 96, and 70 %) and deionized water. Rehydrated slides were stained with hematoxylin for 2 min to visualize all acidic structures in dark violet. After washing the slides under running tap water, slides were counterstained with eosin for 5 min to label basophilic structures like cytoplasm, connective tissue and other extracellular substances in pink. Slides were washed and dehydrated using isopropanol and 96 % ethanol. Slides were incubated in Histoclear before they were covered with mounting medium and coverslips.

2.3.4. Immunohistochemistry

Paraffin sections were deparaffinized and rehydrated (see2.3.3.) for histological analysis. For antigen retrieval, slides were boiled for 10 min in citrate buffer. Endogenous peroxidase activity and non-specific binding respectively were blocked by quenching with hydrogen peroxide (3 % H_2O_2, 10 min). The slides were briefly rinsed with de-ionized water and washed in PBS followed by incubation in 5 % serum for one hour at RT. Slides were incubated overnight at 4 °C with the respective primary antibody diluted in blocking solution (Table 2 -1). The primary antibody was washed off and the biotinylated secondary antibody was applied for one hour at RT followed by color development with diaminobenzidine (DAB) chromogen kit according to manufacturer´s instructions. Slides were briefly counterstained with hematoxylin and dehydrated and mounted as described in2.3.3.. Isotype controls were used at the same concentration as the primary antibodies. Histological images were taken on a Zeiss Axiovert Imager.

2.3.5. Immunofluorescence

Prior to immunofluorescent staining cryo slides were fixed in either 4 %PFA at RT or in chilled Methanol/Acetone (1:1) at -20 °C for 10 minutes. FFPE-slides were treated and incubated with primary antibody as described in 2.3.4., except for H_2O_2 treatment. Fluorochrome-labeled secondary antibodies were used and sections were mounted with

DAPI hard cover mounting medium to counterstain nuclei. Microscopic pictures were taken on a fluorescent microscope.

2.3.6. Morphometric quantification

Following IHC staining for Ki67 and Cleaved Caspase 3, photographs of whole pancreatic tissue sections were taken, and positive cells were scored (N= 3 for each genotype). For proliferation analysis, mice received i.p injections with 100 mg/kg BrdU (Sigma-Aldrich) two hours prior to sacrifice. Counting was performed with AxioVision software (Zeiss). The percentage of positive cells was calculated by dividing the number of cells positively stained with the respective antibody by the total number of cells in the areas of pancreatic tissue, excluding edema, fatty or inflammatory tissue.

For quantification of CK19-positive areas or MUC5AC-positive PanIN lesions, two representative slides per mouse were chosen and at least 5 pictures were taken from each slide and calculated manually or using the AxioVision 4.8 or Definiens software (n = 3 - 4 mice per group).

2.4. DNA analysis

2.4.1. DNA Isolation from mouse tails for genotyping

Genomic DNA was isolated from mouse tails using 200 µl Direct PCR-Tail lysis buffer supplemented with 10 µl Proteinase K to determine the genotype. Tails were incubated overnight at 55 °C subsequently Proteinase K activity was heat-inactivated for 45 min at 85 °C. 1 µl isolated DNA was used as template for the genotyping PCR.

2.4.2. Genotyping PCR

Specific oligonucleotides were used to discriminate between the wildtype and floxed allele by difference in size (Table 2 -2). PCR products were separated via agarose gel electrophoresis. Genotyping results were visualized under UV light with the Molecular Imager Gel Doc XR System.

All genotyping PCRs were performed using the RedTaq Ready Mix according to the manufacturer's protocol with 1 µl genomic DNA template, and primers at a final concentration of 10 pM. The following conditions were applied for amplification:

1.	**Initial denaturation**		**95°C**	**1 min**
2.	**Denaturation**	**40x**	**94°C**	**30 sec**
	Annealing		**56°C**	**30 sec**
	Elongation		**72°C**	**1 min 30 sec**
3.	**Final elongation**		**72°C**	**10 min**
4.	**Storage**		**4°C**	

2.4.3. Extraction of pancreatic DNA from FFPE-blocks

To isolate DNA from FFPE-blocks the DNA blood and tissue kit (Qiagen) was used according to manufacturer´s protocol.

2.5. Detection and Quantitation of Gene Transcription

2.5.1. RNA Isolation

Tissue from three different parts of the pancreas was resected, immediately homogenized in RLT-buffer (supplemented with 1 % v/v -mercaptoethanol), and snap frozen in liquid nitrogen. Lysed tissue samples for RNA extraction were thawed on ice and RNA extraction was performed utilizing the RNeasy kit (Qiagen) according to manufacturer´s protocol. After elution RNA concentration was measured on a Nano-Drop 2000 spectrophotometer (Thermo Scientific) and RNA integrity was checked on a 1% agarose gel.

2.5.2. cDNA Synthesis

cDNA synthesis was performed with 1 µg of total RNA using SuperScript™ II Reverse Transcriptase (Invitrogen) according to manufacturer's protocol. The cDNA was stored at -20°C.

2.5.3. Quantitative RT-PCR

Real-Time PCR was performed on a Lightcycler480 system using the SYBR Green master mix (both Roche) and suitable primers (Table 2 -3). Cyclophilin was used for normalization. Values were calculated with the following exponential equation: $2^{DeltaCT(Cyclophilin) - DeltaCT(target\ gene)}$.

All RT-PCR experiments were performed with n= 3-6 individual biological samples per group. P values were calculated with the Mann-Whitney-test for non-normally distributed, unpaired data using the GraphPad Prism5 statistical software.

2.6. Proteinbiochemistry

2.6.1. Isolation of protein from pancreatic tissue

Tissue samples were thawed in non denaturating lysis buffer (NDLB) supplemented with Protease- and Phosphatase inhibitors and homogenized using an electrical tissue homogenizer. Lysed tissue was sonicated for 10 sec, incubated on ice for 10 min and then centrifuge at 4 °C for 20 min at 13200 rpm. Supernatants were transferred to new vials and stored at -20 °C for short term, and at -80 °C for long term storage.

2.6.2. Protein concentration determination

Protein concentrations were determined using the BCA kit from Thermo Scientific with included Albumin standard according to manufacturer´s instructions. Linear absorbance was measured at 570 nm on an E-max precision microplate reader.

2.6.3. SDS polyacrylamide gel electrophoresis (SDS PAGE) and Western Blot

Protein lysates were supplemented with 5x Laemmli buffer and denaturated at 95 °C for 5 min. Protein separation was performed on a SDS polyacrylamid gel between 7.5 and

15 %, depending on the size of the protein that should be detected at 120 Volt in SDS running buffer.

Western Blot protein transfer to methanol-activated PDVF membranes (Immobilon-PSQ, Millipore) was performed at 350 mA for 1 h to 2.5h, depending on the size of the proteins that should be detected. The membrane and the gel were clamped between a sponge and two filter papers on each side and the blotting chamber was cooled with an ice pack for the time of the transfer.

After transfer membranes were incubated for 30 min with 3 % skim milk powder in TBS-T to block unspecific antibody binding sites and then incubated overnight at 4 °C with the respective primary antibody in 3 % BSA in TBS-T. After washing with TBS-T the membrane was then incubated with the appropriate HRP-coupled secondary antibody in blocking solution for 1 h at RT. After additional washing steps, detection was performed using the ECL Western Blotting Detection Reagents and Amersham Hyperfilms (both GE Healthcare).

2.7. Statistical analysis

Statistical analysis was performed using Graph Pad Prism5 program (GraphPad Software,Inc). Inter-group comparison was performed using the Mann-Whitney Test for non-normal distributed unpaired data. Differences with a P value lower than 0.05 were considered significant. For P values, the following was applied: * $p \leq 0.05$, ** $p \leq 0.01$, *** $p \leq 0.001$. Data is presented as mean±SEM. Kaplan–Meier curves were calculated using the survival time for each mouse from the littermate groups. The log-rank test was used to address significant differences between the groups.

3. Results

3.1. The role of Hes1 in pancreatic development and homeostasis

3.1.1. Characterization of Pancreas-Specific Conditional *Hes1*- Knockout Mice

To examine the functional role of HES1 in pancreatic development and acinar cell maturation and maintenance, *Hes1* was conditionally deleted in the pancreas utilizing a pancreas-specific Cre recombinase. In *Pft1a*$^{Cre/+}$mice, Cre recombinase is specifically expressed in pancreatic progenitor cells starting embryonic day 9.5[27], [140] and its expression persists in mature tissue.

Pft1a$^{Cre/+}$ mice were crossed with homozygous *Hes1*$^{lox/lox}$ mice to obtain *Ptf1a*$^{+/Cre}$*;Hes1*$^{lox/lox}$ mice(named *Hes1*$^{\Delta/\Delta}$ henceforth) (Figure 3 -11A). The *Hes1*$^{\Delta/\Delta}$ model was subsequently used to determine effects of HES1 deletion in pancreatic exocrine development; homeostasis and carcinogenesis. *Hes1*$^{\Delta/\Delta}$ offspring were born at the expected Mendelian ratio and appeared healthy.

Upon recombination with the pancreas specific Ptf1a$^{+/Cre}$, exons 2, 3 and 4 are excised at the loxP sites flanking exons 2 and 4 (red triangles) from the *Hes1* gene (Figure 3 -11 A). The consequence is a shift of the reading frame leading to disturbed protein product generation. Effective deletion of *Hes1* at 4 weeks was confirmed by qRT-PCR and Western Blot analysis (Figure 3 -11B, C). While immunostaining showed nuclear expression of HES1 in centroacinar cells (CAC) of control mice, expression was effectively eliminated in *Hes1*$^{\Delta/\Delta}$ mice. To ensure proper localization of CAC in *Hes1*$^{\Delta/\Delta}$ mice, we performed immunostaining for Notch2-IC (Figure 3 -11D).

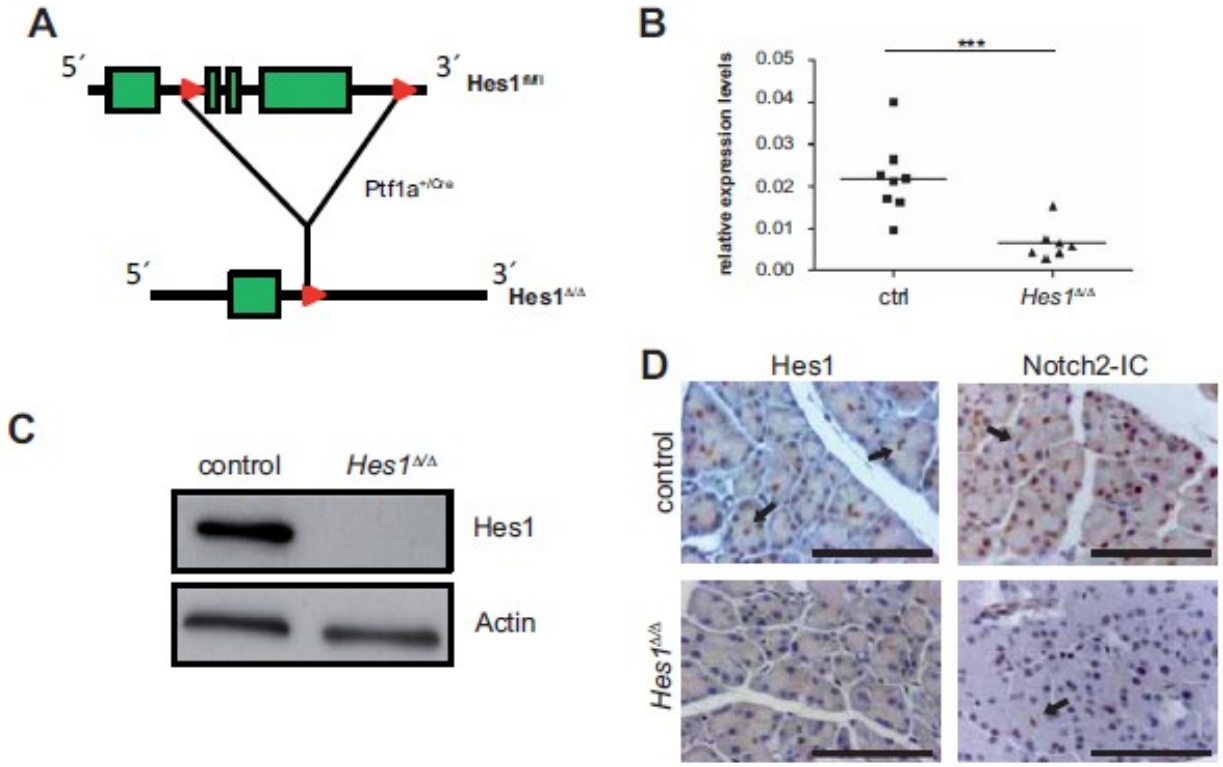

Figure 3-11: Conditional *Hes1*-knockout in the pancreas
A: Gene targeting strategy: *Hes1* gene flanked by loxP sites (red triangles) between exons 2 and 4 (green boxes). Upon recombination with the pancreas specific *Ptf1a*$^{+/Cre}$exons 2, 3 and 4 are excised from the *Hes1* gene generating the HES1 knockout. Adapted from[141]. **B:** Real time PCR for *Hes1* expression levels in pancreas from control or *Hes1*$^{\Delta/\Delta}$ mice (N≥7 per group). Values are shown as mean±SEM. P values: *p<0.05, **p<0.01, ***p<0.001.**C:** Western blot showing expression of HES1 protein in pancreatic tissue from control and *Hes1*$^{\Delta/\Delta}$ mice. Actin is shown as loading control. **D:** Immunohistochemical staining for HES1 and NOTCH2 intracellular domain proteins in control and *Hes1*$^{\Delta/\Delta}$ mice. Positive staining is highlighted with arrows. Scale bars: 100 µm.

To assess potential compensatory mechanisms between different NOTCH family members, transcriptional profiling was carried out. Real-time quantitative reverse-transcription polymerase chain reaction (qRT-PCR) revealed that no difference in expression levels of various Notch receptors (*Notch1* and *Notch2*), Notch ligands (*Dll1*) and Notch target genes (*Hes3, Hes5, Hes7* as well as *Hey1* and *HeyL*) could be detected (Figure 3 -12). These results indicate maintenance of Notch signaling without compensatory effects between NOTCH family members at least on the transcriptomic level.

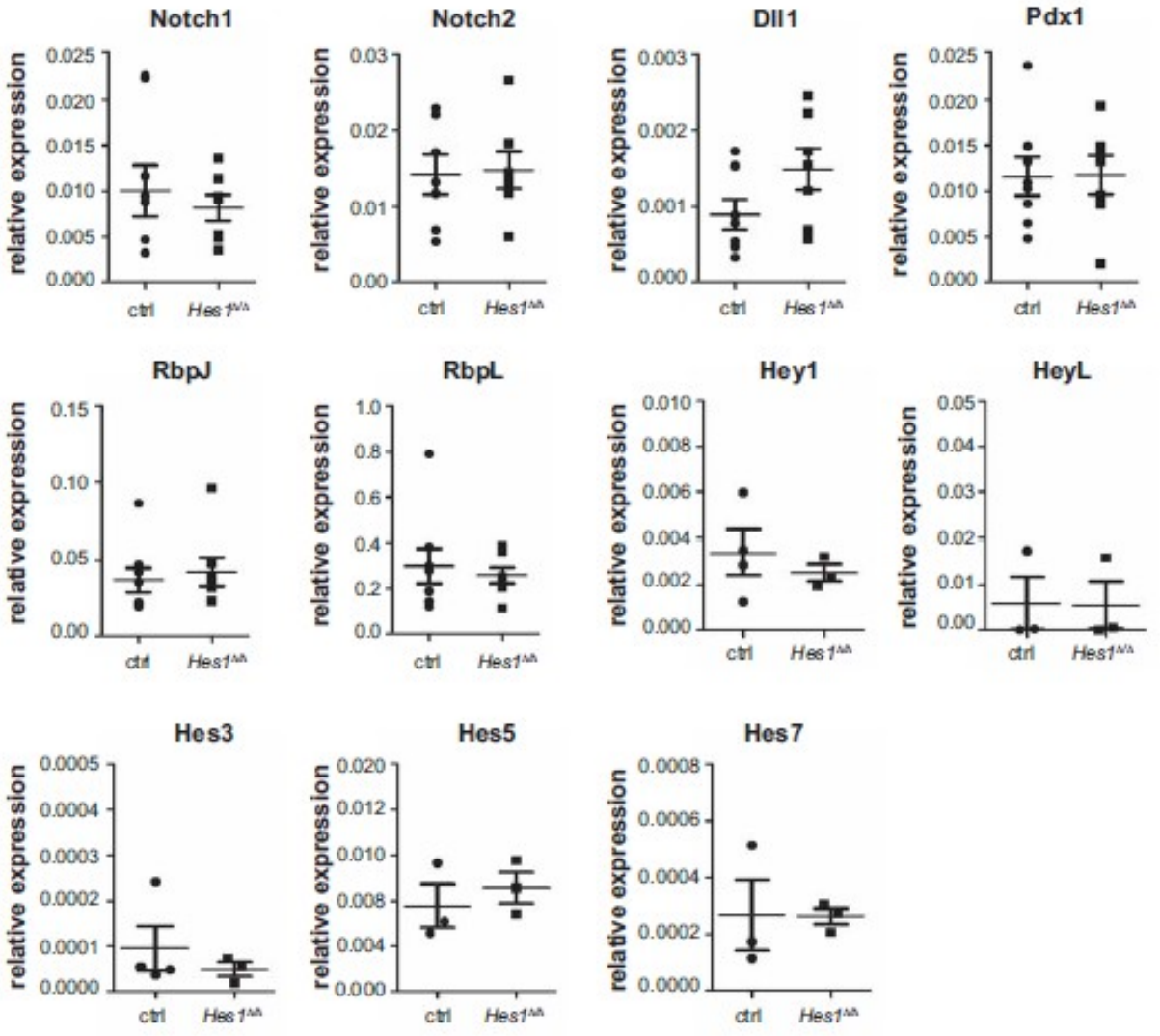

Figure 3-12: Relative expression of different members from the Notch signalling pathway.
Real time PCR in pancreatic tissue from 7-day old control and *Hes1*$^{\Delta/\Delta}$ mice for *Notch1* and *Notch2* receptors, *Delta-Like1* (*Dll1)* ligand, *RbpJ* and *RbpL* transcription factors and *Pdx1*, a transcription factor required for pancreatic development (N≥5 per group). As well as, for the Notch target genes *Hes3*, *Hes5*, *Hes7*, *Hey1*, and *HeyL* (N≥3 per group).

3.1.2. Hes1 as a regulator of acinar cell maturation and maintenance

To investigate the role of HES1 in exocrine compartment maturation and maintenance the effects of *Hes1* deletion at 4 weeks of age were analysed.

Gross morphology and histology as demonstrated by macroscopic images and H&E staining of *Hes1*$^{\Delta/\Delta}$ pancreata showed no apparent differences between 4-week-old control and *Hes1*$^{\Delta/\Delta}$ mice. These results suggest that after E 9.5 HES1 is dispensable for pancreatic development. Higher magnification of the H&E slides of control and *Hes1*$^{\Delta/\Delta}$ mice display comparable acinar, ductal and endocrine cells in both groups (Figure 3 -13 A). Even though no difference in bodyweight could be observed, a significant decrease in pancreas-to-body weight ratio was observed between control and *Hes1*$^{\Delta/\Delta}$ mice (Figure 3 -13 B).

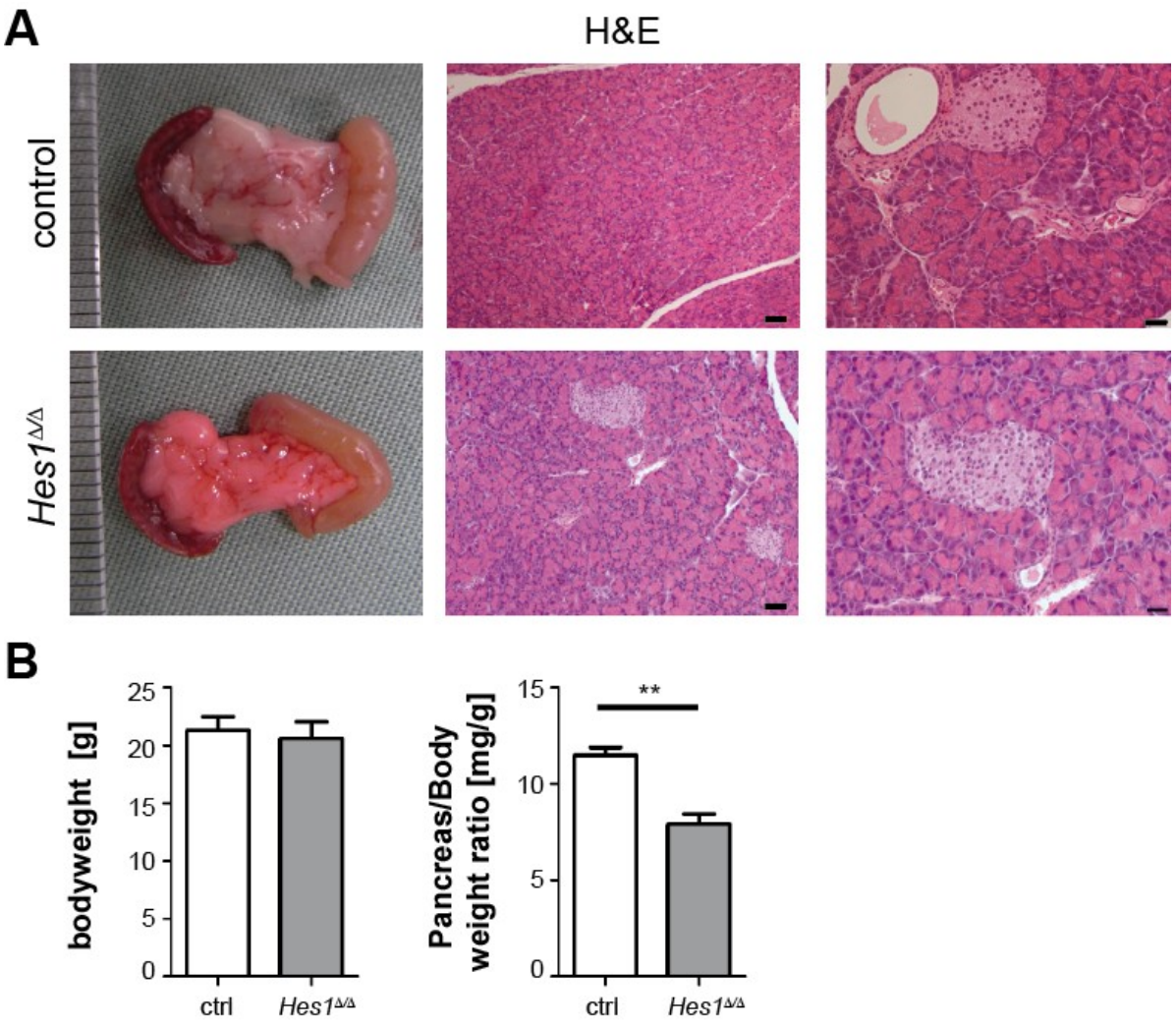

Figure 3-13: Hes1 is dispensable for pancreatic development
A: Macroscopic images of pancreata and H&E staining of control and *Hes1*$^{\Delta/\Delta}$ mice at 4 weeks of age at two different magnifications show no apparent difference in pancreatic morphology in *Hes1*$^{\Delta/\Delta}$ mice compared to control. Scale bars: 50 µm and 100 µm respectively. **B:** Bodyweight and pancreas to bodyweight ratio of control (N=6) and *Hes1*$^{\Delta/\Delta}$ (N=5) mice, at 4 weeks of age. Data are presented as mean+SEM. P values: *p<0.05, **p<0.01, ***p<0.001

To address possible mechanisms responsible for the diminished pancreas-to-body weight ratio in *Hes1*$^{\Delta/\Delta}$ mice, cell proliferation and cell death in control and mutant mice at 4 weeks of age were examined.

Cleaved Caspase 3 is a protein which is activated in apoptotic cells therefore IHC for Cleaved Caspase 3 was used to measure cell death in each cell population. Immunohistochemical staining for Cleaved Caspase 3 showed a lack of apoptotic cells in both groups which is to be expected in healthy adult murine pancreas.

Cell proliferation was quantified by staining for BrdU uptake and subsequent morphometric quantification in both groups. *Hes1*$^{\Delta/\Delta}$ mice exhibited a significant decrease in cell proliferation compared to control mice at 4 weeks of age (Figure 3 -14 A,B). The decrease in proliferation in 4 week old *Hes1*$^{\Delta/\Delta}$ mice is suggestive of a requirement for HES1 in the proper expansion of the acinar cell compartment and is in line with previous studies [10].

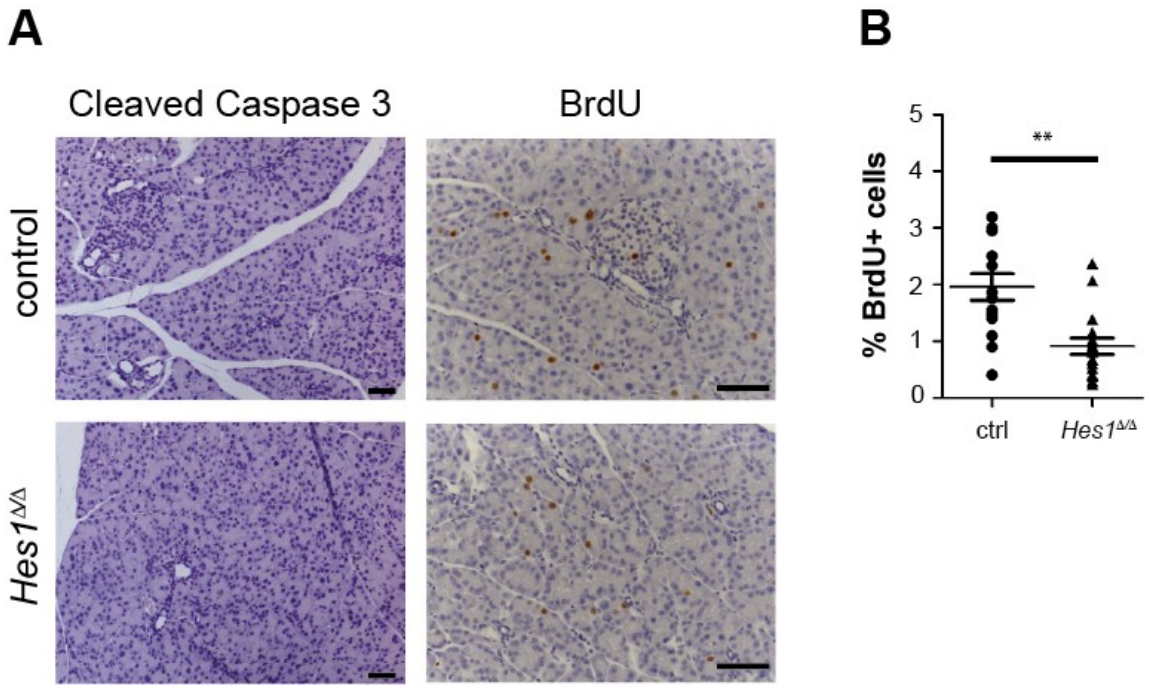

Figure 3-14: Loss of Hes1 leads to decreased proliferation of acinar cells.
A: Left: staining for apoptosis with Cleaved Caspase 3 and right: staining for proliferation with BrdU, on pancreata from 4-week-old mice. Scale bars 50 µm. **B:** Quantification of BrdU positive cells from panel A. In control and *Hes1*$^{\Delta/\Delta}$ mice, data are shown as a percentage of positively stained cells to total cells (N≥12 per group). P values: *p<0.05, **p<0.01, ***p<0.001.

Since other genetic mouse models with impaired acinar cell maturation display decreased pancreatic weight as well as fatty metaplasia [142], [125] the role of HES1 in the context of acinar cell differentiation was further investigated.

To further examine acinar cell maturation and differentiation, H&E and amylase staining of *Hes1*$^{\Delta/\Delta}$ mice was analysed in further detail. Impaired acinar cell intactness could be shown in the H&E staining as demonstrated by the formation of vacuoles within the acinar cells (Figure 3 -15, arrows in magnified figures) whereas amylase staining is somewhat unevenly distributed but nonetheless presents a typical and expected image.

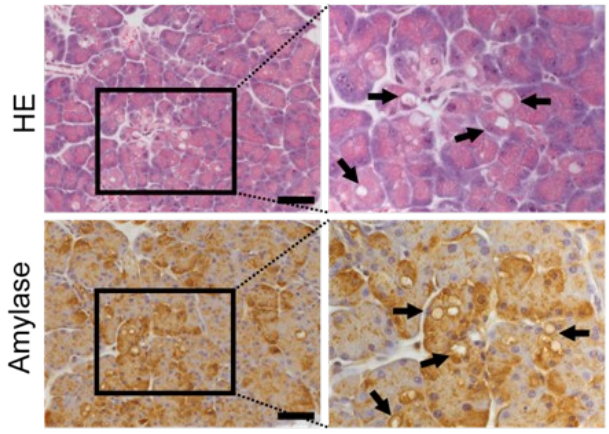

Figure 3-15: H&E and amylase staining of impaired acinar cells in *Hes1*$^{\Delta/\Delta}$ mice
H&E and Amylase staining in *Hes1*$^{\Delta/\Delta}$ mice displaying vacuoles and zymogen granules in the cytoplasm of acinar cells. Scale bar: 50 µm

To examine the differentiation status of acinar and ductal cell compartments, immunofluorescence co-staining for Amylase, a marker for the acinar compartment and CK19, a marker for the ductal compartment was performed in control and *Hes1*$^{\Delta/\Delta}$ mice. Both markers could be detected in both groups and expression as well as distribution seemed comparable. Amylase and Elastase are exocrine markers that are present in developed acinar cells and Mist1 is a transcription factor with importance for acinar cell maturation. To further assess the status of acinar cell maturation we examined expression levels of those acinar specific genes [143] using qRT-PCR and detected significantly decreased levels in*Hes1*$^{\Delta/\Delta}$ mice compared to control mice at 4 week of age (Figure 3 -16 A). These results are in line with the previous results suggesting impaired acinar maturation in *Hes1*$^{\Delta/\Delta}$ mice.

The markersSox9 [21], [18] and Clusterin [6] associated with multipotent progenitor cells [10] were analysed to further assess the maturation status of acinar cells since these previous results suggested impaired acinar maturation in *Hes1*$^{\Delta/\Delta}$ mice. IHC revealed increased expression of Sox9 in acinar and ductal cells in *Hes1*$^{\Delta/\Delta}$ mice while its expression was, as expected, restricted to ductal and CAC in control mice (Figure 3 -16 B). Immunohistochemical staining for Clusterin, a marker of immature acinar cells [10], [6], [144] showed expression in the lumen of acinar cells in *Hes1*$^{\Delta/\Delta}$ mice.

Expression of Sox9 in acinar and ductal cells as well as expression of Clusterin in the acinar cell compartment is suggestive of compromised acinar cell differentiation in 4-week-old *Hes1*$^{\Delta/\Delta}$ mice. These observations point to a requirement of HES1 activity for complete acinar cell differentiation. To further examine a possible difference in acinar cell number and size, immunostaining for E-Cadherin was performed which demonstrated regular acinar cell borders and no difference in cell size (Figure 3 -16B).

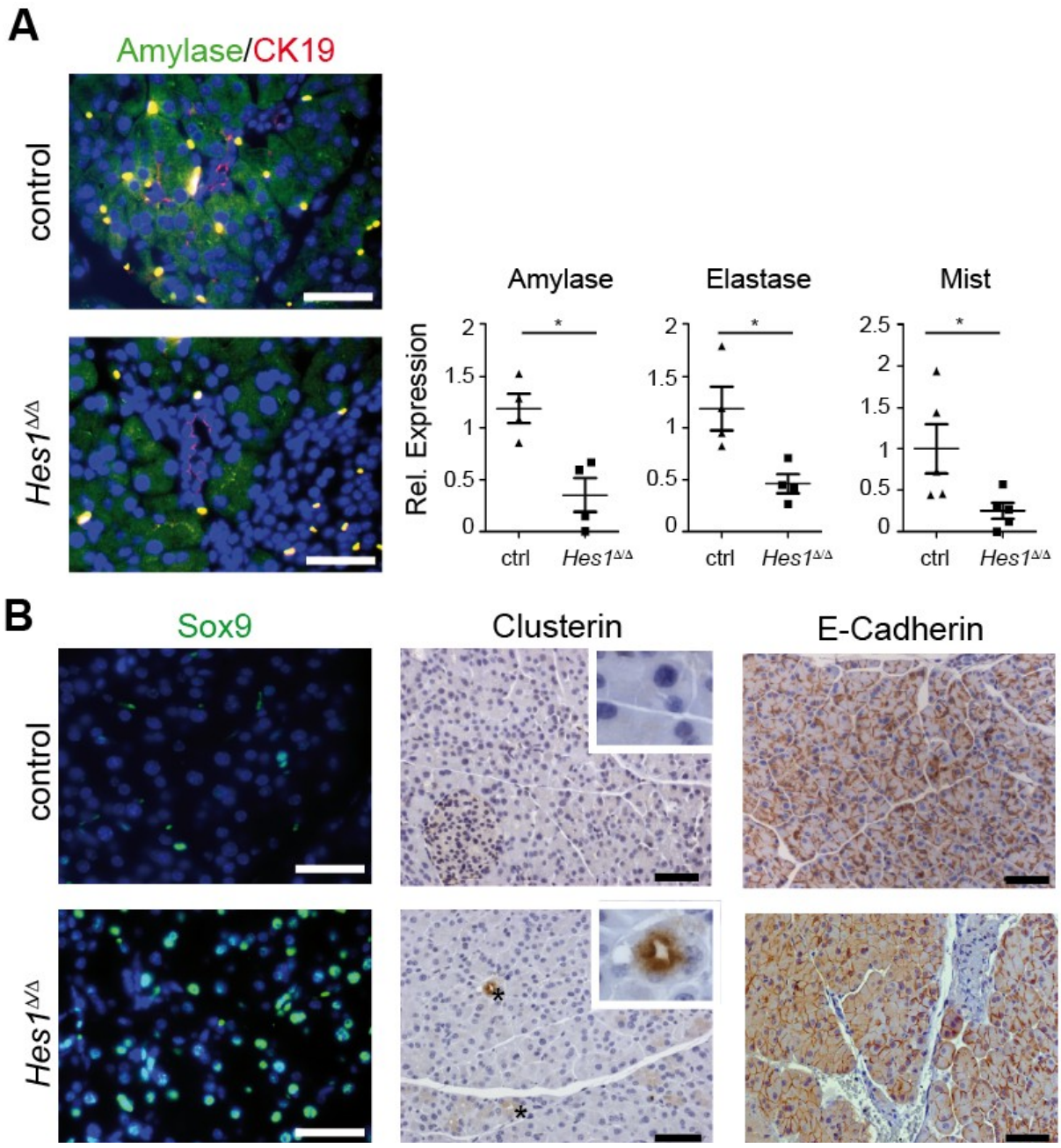

Figure 3-16: Acinar cell maturation and differentiation is impaired in *Hes1*$^{\Delta/\Delta}$
A: Immunofluorescence staining for exocrine markers Amylase (green) and CK19 (red) and DAPI (blue) in 4-week-old mice show no apparent difference in the expression pattern of exocrine markers or morphology of acinar cells in *Hes1*$^{\Delta/\Delta}$ mice compared to control. RT-PCR of acinar markers in*Hes1*$^{\Delta/\Delta}$ and control mice (n= 5 per group) at 4 weeks of age show significantly reduced expression of acinar markers indicative of impaired acinar cell maturation. P values: *p<0.05, **p<0.01, ***p<0.001 **B:** Immunofluorescence of Sox9 (green) and DAPI (blue) showed a significantly increased expression in acinar cells of *Hes1*$^{\Delta/\Delta}$ mice suggesting impairment of acinar cell maturation. Immunohistochemical staining for Clusterin shows beginning impairment of acinar cell intactness. Asterisk shows Clusterin deposits. IHC for E-Cadherin demonstrates regular acinar cell borders. Scale bars: 50 µm.

Immunohistochemical staining for endocrine markers, such as Insulin and Glucagon showed comparable distribution of these hormones in control and *Hes1*$^{\Delta/\Delta}$ mice within the Islets of Langerhans. With insulin expression throughout the Islet of Langerhans and glucagon distributed at the edge. Size of Islets of Langerhans was comparable between the two groups as well (Figure 3 -17A). Intraperitoneal glucose tolerance test showed no significant difference between the two groups with a return to glucose levels close to baseline within the same time frame suggesting a preservation of the endocrine function in *Hes1*$^{\Delta/\Delta}$ mice at 4 weeks of age(Figure 3 -17B).

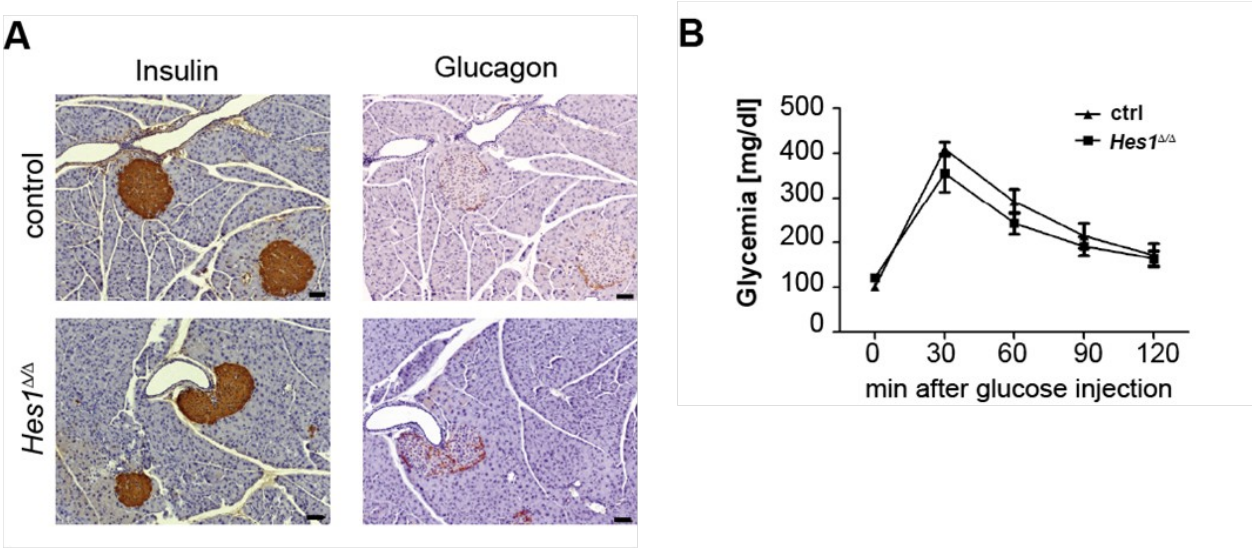

Figure 3-17: Absence of endocrine abnormalities at 4 weeks of age in Hes1Δ/Δ mice
A: Immunohistochemical staining of 4-week-old control and *Hes1*$^{\Delta/\Delta}$ mice for endocrine markers Insulin and Glucagon. Scale bars: 50 µm. **B:** Glucose tolerance test of *Hes1*$^{\Delta/\Delta}$ mice compared to controls at 4 weeks of age.

To assess the impact of incomplete acinar maturation in *Hes1*$^{\Delta/\Delta}$ mice, more advanced time points were looked at. *Hes1*$^{\Delta/\Delta}$ mice at 12 and 52 weeks were looked at in more detail. With advanced age gross appearance and H&E staining of *Hes1*$^{\Delta/\Delta}$ mice show massive pancreatic atrophy and fatty metaplasia, a common reaction to epithelial cell death in the pancreas. Immunohistochemical staining for endocrine markers showed presence of Islets of Langerhans and positive staining for these hormones in *Hes1*$^{\Delta/\Delta}$ mice at 12 weeks of age. Intraperitoneal glucose tolerance testing showed no significant difference in glucose tolerance between the two groups suggestive of a preservation of the endocrine function in *Hes1*$^{\Delta/\Delta}$ mice at 12 weeks of age (Figure 3 -19).

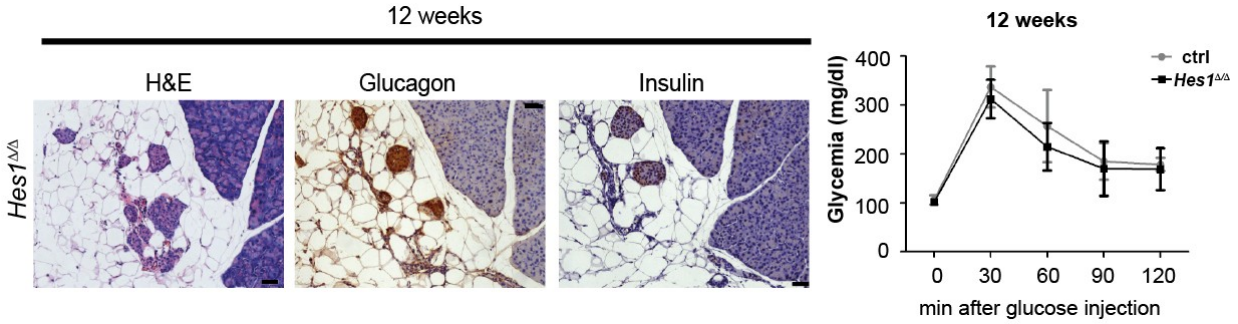

Figure 3-18: Absence of endocrine abnormalities at 12 weeks of age in Hes1$^{\Delta/\Delta}$ mice
H&E and immunohistochemical staining for endocrine markers insulin and glucagon and glucose tolerance test indicate normal endocrine function in control and *Hes1*$^{\Delta/\Delta}$ mice at 12-week-old mice. Some areas of pancreatic tissue have been replaced by fatty tissue Scale bars: 50 µm

At 52 weeks of age only few acinar lobules persist in *Hes1*$^{\Delta/\Delta}$ mice while the majority of the exocrine tissue was replaced by fatty tissue (as outlined in the macroscopic picture of the pancreas), Islets of Langerhans remain functional and are located dispersed within adipose tissue. Old *Hes1*$^{\Delta/\Delta}$ mice appeared healthy and had no diarrhea or steatorrhea, symptoms associated with pancreatic insufficiency (Figure 3 -19).

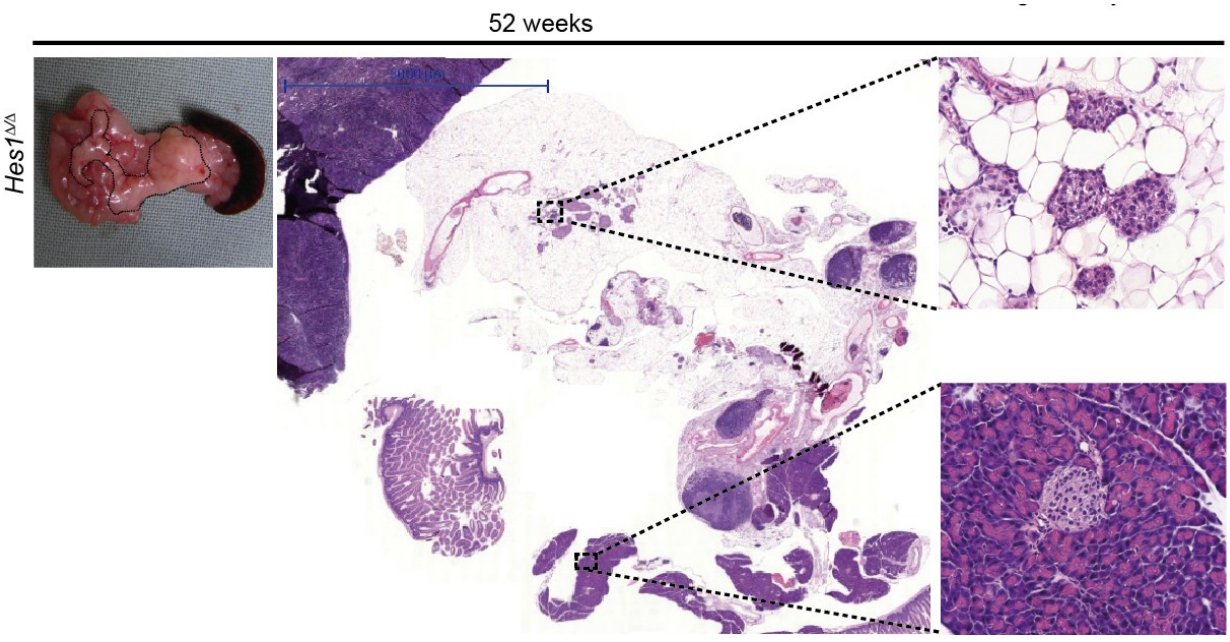

Figure 3-19: Loss of Hes1 leads to fatty metaplasia in advanced aged Hes1$^{\Delta/\Delta}$ mice.
Macroscopic image of pancreas and H&E staining of 52-week-old*Hes1*$^{\Delta/\Delta}$ mice. Notice that small areas of pancreatic tissue are still visible but the majority has been replaced by fatty tissue. Islets of Langerhans are unaffected within remaining exocrine tissue and dispersed in fat (insets). Scale bar: 5000 µm.

Overall these results indicate that even though Hes1 seems to be dispensable for pancreatic development, Hes1 activity affects acinar cell maturity as suggested by positive IHC for SOX9 (Figure 3 -16)and acinar cell compartment maintenance with age (Figure 3 -19). As demonstrated by IHC and IPGTT the endocrine function seems unaffected even in aged mice that presented with massive pancreatic atrophy and fatty metaplasia (Figure 3 -18, Figure 3 -19).

3.2. Effects of acute pancreatitis on *Hes1*$^{\Delta/\Delta}$ mice

Notch signaling is required for exocrine regeneration after acute pancreatitis and expression of HES1 is upregulated in re-differentiating acini but not in duct cells[10]. HES1 expression can be observed at d1 after acute pancreatitis at low levels and is predominant at d3 which indicates that Notch signaling activation takes place during acinar regeneration [135]. Caerulein-induced pancreatitis was used as a model of regeneration in *Hes1*$^{\Delta/\Delta}$ mice to determine the functional role of HES1 in pancreatic exocrine regeneration. The changes in pancreatic regeneration were evaluated 1, 3 and 5 days after the last caerulein injection (d1, d3 and d5). H&E staining was performed to show the progression of caerulein-induced acute pancreatitis and regenerative processes of exocrine tissue thereafter from d1 through d5 (Figure 3 -20 A). Pancreatic tissue from control mice and*Hes1*$^{\Delta/\Delta}$ mice were treated with caerulein to determine whether loss of *Hes1* affects the severity of injury, the effectiveness of regeneration, or both. Caerulein-induced pancreatitis led to abundant inflammation, edema and de-differentiation of acinar cells in both groups at d1 (Figure 3 -20 A). Thus, initial response to acute pancreatitis and extent of exocrine injury seemed to be comparable in both groups at d1. Acinar re-differentiation was apparent at d3 post caerulein treatment only in control pancreas and nearly complete regeneration of exocrine tissue could be observed at d5 in control mice. Start of compromised regeneration is detected at d3 in *Hes1*$^{\Delta/\Delta}$ mice compared to control animals. In *Hes1*$^{\Delta/\Delta}$ mice H&E staining at d5 shows that regeneration is delayed and compromised (Figure 3 -20A).

Cross section H&E staining of the whole pancreas at d3 post caerulein treatment of control mice show acinar regeneration while large areas of exocrine tissue in *Hes1*$^{\Delta/\Delta}$ pancreas were replaced by adipose tissue with remaining exocrine tissue displaying persistent inflammation and duct-like structures. Quantification of total pancreatic area to exocrine area of control and *Hes1*$^{\Delta/\Delta}$ mice illustrates the magnitude of reduced functional exocrine tissue due to the loss of *Hes1* (Figure 3 -20B).

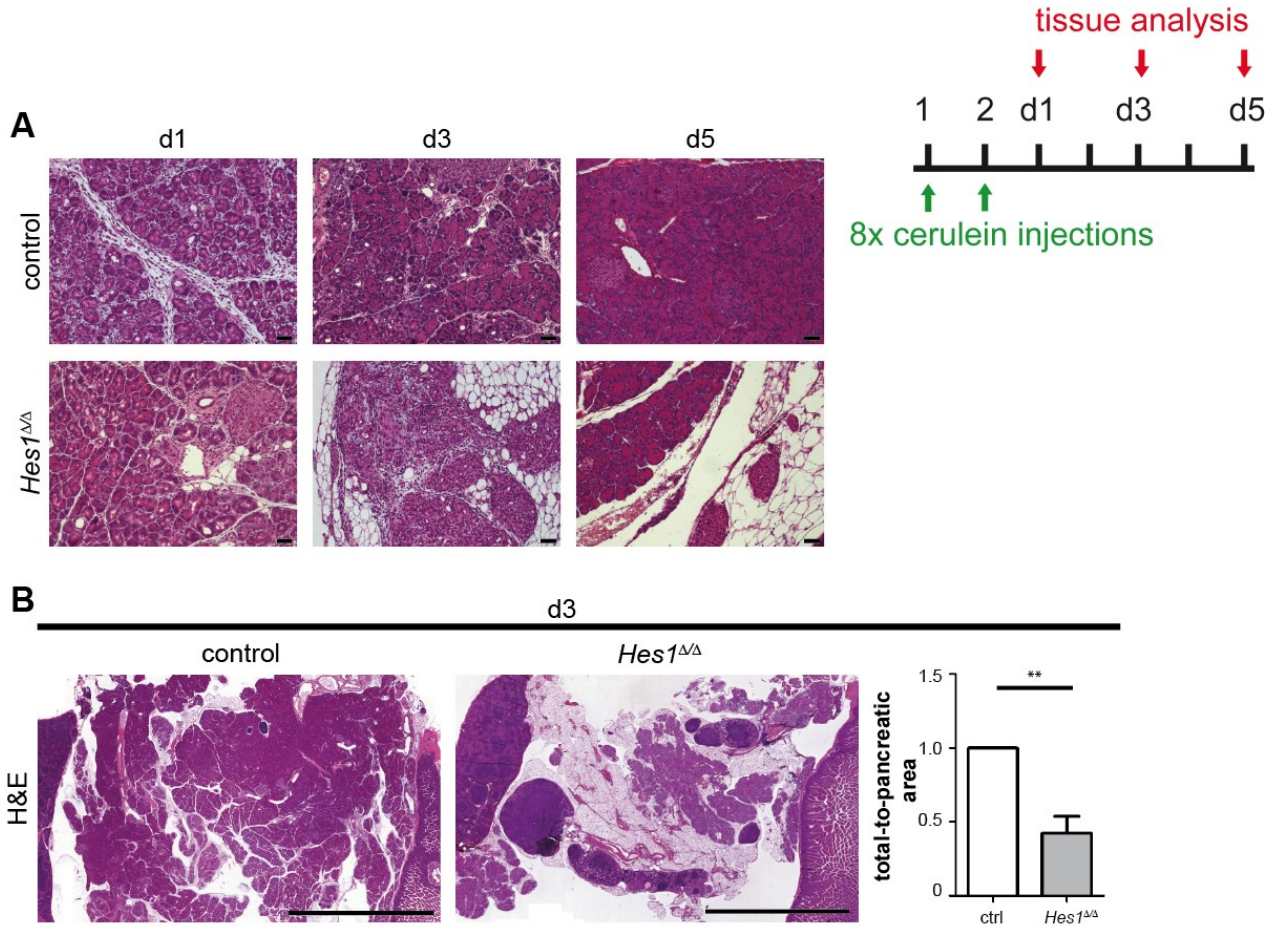

Figure 3-20: Deletion of Hes1 impairs regeneration of exocrine tissue after acute pancreatitis.
A: Representative H&E staining demonstrates histological progression of acute pancreatitis and regeneration over time in control and Hes1$^{\Delta/\Delta}$ miceat the indicated time points (day1, day3 and day5 post caerulein treatment). **B:** While H&E staining at d3 post caerulein treatment of control mice show regenerated acinar tissue, large areas of exocrine tissue in Hes1$^{\Delta/\Delta}$ pancreas are replaced by adipose tissue and remaining exocrine tissue displays persistent inflammation and duct-like structures. Ratio of total pancreatic area to exocrine area at day 3. Values are shown as mean+SEM. P values: *p<0.05, **p<0.01, ***p<0.001.Scale bars in A: 50µm, scale bars in B: 2000 µm

To assess the impact of HES1loss on proliferation and apoptosis in the impaired regeneration processes after acute pancreatitis immunochemistry for Ki67 and Cleaved Caspase3 were performed. Immunostaining and quantification of Ki67 and Cleaved Caspase3 showed significant decrease in Ki67^{+} cells and significant increase in Cleaved Caspase3^{+}cells on d3 in *Hes1*$^{\Delta/\Delta}$ mice compared to control (Figure 3 -21A, B). Proliferative activity in control mice is in line with results of previous studies which showed acinar regeneration is based on preexisting acinar cells after inflammatory injury [145]. Regarding quantification of Ki67, a higher number of total cells due to persistent

inflammation had to be taken into consideration but the decrease in proliferation of duct-like epithelium was still apparent. Thus, the diminished regenerative capacity in *Hes1*$^{\Delta/\Delta}$ mice could be associated with decreased cell proliferation and an increase in apoptosis after acute pancreatitis. These results are in line with previous studies and suggest that HES1 plays a role in acinar regeneration after insult[10].

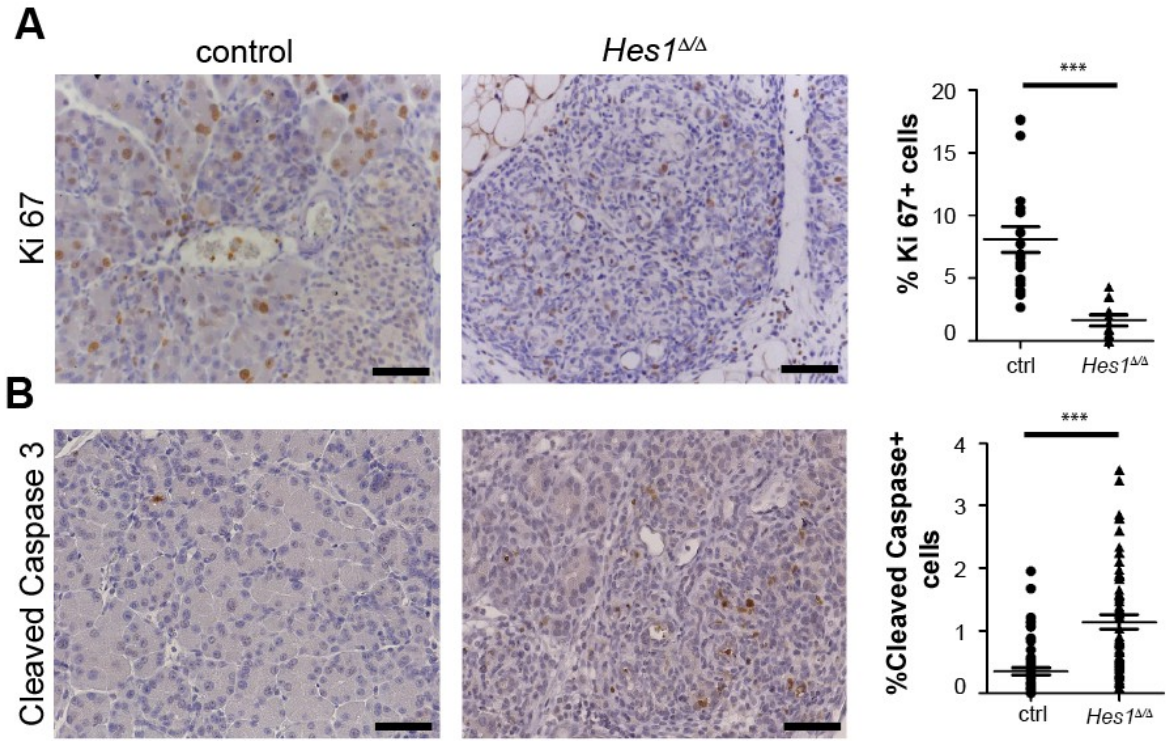

Figure 3-21: Loss of Hes1 reduces proliferation while increasing apoptosis after acute pancreatitis.
A: Representative immunohistochemical staining and morphometric quantification for Ki 67 and
B: Cleaved Caspase 3 (n= 3 per group). Values are shown as mean±SEM. P values: *p<0.05, **p<0.01, ***p<0.001.Scale bars: 50 µm

To further investigate the role of HES1 in acinar regeneration the expression of specific exocrine markers was analysed. Immunostainings at day 3 after induction of acute pancreatitis were performed for markers of exocrine pancreatic cells as well as exocrine cell maturity. Looking at the exocrine markers Amylase and CK19 in control and *Hes1*$^{\Delta/\Delta}$ mice at d3 showed that while Amylase and CK19 patterns were as expected in re-differentiated exocrine tissue in control mice with amylase expressed in acinar cells and CK 19 restricted to ductal cells. In *Hes1*$^{\Delta/\Delta}$ mice a dramatic difference in amylase and

CK19 expression is observed reflecting blocked acinar re-differentiation and persistent ductal metaplasia in *Hes1*$^{\Delta/\Delta}$ mice. The strong expression of progenitor markers Clusterin (a marker of immature, regenerating acini [6], [10]) and Sox9 in duct-like epithelial pancreatic cells in *Hes1*$^{\Delta/\Delta}$ mice suggest that HES1 function is important for pancreatic regeneration, in particular during acinar re-differentiation. Loss of HES1 seems to obstruct re-differentiation of acinar cells and keeping cells locked in a transdifferentiated state. Consistent with previous studies [2], it could be demonstrated that immature acinar cells with strong expression of Sox9 are prone to ADM formation in the setting of acute pancreatitis (Figure 3 -22).

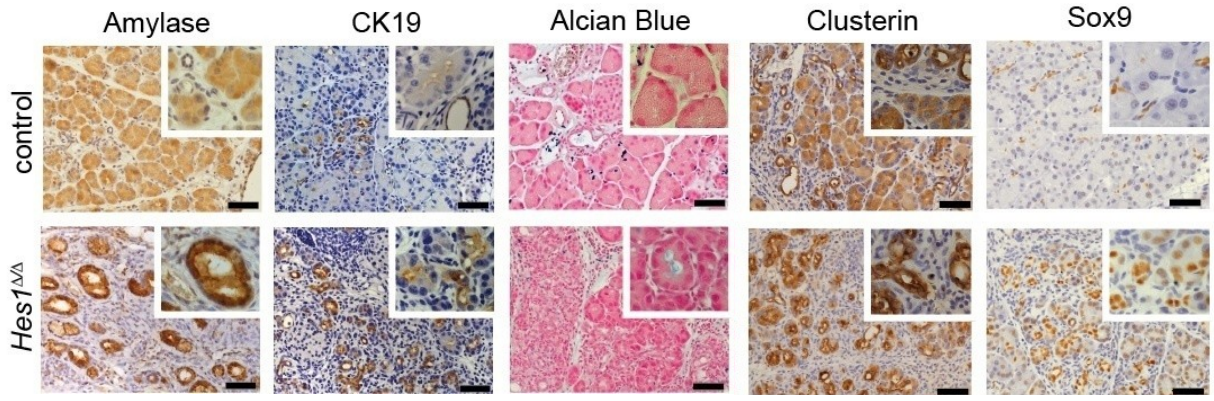

Figure 3-22: Hes1$^{\Delta/\Delta}$ mice show compromised acinar re-differentiation and persistent ductal metaplasia
Immunohistochemical staining in day3 samples for exocrine markers Amylase and CK19 show duct-like epithelial pancreatic cells in Hes1$^{\Delta/\Delta}$; Alcian Blue staining reveals no mucinous deposits in ADM. Clusterin and Sox9 are expressed in duct-like epithelial pancreatic cells. Higher magnification of a detail is shown in the inset. Scale bars: 50µm.

In contrast to other genetic mouse models with impaired acinar regeneration after caerulein-induced pancreatitis [142], [125] no mucinous deposits could be detected within ductal structures in *Hes1*$^{\Delta/\Delta}$ mice as demonstrated by the lack of Alcian Blue staining (Figure 3 -22). The lack of mucinous deposits within the ductal structures is indicative of acinar cells undergoing transdifferentiation and in line with the histology of previously described atypical flat lesions (1.2.2..).

Thus, HES1 function seems to be important not only for complete acinar maturation and maintenance but also critical in regaining acinar differentiation after caerulein-induced acute pancreatitis.

3.3. The role of Hes1 in PDAC initiation and development

Notch pathway activation and HES1 expression are proposed to be requisite for PanIN progression and PDAC development [11], [9]. The previous results in this thesis have demonstrated impairments in acinar cell maturation and maintenance accompanied by over-expression of SOX9as well as compromised regeneration of the acinar compartment after induced acute pancreatitis in*Hes1*$^{\Delta/\Delta}$ mice. Therefore, further investigation into whether HES1 plays a role in ADM in the context of KRAS driven preneoplastic transformation was conducted.

In order to investigate the functional role of HES1 in malignant transformation, conditional Hes1 loss of function GEMM was crossed with constitutively active *Kras*^{G12D} GEMM (*Ptf1a*$^{+/Cre}$;*Kras*$^{+/LSL\text{-}G12D}$;*Hes1*$^{fl/fl}$ henceforth called: *Kras*^{G12D};*Hes1*$^{\Delta/\Delta}$) and the resulting *Kras*^{G12D}; *Hes1*$^{\Delta/\Delta}$ model was utilized. To analyse preneoplastic lesion development and progression, pancreata of the *Kras*^{G12D};*Hes1*$^{\Delta/\Delta}$ GEMM were characterised at defined time points.

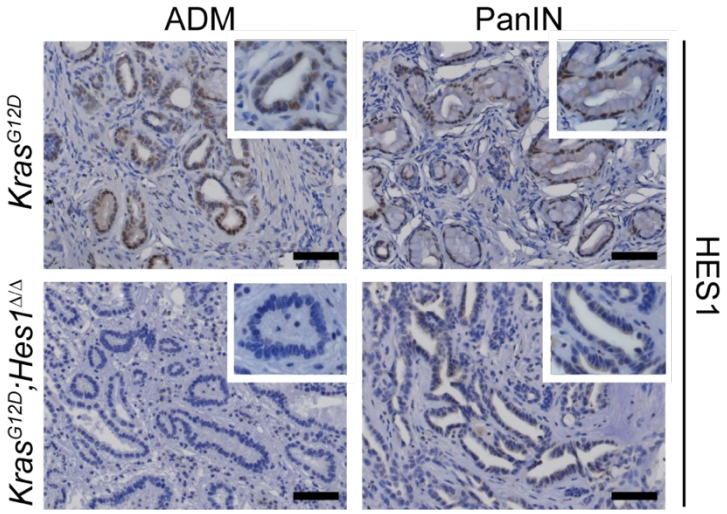

Figure 3-23: IHC of HES1 in *Kras*^{G12D};*Hes1*$^{\Delta/\Delta}$ mice compared to *Kras*^{G12D}controls.
Immunohistochemical staining for HES1 in ADM and PanIN lesions of *Kras*^{G12D} control and *Kras*^{G12D};*Hes1*$^{\Delta/\Delta}$ mice. Scale bars: 50µm.

Absence of Hes1 in Kras driven preneoplastic transformation results in highly proliferative ADM and fewer high grade PanIN lesions

Ptf1a$^{+/Cre}$;*Kras*$^{+/LSL\text{-}G12D}$ mice with *Hes1*$^{fl/fl}$ mice were intercrossed to assess the requirement of *Hes1* in the context of *Kras*^{G12D} mediated PDAC initiation and progression. Loss of HES1 in the context of oncogenic KRAS revealed an abundance of metaplastic ductal structures and cystic transformation with large areas of pancreatic parenchyma affected, in comparison to aged matched controls(Figure 3 -24 A).

Pathological analysis showed that *Kras*^{G12D}*;Hes1*$^{\Delta/\Delta}$ mice presented a higher ADM incidence compared to *Kras*^{G12D} animals. At 12 weeks of age PanIN lesions were focally localized and overall low grade in both groups (Figure 3 -24 B).

To further characterise the lesions of *Kras*^{G12D} and *Kras*^{G12D}*; Hes1*$^{\Delta/\Delta}$ at 12 weeks of age, immunohistochemical analysis of relevant markers was carried out. Claudin 18, a marker located in the cell membrane of PanIN lesions that can be utilized to specifically stain for and identify PanIN lesions [146]. Alcian Blue, a marker for mucin content of lesions which is also used to identify PanIN lesions [147]. Mucin 5AC, a marker that can be detected in the earliest PanIN lesions as well as PDAC but is not expressed in regular ducts allows for further distinctions between lesions and ductal structures [148], [149]. The ductal characteristics of the lesions in *Kras*^{G12D}*;Hes1*$^{\Delta/\Delta}$ were highlighted by positive CK19 staining while lesions in *Kras*^{G12D} mice showed positive staining for Claudin 18, MUC5AC and Alcian Blue, all typical markers for PanIN lesions. Ductal lesions present in *Kras*^{G12D}*;Hes1*$^{\Delta/\Delta}$ mice lacked strong staining for MUC5AC and Alcian Blue, markers of mucin content and indicative of PanIN lesions (Figure 3 -24 C).

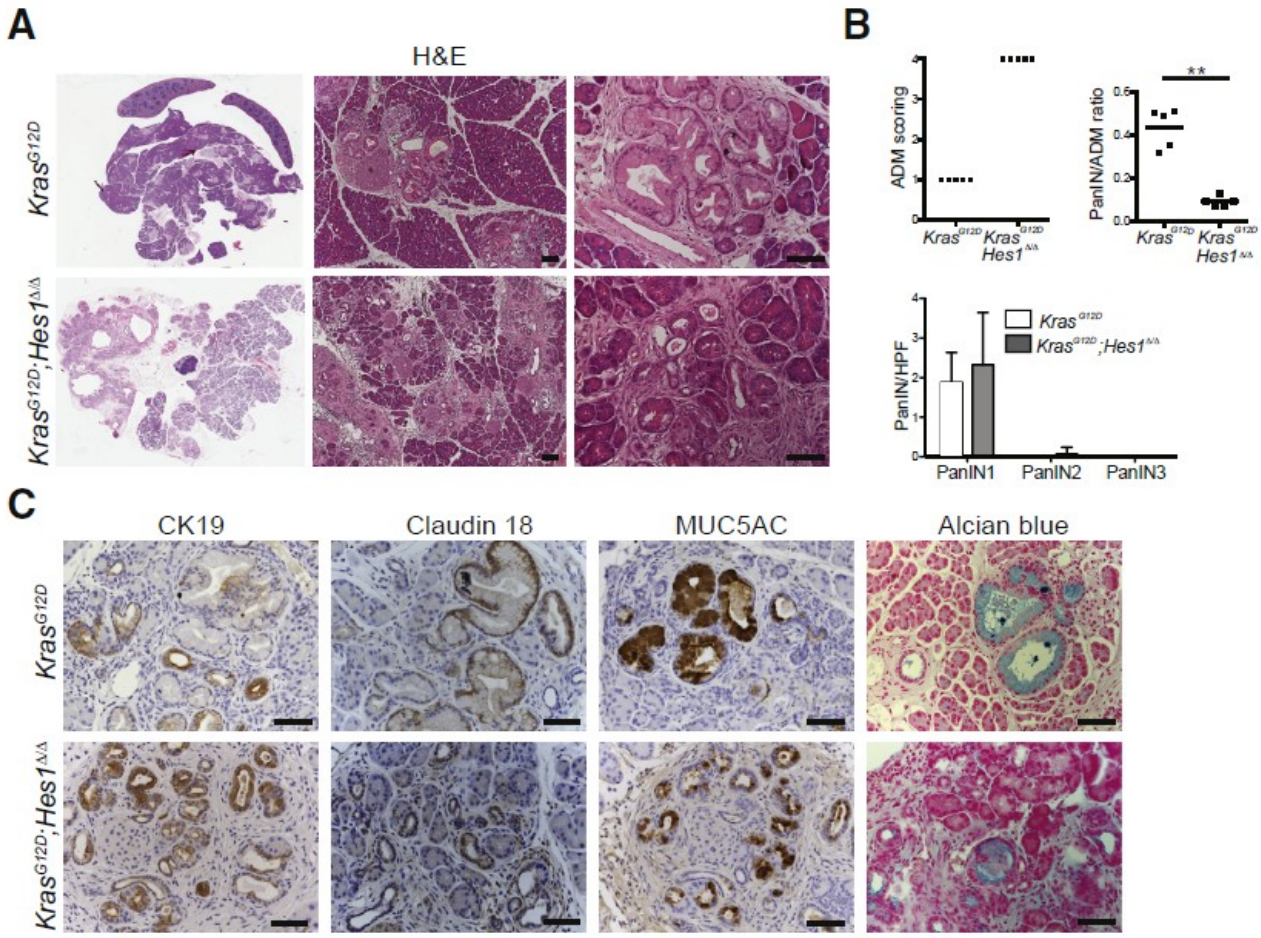

Figure 3-24: Loss of Hes1 leads to increased acinar to ductal metaplasia in Kras^{G12D}-driven neoplasia.

A: Representative H&E staining of *Kras^{G12D}* and *Kras^{G12D};Hes1$^{Δ/Δ}$* at 12 weeks of age. Notice, in the second panel, a more detailed image of the different lesions: PanIN in control mice and ADM in*Kras^{G12D};Hes1$^{Δ/Δ}$* mice. **B:** Quantification of lesion type in *Kras^{G12D};Hes1$^{Δ/Δ}$* mice and aged matched *Kras^{G12D}* controls. Values are shown as mean±SEM. P values: *p<0.05, **p<0.01, ***p<0.001. **C:** Immunohistochemical staining for CK19, Claudin 18, MUC5AC and Alcian Blue of indicated genotypes. Scale bars: 50µm.

To further substantiate the hypothesis that Hes1 is an essential component of the PanIN-to-PDAC route in $Kras^{G12D}$-driven mouse pancreatic carcinogenesis, tissuesof12-week-old $Kras^{G12D}$and $Kras^{G12D};Hes1^{\Delta/\Delta}$ mice were stained with Ki67 and MUC5AC. Sequential slides were used in order to correlate the proliferative status of the lesions present in both phenotypes in order to assess further distinctions of the lesions. While$Kras^{G12D}$ littermates presented with MUC5AC-positive lesions, lesions in the $Kras^{G12D};Hes1^{\Delta/\Delta}$ group were predominately MUC5AC-negative but highly proliferative, as demonstrated by Ki67 staining (A).

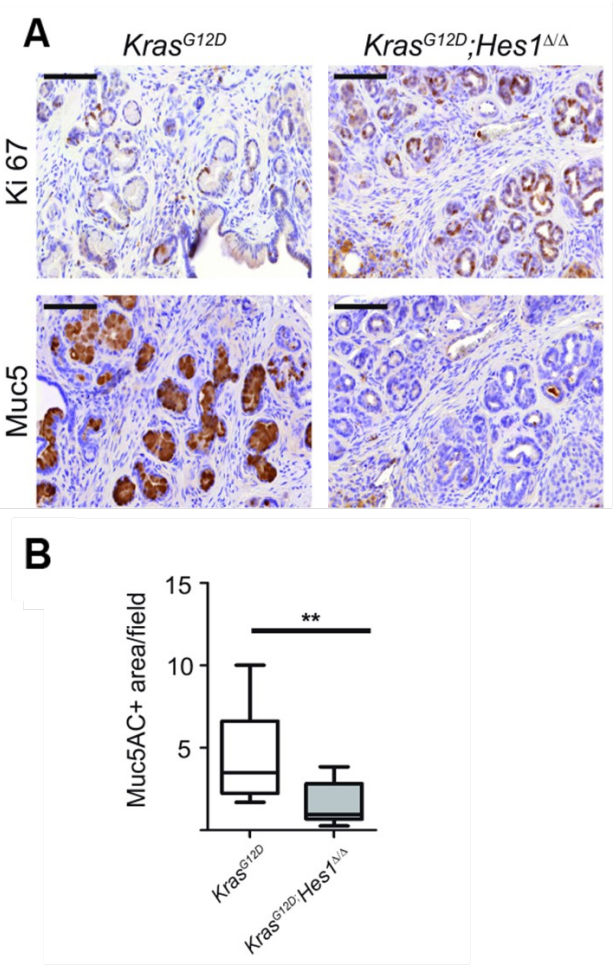

Figure 3-25:Absence of Hes1 in $Kras^{G12D}$-driven preneoplastic transformation results in an abundance of proliferative ADM.
A: Immunohistochemical staining of Ki67 and MUC5AC of the indicated genotypes. **B:** Quantification of MUC5AC-positive lesions per optical field of the indicated genotypes. Values are shown as mean± SEM. P values: *p<0.05, **p<0.01, ***p<0.001.Scale bars: 50 µm.

In order to assess the extent of ADM in *Kras^{G12D};Hes1$^{\Delta/\Delta}$* mice, a pancreatic expert pathologist (Prof. Dr. med. Bence Sipos, Institut für Pathologie und Neuropathologie, Abteilung Allgemeine Pathologie, Universität Tübingen) rated the amount of ADM present at specific time points. The results in the table below(Table 3 -4) demonstrate that a high ADM burden was accompanied by low grade PanIN lesion incidence which persisted with progressing age of *Kras^{G12D};Hes1$^{\Delta/\Delta}$* mice. Besides abundant ADM the H&E staining from *Kras^{G12D};Hes1$^{\Delta/\Delta}$* mice revealed cystic transformation accompanied by fatty metaplasia, fibrosis and ductectasia (Table 3 -4 and).

The obtained data from *Kras^{G12D};Hes1$^{\Delta/\Delta}$* mice suggest that loss of HES1 leads to PDAC formation through an alternative route of highly proliferative ductal lesions.

Table 3-4: Pathological analysis of pancreatic lesions from *Kras^{G12D};Hes1$^{\Delta/\Delta}$* mice.
Amount of lesions were graded by pathologist using the following categories: 4=strong, 3=moderate, 2=minimal, 1=slight or 0=no lesions.

Age (days)	ADM	Fibrosis	Lipomatosis	Duct ectasia	Cystic transf.	PanIN			Tumor	Comments
						1	2	3		
133	3	3	2	1	0	2	1	0		PanINslowproliferating
133	2	3	0		3	0	0	0		Epithelia of cysts low proliferating
133	2	2	2	1	0	2	0	0		
140	2	3	2	3	2	1	0		Incipient G3 carcinoma	Flat atypia, focal moderately proliferating
161	3	3	3		3	0	0	0		
224	3	3	2	2	0	0	1	0		Mucocele-like lesions. Flat atypia, moderately proliferating, epithelia of cysts low proliferating

As noted by the pathologist, disease progression was accompanied by fibrosis, lipomatosis, ductectasia and cycstic transformation during disease progression in some *Kras*^{G12D}*;Hes1*$^{\Delta/\Delta}$ mice(Table 3 -4) which is shown in a representative H&E staining of a whole pancreas section of the *Kras*^{G12D}*;Hes1*$^{\Delta/\Delta}$ phenotype(Figure 3 -26).

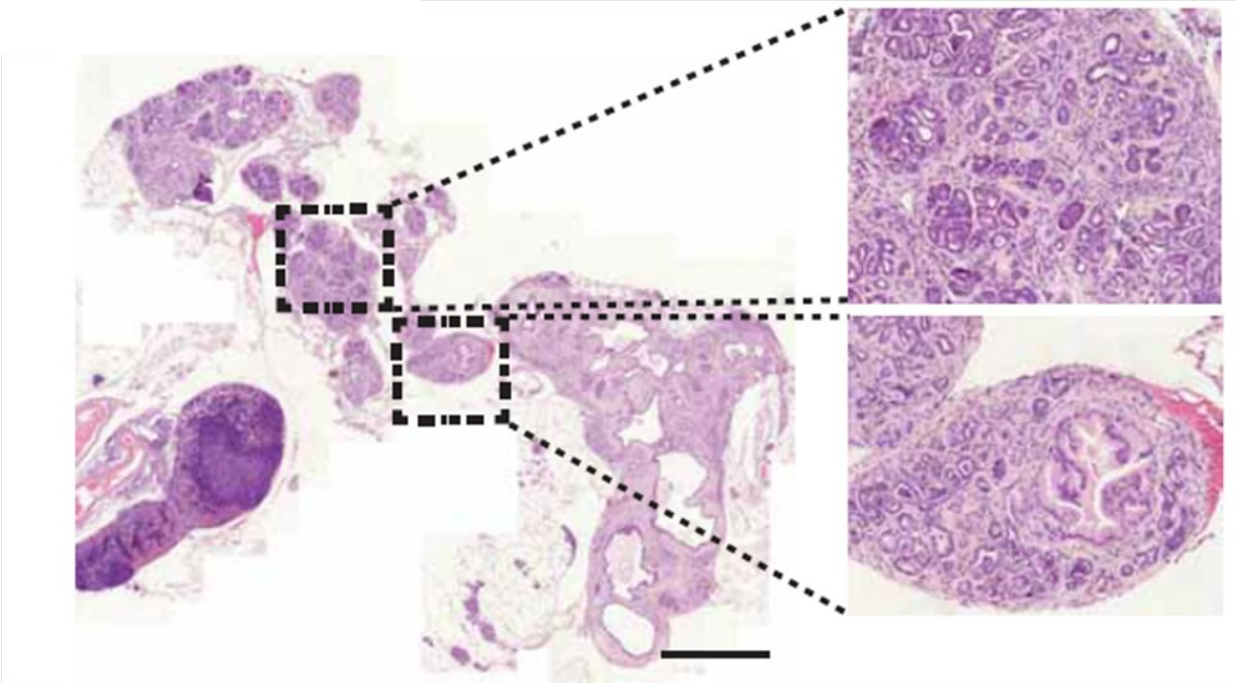

Figure 3-26: Loss of Hes1 leads to fibrosis, lipomatosis, ductectasia and cystic transformation.
Whole pancreas scan of H&E staining from *Kras*^{G12D}*; Hes1*$^{\Delta/\Delta}$ mouse. Note the presence of cysts and adipose tissue. Scale bar: 1000 µm, in zoomed images 100 µm.

The side by side H&E scan of representative whole pancreas of both *Kras*^{G12D} and *Kras*^{G12D};*Hes1*$^{\Delta/\Delta}$ mice underscores the extent of fibrosis, lipomatosis and cystic lesions in the *Kras*^{G12D};*Hes1*$^{\Delta/\Delta}$ mice. Quantification of ADM in both groups showed a significantly higher ADM incidence per high power field (HPF) in *Kras*^{G12D};*Hes1*$^{\Delta/\Delta}$ mice compared to *Kras*^{G12D} mice. As demonstrated in Table 3 -4 coinciding with high ADM incidence is a lack of high grade PanIN formation (Figure 3 -27).

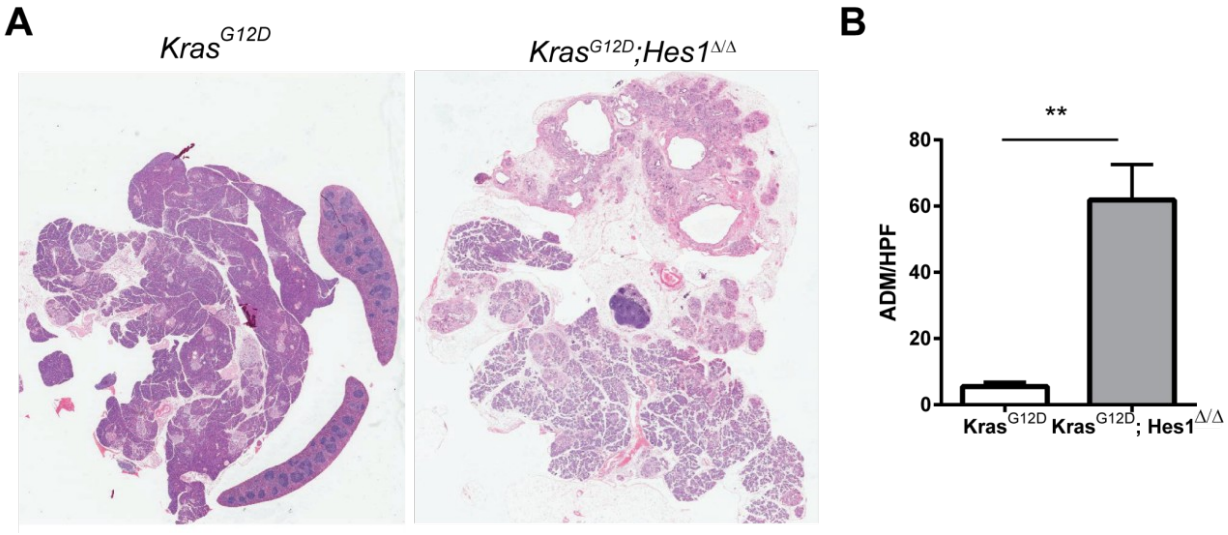

Figure 3-27: Loss of Hes1 leads to ADM and cystic transformation rather than PanIN progression
A: Whole pancreas scan of H&E staining in *Kras*^{G12D} and *Kras*^{G12D};*Hes1*$^{\Delta/\Delta}$ mice. **B**: Quantification of ADM per high power field from (A). Data is shown as mean±SEM. P values: *p<0.05.

Histological evaluation of representative H&E staining of *Kras*^{G12D} and *Kras*^{G12D};*Hes1*$^{\Delta/\Delta}$ mice at 6 and 9 months of age as well as at terminal stage further demonstrate the higher ADM incidence and predominance of low grade PanIN lesions in *Kras*^{G12D};*Hes1*$^{\Delta/\Delta}$ compared to age-matched *Kras*^{G12D} which display high grade PanIN to PDAC progression(Figure 3 -28 A).Survival analysis revealed that the median survival of *Kras*^{G12D};*Hes1*$^{\Delta/\Delta}$ mice compared to *Kras*^{G12D} controls was significantly reduced (Figure 3 -28 B).Interestingly over half of the *Kras*^{G12D};*Hes1*$^{\Delta/\Delta}$ mice developed PDAC at terminal point, without presence of high grade PanIN lesions (Table 3 -5). The results show that loss of HES1 in the context of *Kras*^{G12D} is associated with a high incidence of ADM and cystic transformation leading to a shorter median survival compared to *Kras*^{G12D} controls (Figure 3 -28 B).

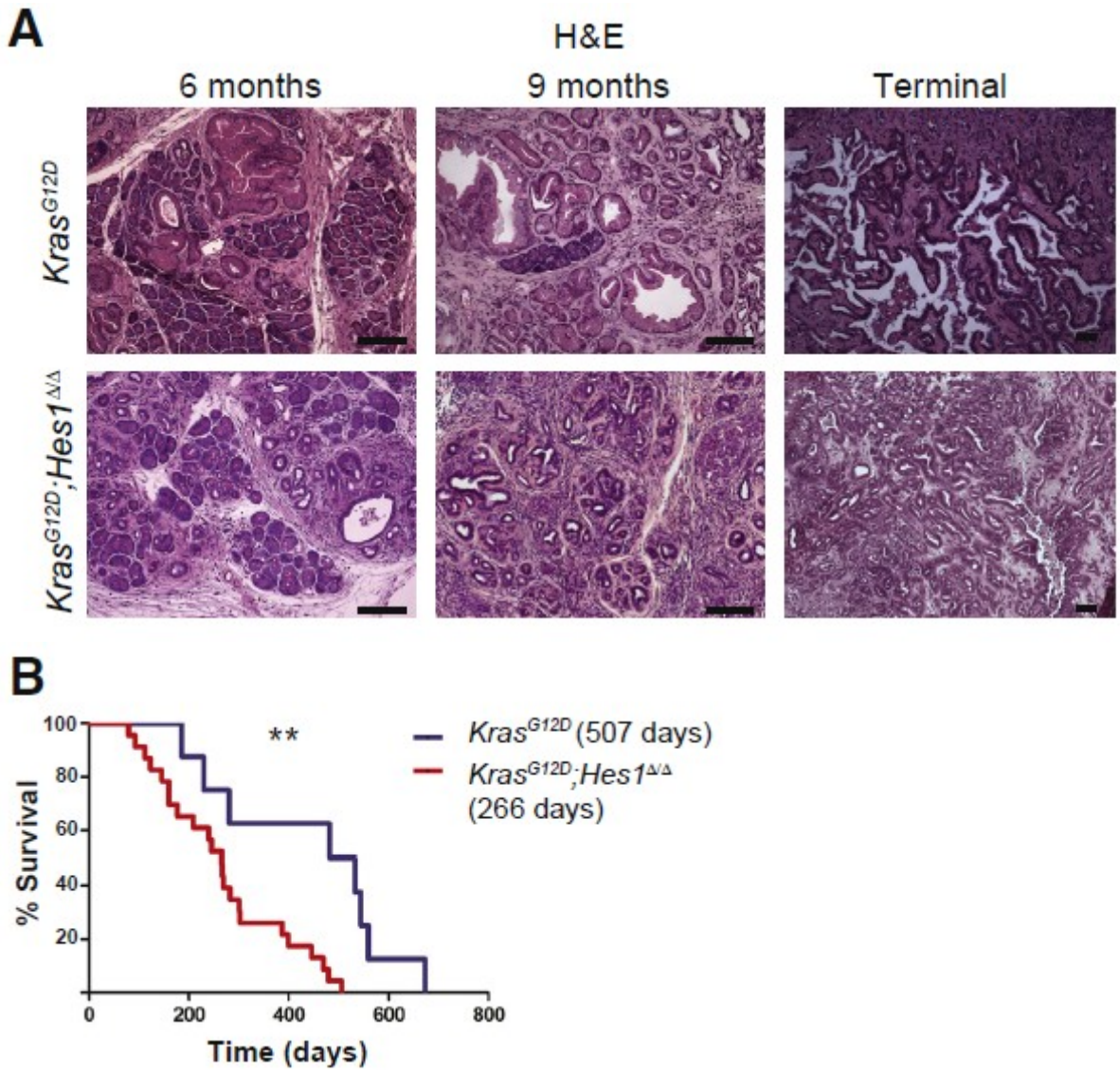

Figure 3-28: Loss of *Hes1* in the *Kras^{G12D}* setting leads to PDAC and reduced survival.
A: Representative H&E staining of *Kras^{G12D}* and *Kras^{G12D};Hes1$^{\Delta/\Delta}$* mice at 6 and 9 months of age and at terminal stage. Scale bars 50 µm. **B:** Kaplan-Meier survival curve of *Kras^{G12D}* and *Kras^{G12D}; Hes1$^{\Delta/\Delta}$* mice. *Kras^{G12D}* mice had significantly prolonged survival compared to *Kras^{G12D};Hes1$^{\Delta/\Delta}$* mice. P values: *p<0.05, **p<0.01, ***p<0.001

Analysis of *Kras^{G12D}; Hes1$^{\Delta/\Delta}$* mice at end point stage showed that mice developed PDAC while at the same time displaying a lack of high grade PanIN lesions consistent with the disease progressing at earlier time points and/or through a different preneoplastic lesion route (Table 3 -5).

Table 3-5: Pathological analysis of lesion type for *Kras^{G12D};Hes1$^{\Delta/\Delta}$* mice at end point stage.
Grading is defined as follows: G1= well differentiated, G2= moderately differentiated, G3= poorly differentiated tumors

Age (days)	PanIN	PDAC	Grade	Parenchyma
112	Minimal 1a	No	-	Marked ductectasia
160	Moderately 1a	No	-	Almost complete cystic
177	No residual pancreas	Yes	G2-G3	Ductectasia
186	Marked 1b, few 2	No	-	Complete fibrosis/ADM
245	Moderately 1a-b, focally 3, flat atypia?	Yes	G3	Moderate ductectasia, marked
269	No residual pancreas	Yes	G2-G3	No residual pancreas
387	Marked 1b and 2	No	-	Complete fibrosis/ADM
399	No residual pancreas	Yes	G1-G2	No residual pancreas
445	Moderately 1a-b, few 2	Yes	ND	Marked fibrosis/ADM
469	Marked 1a-b	Yes	G2-G3	Marked fibrosis/ADM
479	1a	Yes	G1-G2	Marked ductectasia

4. Discussion

4.1. Hes1 is required for acinar cell compartment maintenance and differentiation

The Notch signaling pathway is a key regulator of cell-fate decision, tissue patterning as well as cell differentiation and proliferation in various organs [26], [39]. It plays a major role during pancreatic development by maintaining an undifferentiated precursor cell pool [34], [40]. The Notch signaling effector HES1 is a transcription factor active in pancreatic development involved in the embryonic process of cell fate decision. In adult animals HES1 expression is only present in centroacinar cells which have been proposed to be a source of undifferentiated pancreatic cells. A re-activation of HES1 expression has been shown for acinar cells in acute pancreatitis and PDAC[113], [10]. To determine whether deletion of HES1 would affect regular pancreatic development *Hes1* was conditionally deleted in the pancreas utilizing a pancreas-specific Cre recombinase.

Pancreata of 4-week-old $Hes1^{\Delta/\Delta}$ mice showed no macroscopic differences compared to control animals. Since pancreas increases in size with age; pancreatic weight is usually normalized to body weight. Using a comparative approach, a significant decrease in pancreas-to-body weight ratio could be observed in $Hes1^{\Delta/\Delta}$ mice. Pancreatic size is regulated through both genetic programming and environmental influences and, because the exocrine compartment comprises up to 90 % of the pancreas and consists of acini appearing as berry shaped cell clusters and ductal cells [17],a deletion of HES1 appears to play an important role in exocrine cell mass expansion.

While immunohistochemistry of acinar markers and proliferation were decreased in $Hes1^{\Delta/\Delta}$ mice, markers associated with multipotent progenitor cells such as Clusterin and Sox9 were present in the acinar cell compartment, suggesting compromised acinar cell differentiation and maturation at 4 weeks of age. H&E staining also revealed vacuoles within the acinar cells in line with the previous observations. With progressing age

Hes1$^{\Delta/\Delta}$ mice presented with transdifferentiation of acinar cells to adipocytes, resulting in decreased functional exocrine pancreatic tissue without any endocrine insufficiencies. Interestingly, HES1 seems to be important for complete acinar differentiation and maintenance of adult acinar tissue, as demonstrated by a significant decrease in acinar specific genes Amylase and Elastase and Mist1 in *Hes1*$^{\Delta/\Delta}$ mice compared to control mice at 4 weeks, rather than maintaining an adult progenitor cell pool as previously suggested.

These results are in line with a recent study of forced expression of *Sox9* in acinar cells (*Ptf1a*^{Cre}*; Sox9*^{OE}) that lead to an increase in CK19 and concomitant decrease in acinar cell specific genes. While the observed changes were indicative of acinar cell dedifferentiation, acinar morphology was largely retained suggesting that while Sox9 expression in acinar cells destabilized the acinar cell state and promoted expression of ductal genes, it was not sufficient to induce complete ductal reprogramming[125]. Although these results fall in line with the data of this thesis, here we also observe impaired acinar intactness in young adult mice as evidenced by vacuoles in acinar compartment. These observed differences might be due to the fact, that the deletion of *Hes1* in the centroacinar cell compartment more closely mimics the signaling cascade, suggesting that HES1 expression in centroacinar cells serves as a gatekeeper ensuring cell fate determination and maintenance of acinar structures through several effectors.

Interestingly, a study using a conditional GEMM deleting *Hes1* from adult acinar cells found HES1 not to be essential for maintaining the homeostasis of adult pancreatic acinar cells [150]. The study argues that this might be due to the use of an inducible and acinar cell-specific ablation of Hes1 (using *Elastase1-CreERT2* in which *Hes1* deletion can be restricted to acinar cells in a tamoxifen-dependent manner) and thereby avoiding any possible influence on pancreatic development in contrast to the approach that was used in this present study. Namely, using *Ptf1aCre* which induces recombination in pancreatic multipotent progenitor cells in the embryonic stage, but it could be argued, that the lack of impact of Hes1 deletion in adult acinar cells is due to a lack of active Notch signaling in the normal adult acinar compartment.

To check for possible redundancies between Notch target genes real-time quantitative reverse-transcription polymerase chain reaction (qRT-PCR) was carried out. The qRT-PCR results revealed no difference in expression levels of various Notch receptors (*Notch1* and *Notch2*), Notch ligands (*Dll1*) and Notch target genes (*Hes3, Hes5, Hes7* as well as *Hey1* and *HeyL*) demonstrating no compensatory effects occurred between Notch target genes.

A recent study looked at the role of Notch ligands Delta-like (Dll1) or Jagged (Jag1) during pancreatic development. It could be shown that in mice, in which both ligands were deleted a loss of centroacinar cells in the developing pancreas could be detected [151]. The study hypothesized that a defined boundary between Notch-active and Notch-inactive cells is important in cell fate determination and maintenance of acinar structures. This gatekeeping function was attributed to centroacinar cells and an important role for Notch ligands in this process was stipulated. It was observed that double knock-out mice (Dll1/Jag1) were presenting a vacant space in the center of the primitive acini. In control mice these vacant spaces were gradually occupied and only few vacuoles could be detected upon maturation, whereas they remained present in Dll1/Jag1 cKO. Due to normal shape and size as well as basal nucleus localization of acinar cells they speculated, that rather than a disorganization or shrinkage of acinar cells a loss of centroacinar cell population was responsible for the observed effect. In the study on hand vacuoles in the acinar structures could also be observed, indicating instability of the centroacinar cells and concomitant issues in acinar cell compartment differentiation and maintenance.

Other studies have also shown that inactivation of genes involved in pancreatic development can lead to defective acinar cell maturation and transdifferentation of acinar cells and accumulation of adipocytes within pancreatic parenchyma [91], [85], [152], [153], [154], [155], [156]. Moreover, affected acinar cell differentiation and proliferation are associated with susceptibility to injury with ageing, leading to acinar cell regression and accumulation of adipose tissue[157], [158], [159].

In conclusion, the data demonstrate that while HES1 is dispensable for pancreatic development, it is required for normal acinar mass expansion, complete acinar

differentiation and acinar compartment maintenance. These results point to a role of centroacinar cells with HES1 expression as a gatekeeper ensuring cell fate determination and maintenance of acinar structures, rather than functioning as an adult progenitor cell pool. These results are in line with previous studies of Notch family loss of function GEMMs [77], [10].

4.2. *Hes1* is essential for acinar cell regeneration after acute pancreatitis

To characterise the role of the Notch pathways effector HES1 in acinar regeneration, a model of caerulein-induced acute pancreatitis was employed. During caerulein-induced acute pancreatitis, short term caerulein administration at supramaximal levels leads to severe pancreatitis resulting in a loss of a majority of the exocrine pancreatic cells. Acinar cells dedifferentiate during the course of acute pancreatitis which is marked by a decrease in acinar markers and reactivation of signaling pathways that are important during pancreatic development [135]. Interestingly, developmental pathways that are reactivated in regenerative processes during acute pancreatitis are also activated in PanIN formation and PDAC initiation[113]. During the dedifferentiation and subsequent redifferentiation process, acinar cells undergo transient ductal morphology. In wild type animals the acinar cells redifferentiate and eventually fully regenerate due to the strong regenerative ability of the pancreas. In the dedifferentiating acini of wild type animals, HES1 is expressed which indicates a reactivation of the Notch signaling pathway in adult acinar cells. Dedifferentiation and subsequent redifferentiation is recapitulated during acute pancreatitis which makes acute pancreatitis a good model to examine the cellular plasticity of pancreatic cells in the context of HES1 loss.

Notch signaling is reactivated during acinar regeneration [126] and has been shown to promote ADM [160]. Since ADM is a proposed initial step in PanIN-to-PDAC progression, this thesis looked at the impact of loss of HES1 in the context of exocrine regeneration after acute pancreatitis. In this thesis it could be demonstrated that loss of HES1 resulted in disrupted acinar cell regeneration after caerulein-mediated acute

pancreatitis and lead to divergence of acinar cell redifferentiation and persistent ADM formation. Large areas of exocrine tissue were replaced by adipose tissue upon inflammatory insult. The diminished regenerative capacity in *Hes1*$^{\Delta/\Delta}$ mice could be associated with lower proliferative activity and an increase in apoptosis during acute pancreatitis as demonstrated by immunohistochemistry for the markers Ki67 and Cleaved Caspase3 respectively. The remaining exocrine tissue displayed persistent inflammation and ADM. Duct-like epithelial pancreatic cells in *Hes1*$^{\Delta/\Delta}$ mice strongly expressed the progenitor markers Clusterin and Sox9, suggestive of HES1 acting as an important agent in pancreatic regeneration. It could also be shown that immature acinar cells with strong expression of Sox9 are prone to ADM formation in the setting of acute pancreatitis. This is in line with previous studies that have shown that forced SOX9 expression in acinar cells destabilizes acinar cell identity and promoted expression of ductal genes and ADM [125].

In contrast to other genetic mouse models with impaired acinar regeneration *Hes1*$^{\Delta/\Delta}$ mice were lacking Alcian Blue staining. The lack of Alcian Blue staining is indicative of acinar cells undergoing transdifferentiation rather than ADM being derived from preexisting ductal cells. Previous studies have suggested that mature exocrine cells harbor progenitor-like properties that are “unlocked” during organ regeneration [135]. In line with that observation, this thesis demonstrates that loss of *Hes1* prevents acinar cell maturation and the ability to take advantage of their inherent regenerative capabilities. *Hes1*$^{\Delta/\Delta}$ mice seem to “lock” acinar cells in an immature state that prevents them from regenerating through processes of redifferentiation after acute injury mediated dedifferentation.

Nishikawa et al., using their acinar cell-specific Hes1 deletion GEMM, showed that although initial ADM formation can be observed upon acute pancreatitis induction, acinar cells were able to fully re-differentiate after an acute injury demonstrating that Hes1 is dispensable for maintenance of mature acinar cell homeostasis under injured conditions [150]. In contrast, we observed an increase of SOX9 expression in immature acinar cells and propose that the combination of loss of *Hes1*in centroacinar cells and

concurrent SOX9 expression in acinar cells constitute an impaired regenerative potential and persistent dedifferentiation of acinar cells (as previously discussed in 3.2.).

Interestingly, a study that used the approach of using two different GEMMS namely a Cre driver to ablate a Hh key signaling transducer Shh throughout the entire pancreatic epithelium (using Pdx1-*Cre,* similar to the approach in this thesis) or specifically in adult acinar cells (Ela-CreER^{T2}) found Hh signaling to be dispensable for normal pancreatic development in mice undergoing either multilineage or acinar cell-specific *Cre*-mediated deletion of *smoothened (Shh)* but demonstrated an impaired regenerative response to exocrine injury with diminished acinar tissue repair[85]. The Hedgehog (Hh) pathway is a developmentally relevant pathway with no detectable expression of its key signal transducer Shh in the ductal, acinar, or islet compartments of uninjured pancreas but is widely expressed following caerulein-induced injury, with expression noted in residual acinar cells as well as in regenerating metaplastic epithelium. Similar to Nishikawa et al. [150] this study demonstrated that blockade of Hh signaling had minimal impact on the ability of acinar cells to generate metaplastic intermediates in response to injury. But in contrast to the model of acinar restricted deletion of Hes1, the absence of Hh signaling lead to a “redifferentiation arrest,” in which metaplastic intermediates don’t reactivate an exocrine differentiation program – much more in line with the results of this thesis. It should be noted that even though some similarities to Nishikawa et al. as well as this thesis could be observed Hh signaling and Shh expression are only present after Kras-mediated activation in the acinar cell compartment, whereas HES1 is present in the centroacinar and terminal duct cells of adult mice. The results of Fendrich et al. as well as Nishikawa et el. undermine the highly cell- and context-dependent role of Notch signaling and HES1 herein.

HES1 expression in centroacinar cells could potentially work to maintain normal differentiation of neighboring acinar cells. This phenotype supports previous studies that link impaired acinar cell maturation with NOTCH signaling [35, 117, 144, 161, 162]. The results in this thesis lead to the conclusion that the regenerative ability of NOTCH1requires its target gene HES1. In the adult pancreas, NOTCH1 is expressed in acinar cells whereas NOTCH2 expression is restricted to the ductal/CAC compartment,

therefore, it is conceivable that regeneration after pancreatitis occurs from the acinar compartment (through NOTCH1), while acinar maintenance and integrity may involve CACs (through NOTCH2).

4.3. Deletion of *Hes1* results in highly proliferative ADMs but fewer high grade PanIN lesion incidence

Despite the ductal phenotype of most PDAC, acinar cells undergoing ADM have been proposed to act as cell of origin of PDAC, and acinar differentiation has been shown to be critical for malignant transformation [6], [125]. Recent studies have provided evidence for ADM and related atypical flat lesions (AFL) to be PDAC precursors in mice and humans [8], [18]. Based on the previous results of this work, the role of murine HES1 in PDAC development was investigated.

Previous studies have shown an involvement of Notch during initiating events such as the development of ADM [126], [92], [9] and PanIN lesions [81], [113], suggesting a role during PDAC initiation and progression. Impaired development of acinar compartment and impaired acinar cell integrity is believed to be a key factor for ADM development and thus PDAC initiation [118, 144, 163]. Therefore, we looked at the impact of loss of HES1 in the context of *Kras*^{G12D}-driven PDAC development. Previous studies have addressed the roles of NOTCH1 and NOTCH2 in the context of PDAC development and progression and have proved to have different roles [9], [10], [164]. Since acinar cell maintenance is an important factor in preventing ADM [79] and Notch signaling and its downstream target HES1 have been shown to be required for the maintenance of centroacinar cell identity and acinar cell differentiation [76], it was crucial to look at the role of HES1in this context in further detail.

Loss of HES1 in the context of oncogenic KRAS revealed an abundance of metaplastic ductal structures and cystic transformation with large areas of pancreatic parenchyma affected. Pathological analysis showed, that *Kras*^{G12D}*;Hes1*$^{\Delta/\Delta}$ mice presented a higher

ADM incidence compared to *Kras*^{G12D} animals. To further characterise the lesions immunohistological analysis of relevant markers was carried out. The ductal characteristics of the lesions in *Kras*^{G12D}*; Hes1*$^{\Delta/\Delta}$ were highlighted by positive CK19 staining while lesions in *Kras*^{G12D} mice showed positive staining for Claudin 18, MUC5AC and Alcian Blue, all typical markers for PanIN lesions. In contrast, ductal lesions present in *Kras*^{G12D}*; Hes1*$^{\Delta/\Delta}$ mice lacked strong staining for MUC5AC and Alcian Blue, markers of mucin content and indicative of PanIN lesions. In order to correlate the proliferative status of the lesions present in both phenotypes and to assess further distinctions of the lesions, consecutive slides of both groups were stained for Ki67 and MUC5AC. The lesions present in *Kras*^{G12D}*; Hes1*$^{\Delta/\Delta}$mice were predominately MUC5AC-negative but highly proliferative, as demonstrated by Ki67 staining. Quantification of present MUC5AC^{+} lesions as well as grading of the lesions by a pathologist revealed significantly reduced high grade PanIN formation in the knockout model compared to age-matched*Kras*^{G12D} which display high grade PanIN to PDAC progression. Survival analysis revealed that the median survival of *Kras*^{G12D}*; Hes1*$^{\Delta/\Delta}$ mice compared to *Kras*^{G12D} controls was significantly reduced with over half of the *Kras*^{G12D}*; Hes1*$^{\Delta/\Delta}$ mice having developed PDAC at terminal point without presence of high grade PanIN lesions. The results show that loss of HES1 in the context of *Kras*^{G12D} is associated with a high incidence of ADM and cystic transformation leading to a shorter median survival compared to *Kras*^{G12D} controls. Taken together, these observations led to the conclusion that HES1is an essential component of the PanIN-to-PDAC route in *Kras*^{G12D}-driven pancreatic carcinogenesis.

In order to assess the extent of ADM in *Kras*^{G12D}*; Hes1*$^{\Delta/\Delta}$ mice, the scale of ADM present at specific time points was rated. In *Kras*^{G12D}*; Hes1*$^{\Delta/\Delta}$ mice a high ADM burden was accompanied by low grade PanIN lesion incidence which persisted with progressing age. Besides abundant ADM, the H&E staining from *Kras*^{G12D}*; Hes1*$^{\Delta/\Delta}$ mice revealed cystic transformation accompanied by fatty metaplasia, fibrosis and ductectasia. The obtained data from *Kras*^{G12D}*; Hes1*$^{\Delta/\Delta}$ mice suggest that HES1 is necessary for classical PanIN progression and a loss of HES1 leads to PDAC formation through an alternative route of highly proliferative ductal lesions. This is suggestive of HES1 having an influence on high grade PanIN formation and PDAC development. These results are in

line with studies by Aichler et al.[8] which showed ADM with progressive flattening of acinar cells and lumen formation and manifestation of tubular complexes (TC). In areas of ADM TCs display accumulation of mucins and mucinous tubular complexes making them indistinguishable from low-grade PanIN. In these areas of ADM no high grade PanIN were detected. The described atypical flat lesions had high proliferative capacity while PanIN had low proliferation rates. Aichler et al. suggest that regions of ADM are probable site of PDAC origin, and ADM associated AFL are most probable precursors of PDAC in *Kras*^{G12D} mice and furthermore are supposed to be an alternative or additional to the classical PanIN-to-PDAC route.

In the context of *Kras*^{G12D}-driven PDAC development, Nishikawa et al. found lower expression of Sox9 in their acinar-restricted Hes1 loss of function model compared to *Kras*^{G12D} GEMM. They went on to demonstrate an essential role of Hes1 in the progression from ADM to PanIN by escaping *Kras*^{G12D}-driven progression to PanIN by re-differentiating into acinar cells and regulation of ADR-related genes. A stark difference to the GEMM studied in this thesis, in which loss of *Hes1* in the context of *Kras*^{G12D} is associated with a high incidence of ADM and cystic transformation leading to a shorter median survival compared to *Kras*^{G12D} controls whereas in their model no PDAC formation was observed. Nishikawa et al. observed fewer high grade PanINs which is consistent with our results, where over half of the *Kras*^{G12D}*; Hes1*$^{\Delta/\Delta}$ mice actually developed PDAC at terminal point but without presence of high grade PanIN lesions. Taken together, both approaches suggest that Hes1 has an essential role in the process of PanIN progression irrespective of GEMM. The results of Nishikawa et al. that are seemingly contradictory to the results in this present study underline the highly cell-specific functions of the Notch signaling pathway and its target HES1 as well as the pivotal role of HES1/SOX9 interplay. Both studies underline the role of Notch signaling and specifically the role of HES1 in the regulation of genes involved in acinar-to-ductal reprogramming. Interestingly, looking at the Tamoxifen induced Cre-mediated pancreatic acinar cell-specific KrasG12D and Trp53R172H activation, and concomittant Hes1 ablation, this GEMM seems to also present with loss of functional acinar cells and fatty metaplasia interspersed with endocrine Islets of Langerhans, similar to *Kras*^{G12D}*; Hes1*$^{\Delta/\Delta}$ mice with progressing age.

Kopp et al. [125] investigated the role of Sox9 in ADM in regards to PanIN formation and PDAC progression. Employing the GEMM of induced acinar *Kras*^{G12D} activation (*Ptf1a*^{Cre}*; Kras*^{G12D} mice), they could show that Sox9 was induced in Kras G12D-expressing acinar cells prior to ADM, indicating initiation of Sox9 expression before Kras-active acinar cells progress to a duct-like state, demonstrating a necessity of Sox9 for PanIN induction. They could show synergy between *Sox9* and *Kras*^{G12D} in a GEMM of forced Sox9 expression in the acinar compartment and active *Kras*^{G12D} (*Ptf1a*^{Cre}*; Kras*^{G12D}*; Sox9*^{OE}) as evidenced by replacement of normal pancreas parenchyma by large areas of Sox9+ ADM and Alcian blue+ PanINs. These results were in line with the results in this thesis regarding impairments in acinar cell maturation and maintenance accompanied by over-expression of SOX9 which is expressed in ductal and centroacinar but not acinar cells in normal adult mice [21]. Kopp et al. showed that Sox9 deletion in the presence of oncogenic Kras abrogated caerulein-induced PanIN formation, while some duct-like lesions persisted, demonstrating that Sox9 is critically required for reprogramming of acini into PanINs. These results were similar to the results of Nishikawa et al. demonstrating the importance of maintenance of acinar cell identity. Previous studies have shown that forced expression of an acinar-restricted transcription factor (*Mist1*), which is critical to acinar cell organization, significantly attenuated *Kras*^{G12D}-induced ADM/PanIN formation. Demonstrating that maintenance of acinar identity is essential in mitigating the transformational force of oncogenic KRAS [19].

While loss of Hes1 in the acinar cell compartment in the context of oncogenic Kras lead to stronger phenotypic fidelity of the acinar compartment and decreased Sox9 expression (Nishikawa et al.), loss of Hes1 in the centroacinar and terminal duct cells lead to impaired acinar cell maturity and increased Sox9 in immature acinar cells. Taken together, these results show a pivotal role of Hes1 and Sox9 interplay in ADM formation and progression to PanIN.Since Notch signaling has been shown to control SOX9 expression and induce ductal genes in the pancreas [165], [166], [20] and given our results, SOX9 seems to be a critical effector of Notch signaling and downstream of HES1 during PanIN induction.

5. Conclusion

To improve therapeutic strategies and prognosis of patients with PDAC, a clear understanding of tumor initiation and progression is needed. Aim of this thesis was to analyse the specific role of the Notch pathway downstream target HES1 in pancreatic development as well as in the initiation and progression of pancreatic ductal adenocarcinoma using various genetically engineered mouse models. To closer characterise the function of *Hes1* in cellular plasticity involved in regeneration and tumor initiation, mouse models with a pancreas specific deletion of *Hes1* by itself or in the context of pancreas specific activation of the Kras oncogene were generated.

The data acquired support the notion that acinar homeostasis is dependent on the centroacinar cell compartment with HES1 expression ensuring cell fate determination and maintenance of acinar structures rather than functioning as an adult progenitor cell pool. The deletion of *Hes1* initiated a gene expression program leading to the destabilization of the acinar cell phenotype, with Sox9 activation in the acinar compartment as pivotal result. After caerulein-mediated acute pancreatitis the deletion of Hes1 triggered a “redifferentiation arrest,” in which the metaplastic intermediates continued to express markers of pancreatic progenitor cells and failed to reactivate an acinar differentiation program. The results in this thesis lead to the conclusion that the regenerative ability of NOTCH1 requires its target gene HES1. In the adult pancreas, NOTCH1 is expressed in acinar cells whereas NOTCH2 expression is restricted to the ductal/CAC compartment, therefore, it is conceivable that regeneration after pancreatitis occurs from the acinar compartment (through NOTCH1), while acinar maintenance and integrity may involve CACs (through NOTCH2). Highlighting the highly cell-type and context-dependent effects of Notch signaling and its target *Hes1.* In the context of $Kras^{G12D}$ loss of HES1 was associated with a high incidence of ADM and cystic transformation while attenuating PanIN formation. Therefore, these results suggest that HES1 is a critical determinant in exocrine cell plasticity and maintenance of acinar cell identity which critically affects Kras-mediated PDAC development.

Overall, the results in this thesis demonstrate that the loss of HES1 may increase PDAC risk by rendering acinar cells more plastic and reducing the threshold for ADM which has been shown to be an essential early event in the initiation of pancreatic neoplasia. As ADM proved to be the initializing step in *Kras*^{G12D}-induced PDAC initiation and progression, stabilizing acinar cell identity and thereby reducing ductal reprogramming of acinar cells could be a potential therapeutic targeting approach in preventing PDA initiation and progression.

6. References

1. Vincent, A., et al., *Pancreatic cancer.* Lancet, 2011. **378**(9791): p. 607-20.
2. Siegel, R., D. Naishadham, and A. Jemal, *Cancer statistics, 2012.* CA Cancer J Clin, 2012. **62**(1): p. 10-29.
3. Krapp, A., et al., *The bHLH protein PTF1-p48 is essential for the formation of the exocrine and the correct spatial organization of the endocrine pancreas.* Genes Dev, 1998. **12**(23): p. 3752-63.
4. Siegel, R.L., K.D. Miller, and A. Jemal, *Cancer statistics, 2020.* CA Cancer J Clin, 2020. **70**(1): p. 7-30.
5. Luchini, C., P. Capelli, and A. Scarpa, *Pancreatic Ductal Adenocarcinoma and Its Variants.* Surg Pathol Clin, 2016. **9**(4): p. 547-560.
6. Morris, J.P.t., et al., *Beta-catenin blocks Kras-dependent reprogramming of acini into pancreatic cancer precursor lesions in mice.* J Clin Invest, 2010. **120**(2): p. 508-20.
7. Zhu, L., et al., *Acinar cells contribute to the molecular heterogeneity of pancreatic intraepithelial neoplasia.* Am J Pathol, 2007. **171**(1): p. 263-73.
8. Aichler, M., et al., *Origin of pancreatic ductal adenocarcinoma from atypical flat lesions: a comparative study in transgenic mice and human tissues.* J Pathol, 2012. **226**(5): p. 723-34.
9. Mazur, P.K., et al., *Notch2 is required for progression of pancreatic intraepithelial neoplasia and development of pancreatic ductal adenocarcinoma.* Proc Natl Acad Sci U S A, 2010. **107**(30): p. 13438-43.
10. Siveke, J.T., et al., *Notch Signaling Is Required for Exocrine Regeneration After Acute Pancreatitis.* Gastroenterology, 2008. **134**(2): p. 544-555.e3.
11. Miyamoto, Y., et al., *Notch mediates TGFÎ±-induced changes in epithelial differentiation during pancreatic tumorigenesis.* Cancer Cell, 2003. **3**(6): p. 565-576.
12. Thayer, S.P., et al., *Hedgehog is an early and late mediator of pancreatic cancer tumorigenesis.* Nature, 2003. **425**(6960): p. 851-6.
13. Slack, J.M., *Developmental biology of the pancreas.* Development, 1995. **121**(6): p. 1569-80.
14. Cano, D.A., M. Hebrok, and M. Zenker, *Pancreatic development and disease.* Gastroenterology, 2007. **132**(2): p. 745-62.
15. Prado, C.L., et al., *Ghrelin cells replace insulin-producing beta cells in two mouse models of pancreas development.* Proc Natl Acad Sci U S A, 2004. **101**(9): p. 2924-9.
16. Bardeesy, N. and R.A. DePinho, *Pancreatic cancer biology and genetics.* Nat Rev Cancer, 2002. **2**(12): p. 897-909.
17. Rovira, M., et al., *Isolation and characterization of centroacinar/terminal ductal progenitor cells in adult mouse pancreas.* Proc Natl Acad Sci U S A, 2010. **107**(1): p. 75-80.
18. Kopp, J.L., et al., *Sox9+ ductal cells are multipotent progenitors throughout development but do not produce new endocrine cells in the normal or injured adult pancreas.* Development, 2011. **138**(4): p. 653-65.
19. Shi, G., et al., *Maintenance of acinar cell organization is critical to preventing Kras-induced acinar-ductal metaplasia.* Oncogene, 2013. **32**(15): p. 1950-8.

20. Shih, H.P., et al., *A Notch-dependent molecular circuitry initiates pancreatic endocrine and ductal cell differentiation.* Development, 2012. **6**: p. 6.
21. Seymour, P.A., et al., *SOX9 is required for maintenance of the pancreatic progenitor cell pool.* Proc Natl Acad Sci U S A, 2007. **104**(6): p. 1865-70.
22. Stanger, B.Z., et al., *Pten constrains centroacinar cell expansion and malignant transformation in the pancreas.* Cancer Cell, 2005. **8**(3): p. 185-195.
23. Cleveland, M.H., et al., *Exocrine ontogenies: on the development of pancreatic acinar, ductal and centroacinar cells.* Semin Cell Dev Biol, 2012. **23**(6): p. 711-9.
24. Beer, R.L., M.J. Parsons, and M. Rovira, *Centroacinar cells: At the center of pancreas regeneration.* Dev Biol, 2016. **413**(1): p. 8-15.
25. Jonsson, J., et al., *Insulin-promoter-factor 1 is required for pancreas development in mice.* Nature, 1994. **371**(6498): p. 606-9.
26. Artavanis-Tsakonas, S., M.D. Rand, and R.J. Lake, *Notch signaling: cell fate control and signal integration in development.* Science, 1999. **284**(5415): p. 770-6.
27. Gittes, G.K., *Developmental biology of the pancreas: a comprehensive review.* Dev Biol, 2009. **326**(1): p. 4-35.
28. Kumar, M. and D. Melton, *Pancreas specification: a budding question.* Curr Opin Genet Dev, 2003. **13**(4): p. 401-7.
29. Habener, J.F., D.M. Kemp, and M.K. Thomas, *Minireview: Transcriptional Regulation in Pancreatic Development.* Endocrinology, 2005. **146**(3): p. 1025-1034.
30. Spagnoli, F.M., *From endoderm to pancreas: a multistep journey.* Cell Mol Life Sci, 2007. **64**(18): p. 2378-90.
31. Kopp, J.L., et al., *Progenitor cell domains in the developing and adult pancreas.* Cell Cycle, 2011. **10**(12): p. 1921-7.
32. Dubois, C.L., et al., *Sox9-haploinsufficiency causes glucose intolerance in mice.* PLoS One, 2011. **6**(8): p. 2.
33. Pan, F.C. and C. Wright, *Pancreas organogenesis: from bud to plexus to gland.* Dev Dyn, 2011. **240**(3): p. 530-65.
34. Apelqvist, A., et al., *Notch signalling controls pancreatic cell differentiation.* Nature, 1999. **400**(6747): p. 877-881.
35. Esni, F., et al., *Notch inhibits Ptf1 function and acinar cell differentiation in developing mouse and zebrafish pancreas.* Development, 2004. **131**(17): p. 4213-4224.
36. Ghosh, B. and S.D. Leach, *Interactions between hairy/enhancer of split-related proteins and the pancreatic transcription factor Ptf1-p48 modulate function of the PTF1 transcriptional complex.* Biochem J, 2006. **393**(Pt 3): p. 679-85.
37. Jensen, J., et al., *Independent development of pancreatic alpha- and beta-cells from neurogenin3-expressing precursors: a role for the notch pathway in repression of premature differentiation.* Diabetes, 2000. **49**(2): p. 163-76.
38. Edlund, H., *Pancreatic organogenesis--developmental mechanisms and implications for therapy.* Nat Rev Genet, 2002. **3**(7): p. 524-32.
39. Jarriault, S., et al., *Signalling downstream of activated mammalian Notch.* Nature, 1995. **377**(6547): p. 355-8.
40. Jensen, J., et al., *Control of endodermal endocrine development by Hes-1.* Nat Genet, 2000. **24**(1): p. 36-44.

41. Ellisen, L.W., et al., *TAN-1, the human homolog of the Drosophila notch gene, is broken by chromosomal translocations in T lymphoblastic neoplasms.* Cell, 1991. **66**(4): p. 649-61.
42. Weinmaster, G., V.J. Roberts, and G. Lemke, *Notch2: a second mammalian Notch gene.* Development, 1992. **116**(4): p. 931-41.
43. del Amo, F.F., et al., *Cloning, analysis, and chromosomal localization of Notch-1, a mouse homolog of Drosophila Notch.* Genomics, 1993. **15**(2): p. 259-64.
44. Lardelli, M., J. Dahlstrand, and U. Lendahl, *The novel Notch homologue mouse Notch 3 lacks specific epidermal growth factor-repeats and is expressed in proliferating neuroepithelium.* Mech Dev, 1994. **46**(2): p. 123-36.
45. Uyttendaele, H., et al., *Notch4/int-3, a mammary proto-oncogene, is an endothelial cell-specific mammalian Notch gene.* Development, 1996. **122**(7): p. 2251-9.
46. Lai, E.C., *Notch signaling: control of cell communication and cell fate.* Development, 2004. **131**(5): p. 965-73.
47. De Strooper, B., et al., *A presenilin-1-dependent gamma-secretase-like protease mediates release of Notch intracellular domain.* Nature, 1999. **398**(6727): p. 518-22.
48. Bray, S.J., *Notch signalling: a simple pathway becomes complex.* Nat Rev Mol Cell Biol, 2006. **7**(9): p. 678-89.
49. Kovall, R.A. and W.A. Hendrickson, *Crystal structure of the nuclear effector of Notch signaling, CSL, bound to DNA.* Embo J, 2004. **23**(17): p. 3441-51.
50. Miele, L., *Notch signaling.* Clin Cancer Res, 2006. **12**(4): p. 1074-9.
51. Lai, E.C., *Keeping a good pathway down: transcriptional repression of Notch pathway target genes by CSL proteins.* EMBO Rep, 2002. **3**(9): p. 840-5.
52. Oswald, F., et al., *SHARP is a novel component of the Notch/RBP-Jkappa signalling pathway.* Embo J, 2002. **21**(20): p. 5417-26.
53. Oswald, F., et al., *RBP-Jkappa/SHARP recruits CtIP/CtBP corepressors to silence Notch target genes.* Mol Cell Biol, 2005. **25**(23): p. 10379-90.
54. Petcherski, A.G. and J. Kimble, *Mastermind is a putative activator for Notch.* Curr Biol, 2000. **10**(13): p. R471-3.
55. Wu, L., et al., *MAML1, a human homologue of Drosophila mastermind, is a transcriptional co-activator for NOTCH receptors.* Nat Genet, 2000. **26**(4): p. 484-9.
56. Iso, T., L. Kedes, and Y. Hamamori, *HES and HERP families: multiple effectors of the Notch signaling pathway.* J Cell Physiol, 2003. **194**(3): p. 237-55.
57. Alfred, F. and C. Michael, *The function of hairy-related bHLH repressor proteins in cell fate decisions.* BioEssays, 1998. **20**(4): p. 298-306.
58. Dawson, S.R., et al., *Specificity for the hairy/enhancer of split basic helix-loop-helix (bHLH) proteins maps outside the bHLH domain and suggests two separable modes of transcriptional repression.* Mol Cell Biol, 1995. **15**(12): p. 6923-31.
59. Sasai, Y., et al., *Two mammalian helix-loop-helix factors structurally related to Drosophila hairy and Enhancer of split.* Genes & Development, 1992. **6**(12b): p. 2620-2634.

60. Ishibashi, M., et al., *Molecular characterization of HES-2, a mammalian helix-loop-helix factor structurally related to Drosophila hairy and Enhancer of split.* Eur J Biochem, 1993. **215**(3): p. 645-52.
61. Bae, S., et al., *The bHLH gene Hes6, an inhibitor of Hes1, promotes neuronal differentiation.* Development, 2000. **127**(13): p. 2933-43.
62. Pissarra, L., D. Henrique, and A. Duarte, *Expression of hes6, a new member of the Hairy/Enhancer-of-split family, in mouse development.* Mech Dev, 2000. **95**(1-2): p. 275-8.
63. Bessho, Y., et al., *Hes7: a bHLH-type repressor gene regulated by Notch and expressed in the presomitic mesoderm.* Genes Cells, 2001. **6**(2): p. 175-85.
64. Leimeister, C., et al., *Hey genes: a novel subfamily of hairy- and Enhancer of split related genes specifically expressed during mouse embryogenesis.* Mech Dev, 1999. **85**(1-2): p. 173-7.
65. Nakagawa, O., et al., *Members of the HRT family of basic helix-loop-helix proteins act as transcriptional repressors downstream of Notch signaling.* Proc Natl Acad Sci U S A, 2000. **97**(25): p. 13655-60.
66. Iso, T., et al., *HERP, a new primary target of Notch regulated by ligand binding.* Mol Cell Biol, 2001. **21**(17): p. 6071-9.
67. Ohtsuka, T., et al., *Hes1 and Hes5 as notch effectors in mammalian neuronal differentiation.* Embo J, 1999. **18**(8): p. 2196-207.
68. Nishimura, M., et al., *Structure, chromosomal locus, and promoter of mouse Hes2 gene, a homologue of Drosophila hairy and Enhancer of split.* Genomics, 1998. **49**(1): p. 69-75.
69. Koyano-Nakagawa, N., et al., *Hes6 acts in a positive feedback loop with the neurogenins to promote neuronal differentiation.* Development, 2000. **127**(19): p. 4203-16.
70. Fischer, A. and M. Gessler, *Delta-Notch--and then? Protein interactions and proposed modes of repression by Hes and Hey bHLH factors.* Nucleic Acids Res, 2007. **35**(14): p. 4583-96.
71. Murtaugh, L.C., et al., *Notch signaling controls multiple steps of pancreatic differentiation.* Proceedings of the National Academy of Sciences, 2003. **100**(25): p. 14920-14925.
72. Norgaard, G.A., J.N. Jensen, and J. Jensen, *FGF10 signaling maintains the pancreatic progenitor cell state revealing a novel role of Notch in organ development.* Dev Biol, 2003. **264**(2): p. 323-38.
73. Offield, M.F., et al., *PDX-1 is required for pancreatic outgrowth and differentiation of the rostral duodenum.* Development, 1996. **122**(3): p. 983-95.
74. Hald, J., et al., *Activated Notch1 prevents differentiation of pancreatic acinar cells and attenuate endocrine development.* Dev Biol, 2003. **260**(2): p. 426-37.
75. Fujikura, J., et al., *Notch/Rbp-j signaling prevents premature endocrine and ductal cell differentiation in the pancreas.* Cell Metabolism, 2006. **3**(1): p. 59-65.
76. Kopinke, D., et al., *Lineage tracing reveals the dynamic contribution of Hes1+ cells to the developing and adult pancreas.* Development, 2011. **138**(3): p. 431-41.
77. Nakhai, H., et al., *Conditional ablation of Notch signaling in pancreatic development.* Development, 2008. **135**(16): p. 2757-65.

78. Kopinke, D., et al., *Ongoing Notch signaling maintains phenotypic fidelity in the adult exocrine pancreas.* Dev Biol, 2012. **362**(1): p. 57-64.
79. Shi, G., et al., *Maintenance of acinar cell organization is critical to preventing Kras-induced acinar-ductal metaplasia.* Oncogene, 2012. **4**(10): p. 210.
80. Carriere, C., et al., *Acute pancreatitis markedly accelerates pancreatic cancer progression in mice expressing oncogenic Kras.* Biochem Biophys Res Commun, 2009. **382**(3): p. 561-5.
81. Guerra, C., et al., *Chronic pancreatitis is essential for induction of pancreatic ductal adenocarcinoma by K-Ras oncogenes in adult mice.* Cancer Cell, 2007. **11**(3): p. 291-302.
82. Otsuki, M., et al., *Criteria for the diagnosis and severity stratification of acute pancreatitis.* World J Gastroenterol, 2013. **19**(35): p. 5798-805.
83. Schoenberg, M.H., D. Birk, and H.G. Beger, *Oxidative stress in acute and chronic pancreatitis.* Am J Clin Nutr, 1995. **62**(6 Suppl): p. 1306S-1314S.
84. Bhanot, U.K. and P. Moller, *Mechanisms of parenchymal injury and signaling pathways in ectatic ducts of chronic pancreatitis: implications for pancreatic carcinogenesis.* Lab Invest, 2009. **89**(5): p. 489-97.
85. Fendrich, V., et al., *Hedgehog signaling is required for effective regeneration of exocrine pancreas.* Gastroenterology, 2008. **135**(2): p. 621-31.
86. Basturk, O., et al., *A Revised Classification System and Recommendations From the Baltimore Consensus Meeting for Neoplastic Precursor Lesions in the Pancreas.* Am J Surg Pathol, 2015. **39**(12): p. 1730-41.
87. Tosh, D. and J.M. Slack, *How cells change their phenotype.* Nat Rev Mol Cell Biol, 2002. **3**(3): p. 187-94.
88. Means, A.L., et al., *Pancreatic epithelial plasticity mediated by acinar cell transdifferentiation and generation of nestin-positive intermediates.* Development, 2005. **132**(16): p. 3767-76.
89. Reichert, M. and A.K. Rustgi, *Pancreatic ductal cells in development, regeneration, and neoplasia.* J Clin Invest, 2011. **121**(12): p. 4572-8.
90. Habbe, N., et al., *Spontaneous induction of murine pancreatic intraepithelial neoplasia (mPanIN) by acinar cell targeting of oncogenic Kras in adult mice.* Proc Natl Acad Sci U S A, 2008. **105**(48): p. 18913-8.
91. Bonal, C., et al., *Pancreatic Inactivation of c-Myc Decreases Acinar Mass and Transdifferentiates Acinar Cells Into Adipocytes in Mice.* Gastroenterology, 2009. **136**(1): p. 309-319.e9.
92. De La, O.J., et al., *Notch and Kras reprogram pancreatic acinar cells to ductal intraepithelial neoplasia.* Proc Natl Acad Sci U S A, 2008. **105**(48): p. 18907-12.
93. Husain, S. and E. Thrower, *Molecular and cellular regulation of pancreatic acinar cell function.* Curr Opin Gastroenterol, 2009. **25**(5): p. 466-71.
94. Siveke, J.T., et al., *Concomitant pancreatic activation of Kras(G12D) and Tgfa results in cystic papillary neoplasms reminiscent of human IPMN.* Cancer Cell, 2007. **12**(3): p. 266-79.
95. Fukushima, N. and K. Mukai, *'Ovarian-type' stroma of pancreatic mucinous cystic tumor expresses smooth muscle phenotype*. Pathol Int. 1997 Nov;47(11):806-8.
96. Hruban, R.H., et al., *Precursors to pancreatic cancer.* Gastroenterol Clin North Am, 2007. **36**(4): p. 831-49.

97. Izeradjene, K., et al., *Kras(G12D) and Smad4/Dpc4 haploinsufficiency cooperate to induce mucinous cystic neoplasms and invasive adenocarcinoma of the pancreas.* Cancer Cell, 2007. **11**(3): p. 229-43.
98. Hruban, R.H., et al., *An illustrated consensus on the classification of pancreatic intraepithelial neoplasia and intraductal papillary mucinous neoplasms.* Am J Surg Pathol, 2004. **28**(8): p. 977-87.
99. Hruban, R.H., et al., *Pancreatic intraepithelial neoplasia: a new nomenclature and classification system for pancreatic duct lesions.* Am J Surg Pathol, 2001. **25**(5): p. 579-86.
100. Almoguera, C., et al., *Most human carcinomas of the exocrine pancreas contain mutant c-K-ras genes.* Cell, 1988. **53**(4): p. 549-54.
101. Deramaudt, T. and A.K. Rustgi, *Mutant KRAS in the initiation of pancreatic cancer.* Biochim Biophys Acta, 2005. **1756**(2): p. 97-101.
102. Hansel, D.E., S.E. Kern, and R.H. Hruban, *Molecular pathogenesis of pancreatic cancer.* Annu Rev Genomics Hum Genet, 2003. **4**: p. 237-56.
103. Collins, M.A., et al., *Oncogenic Kras is required for both the initiation and maintenance of pancreatic cancer in mice.* J Clin Invest, 2012. **122**(2): p. 639-53.
104. Hruban, R.H., et al., *Progression model for pancreatic cancer.* Clin Cancer Res, 2000. **6**(8): p. 2969-72.
105. Furukawa, T., M. Sunamura, and A. Horii, *Molecular mechanisms of pancreatic carcinogenesis.* Cancer Sci, 2006. **97**(1): p. 1-7.
106. Goggins, M., *Molecular markers of early pancreatic cancer.* J Clin Oncol, 2005. **23**(20): p. 4524-31.
107. Hahn, S.A., et al., *DPC4, a candidate tumor suppressor gene at human chromosome 18q21.1.* Science, 1996. **271**(5247): p. 350-3.
108. Hayashi, A., J. Hong, and C.A. Iacobuzio-Donahue, *The pancreatic cancer genome revisited.* Nat Rev Gastroenterol Hepatol, 2021. **18**(7): p. 469-481.
109. Maitra, A., et al., *Multicomponent analysis of the pancreatic adenocarcinoma progression model using a pancreatic intraepithelial neoplasia tissue microarray.* Mod Pathol, 2003. **16**(9): p. 902-12.
110. Mulkeen, A.L., P.S. Yoo, and C. Cha, *Less common neoplasms of the pancreas.* World J Gastroenterol, 2006. **12**(20): p. 3180-5.
111. Koorstra, J.B., et al., *Morphogenesis of pancreatic cancer: role of pancreatic intraepithelial neoplasia (PanINs).* Langenbecks Arch Surg, 2008. **393**(4): p. 561-70.
112. Hezel, A.F., et al., *Genetics and biology of pancreatic ductal adenocarcinoma.* Genes Dev, 2006. **20**(10): p. 1218-49.
113. Hingorani, S.R., et al., *Preinvasive and invasive ductal pancreatic cancer and its early detection in the mouse.* Cancer Cell, 2003. **4**(6): p. 437-50.
114. Schneider, G., et al., *Pancreatic cancer: basic and clinical aspects.* Gastroenterology, 2005. **128**(6): p. 1606-25.
115. Mazur, P.K. and J.T. Siveke, *Genetically engineered mouse models of pancreatic cancer: unravelling tumour biology and progressing translational oncology.* Gut, 2011.
116. Morris, J.P.t., S.C. Wang, and M. Hebrok, *KRAS, Hedgehog, Wnt and the twisted developmental biology of pancreatic ductal adenocarcinoma.* Nat Rev Cancer, 2010. **10**(10): p. 683-95.

117. Martinelli, P., et al., *Gata6 is required for complete acinar differentiation and maintenance of the exocrine pancreas in adult mice.* Gut, 2013. **62**(10): p. 1481-8.
118. Greer, R.L., et al., *Numb regulates acinar cell dedifferentiation and survival during pancreatic damage and acinar-to-ductal metaplasia.* Gastroenterology, 2013. **145**(5): p. 1088-1097 e8.
119. Bockman, D.E., *Morphology of the exocrine pancreas related to pancreatitis.* Microsc Res Tech, 1997. **37**(5-6): p. 509-19.
120. Gorelick, F.S., G. Adler, and H.F. Kern, *Cerulein-Induced Pancreatitis*, in *The Pancreas: Biology, Pathobiology, and Disease*, V.L.W. Go, et al., Editors. 1993, Raven Press, Ltd.: New York. p. 501-526.
121. Reid, L.E. and N.I. Walker, *Acinar cell apoptosis and the origin of tubular complexes in caerulein-induced pancreatitis.* International journal of experimental pathology, 1999. **80**(4): p. 205-15.
122. Willemer, S., H.P. Elsasser, and G. Adler, *Hormone-induced pancreatitis.* Eur Surg Res, 1992. **24 Suppl 1**: p. 29-39.
123. Yoo, B.M., et al., *Novel antioxidant ameliorates the fibrosis and inflammation of cerulein-induced chronic pancreatitis in a mouse model.* Pancreatology, 2005. **5**(2-3): p. 165-76.
124. Guerra, C., et al., *Pancreatitis-induced inflammation contributes to pancreatic cancer by inhibiting oncogene-induced senescence.* Cancer Cell, 2011. **19**(6): p. 728-39.
125. Kopp, J.L., et al., *Identification of Sox9-dependent acinar-to-ductal reprogramming as the principal mechanism for initiation of pancreatic ductal adenocarcinoma.* Cancer Cell, 2012. **22**(6): p. 737-50.
126. Miyamoto, Y., et al., *Notch mediates TGF alpha-induced changes in epithelial differentiation during pancreatic tumorigenesis.* Cancer Cell, 2003. **3**(6): p. 565-76.
127. Jensen, J.N., et al., *Recapitulation of elements of embryonic development in adult mouse pancreatic regeneration.* Gastroenterology, 2005. **128**(3): p. 728-41.
128. Siveke, J.T., et al., *Notch signaling is required for exocrine regeneration after acute pancreatitis.* Gastroenterology, 2008. **134**(2): p. 544-55.
129. Obata, J., et al., *p48 subunit of mouse PTF1 binds to RBP-Jkappa/CBF-1, the intracellular mediator of Notch signalling, and is expressed in the neural tube of early stage embryos.* Genes Cells, 2001. **6**(4): p. 345-60.
130. Brembeck, F.H., et al., *The mutant K-ras oncogene causes pancreatic periductal lymphocytic infiltration and gastric mucous neck cell hyperplasia in transgenic mice.* Cancer Res, 2003. **63**(9): p. 2005-9.
131. Grippo, P.J., et al., *Preinvasive pancreatic neoplasia of ductal phenotype induced by acinar cell targeting of mutant Kras in transgenic mice.* Cancer Res, 2003. **63**(9): p. 2016-9.
132. Hanlon, L., et al., *Notch1 functions as a tumor suppressor in a model of K-ras-induced pancreatic ductal adenocarcinoma.* Cancer Res, 2010. **70**(11): p. 4280-6.
133. Plentz, R., et al., *Inhibition of gamma-secretase activity inhibits tumor progression in a mouse model of pancreatic ductal adenocarcinoma.* Gastroenterology, 2009. **136**(5): p. 1741-9.

134. Avila, J.L., et al., *Notch1 is not required for acinar-to-ductal metaplasia in a model of Kras-induced pancreatic ductal adenocarcinoma.* PLoS One, 2012. **7**(12): p. e52133.
135. Jensen, J.N., et al., *Recapitulation of elements of embryonic development in adult mouse pancreatic regeneration.* Gastroenterology, 2005. **128**(3): p. 728-41.
136. Stanger, B.Z., et al., *Pten constrains centroacinar cell expansion and malignant transformation in the pancreas.* Cancer Cell, 2005. **8**(3): p. 185-95.
137. Gomez, G., et al., *Increased expression of hypoxia-inducible factor-1alpha, p48, and the Notch signaling cascade during acute pancreatitis in mice.* Pancreas, 2004. **28**(1): p. 58-64.
138. Wagner, M., et al., *A murine tumor progression model for pancreatic cancer recapitulating the genetic alterations of the human disease.* Genes Dev, 2001. **15**(3): p. 286-93.
139. Crawford, H.C., et al., *Matrix metalloproteinase-7 is expressed by pancreatic cancer precursors and regulates acinar-to-ductal metaplasia in exocrine pancreas.* J Clin Invest, 2002. **109**(11): p. 1437-44.
140. Nakhai, H., et al., *Ptf1a is essential for the differentiation of GABAergic and glycinergic amacrine cells and horizontal cells in the mouse retina.* Development, 2007. **134**(6): p. 1151-60.
141. Imayoshi, I., et al., *Hes genes and neurogenin regulate non-neural versus neural fate specification in the dorsal telencephalic midline.* Development, 2008. **135**(15): p. 2531-2541.
142. Zhou, Q., et al., *A multipotent progenitor domain guides pancreatic organogenesis.* Dev Cell, 2007. **13**(1): p. 103-14.
143. Pin, C.L., et al., *The bHLH transcription factor Mist1 is required to maintain exocrine pancreas cell organization and acinar cell identity.* The Journal of Cell Biology, 2001. **155**(4): p. 519-530.
144. von Figura, G., et al., *Nr5a2 maintains acinar cell differentiation and constrains oncogenic Kras-mediated pancreatic neoplastic initiation.* Gut, 2013. **63**(4): p. 656-64.
145. Strobel, O., et al., *In vivo lineage tracing defines the role of acinar-to-ductal transdifferentiation in inflammatory ductal metaplasia.* Gastroenterology, 2007. **133**(6): p. 1999-2009.
146. Sanada, Y., et al., *Immunohistochemical study of claudin 18 involvement in intestinal differentiation during the progression of intraductal papillary mucinous neoplasm.* Anticancer Res, 2010. **30**(7): p. 2995-3003.
147. Albores-Saavedra, J., et al., *The foamy variant of pancreatic intraepithelial neoplasia.* Ann Diagn Pathol, 2008. **12**(4): p. 252-9.
148. Kim, G.E., et al., *Aberrant expression of MUC5AC and MUC6 gastric mucins and sialyl Tn antigen in intraepithelial neoplasms of the pancreas.* Gastroenterology, 2002. **123**(4): p. 1052-60.
149. Rachagani, S., et al., *Activated KrasG^{12}D is associated with invasion and metastasis of pancreatic cancer cells through inhibition of E-cadherin.* Br J Cancer, 2011. **104**(6): p. 1038-48.
150. Nishikawa, Y., et al., *Hes1 plays an essential role in Kras-driven pancreatic tumorigenesis.* Oncogene, 2019. **38**(22): p. 4283-4296.

151. Nakano, Y., et al., *Disappearance of centroacinar cells in the Notch ligand-deficient pancreas.* Genes Cells, 2015. **20**(6): p. 500-11.
152. Westmoreland, J.J., et al., *Pancreas-specific deletion of Prox1 affects development and disrupts homeostasis of the exocrine pancreas.* Gastroenterology, 2012. **142**(4): p. 999-1009.
153. Hess, D.A., et al., *Extensive pancreas regeneration following acinar-specific disruption of Xbp1 in mice.* Gastroenterology, 2011. **141**(4): p. 1463-72.
154. Molero, X., et al., *Gene expression dynamics after murine pancreatitis unveils novel roles for Hnf1{alpha} in acinar cell homeostasis.* Gut, 2011. **23**: p. 23.
155. Fukuda, A., J.P.t. Morris, and M. Hebrok, *Bmi1 is Required for Regeneration of the Exocrine Pancreas in Mice.* Gastroenterology, 2012. **17**: p. 17.
156. Shi, G., et al., *Loss of the acinar-restricted transcription factor Mist1 accelerates Kras-induced pancreatic intraepithelial neoplasia.* Gastroenterology, 2009. **136**(4): p. 1368-78.
157. Iglesias, A., et al., *Diabetes and exocrine pancreatic insufficiency in E2F1/E2F2 double-mutant mice.* J Clin Invest, 2004. **113**(10): p. 1398-407.
158. Zhu, L., et al., *Inhibition of Mist1 Homodimer Formation Induces Pancreatic Acinar-to-Ductal Metaplasia.* Molecular and Cellular Biology, 2004. **24**(7): p. 2673-2681.
159. Rukstalis, J.M., et al., *Exocrine specific expression of Connexin32 is dependent on the basic helix-loop-helix transcription factor Mist1.* Journal of Cell Science, 2003. **116**(16): p. 3315-3325.
160. Miyatsuka, T., et al., *Ectopically expressed PDX-1 in liver initiates endocrine and exocrine pancreas differentiation but causes dysmorphogenesis.* Biochem Biophys Res Commun, 2003. **310**(3): p. 1017-25.
161. Golson, M.L., et al., *Jagged1 is a competitive inhibitor of Notch signaling in the embryonic pancreas.* Mech Dev, 2009. **126**(8-9): p. 687-99.
162. Thomas, M.M., et al., *Epithelial Notch signaling is a limiting step for pancreatic carcinogenesis.* BMC Cancer, 2014. **14**: p. 862.
163. Prevot, P.P., et al., *Role of the ductal transcription factors HNF6 and Sox9 in pancreatic acinar-to-ductal metaplasia.* Gut, 2012. **61**(12): p. 1723-32.
164. Mazur, P.K., et al., *Identification of epidermal Pdx1 expression discloses different roles of Notch1 and Notch2 in murine Kras(G12D)-induced skin carcinogenesis in vivo.* PLoS One, 2010. **5**(10).
165. Delous, M., et al., *Sox9b is a key regulator of pancreaticobiliary ductal system development.* PLoS Genet, 2012. **8**(6): p. e1002754.
166. Manfroid, I., et al., *Zebrafish sox9b is crucial for hepatopancreatic duct development and pancreatic endocrine cell regeneration.* Dev Biol, 2012. **366**(2): p. 268-78.

7. Appendix

List of Abbreviations

ADM	Acinar ductal metaplasia
AKT	v-akt murine thymoma viral oncogene homolog
bHLH	basic Helix-Loop-Helix
bp	base pairs
CCK	Cholecystokinin
CK	Cytokeratin
Da	Dalton
ERK	Extracellular signal-related protein kinase
FFPE	Formalin-fixed, paraffin-embedded
GEMM	Genetically engineered mouse model
H&E	Hematoxylin and eosin
IF	Immunofluorescence
IPGTT	Intraperitoneal glucose tolerance test
IHC	Immunohistochemistry
IPMN	Intraductal papillary mucinous neoplasia
KRAS	Kirsten-Ras
LSL	Lox-Stop-Lox
MAPK	Mitogen activated protein kinase
MCN	Mucinous cystic neoplasia
MEK	Mitogen activated protein kinase kinase
NIC	Notch Intracellular Domain
PanIN	Pancreatic intraepithelial neoplasia
PDAC	Pancreatic ductal adenocarcinoma
PI3K	Phosphoinositid-3-Kinase
RAS	Rat sarcoma
RT-PCR	Reverse transcription-Polymerase-chainreaction
WT	Wild type

Anhang I

Eidesstattliche Erklärung

Ich erkläre an Eides statt, dass ich die bei der promotionsführenden Einrichtung
Lehrstuhl für molekulare Ernährungsmedizin

der TUM zur Promotionsprüfung vorgelegte Arbeit mit dem Titel:

Mechanisms of Notch signaling in pancreatic development and carcinogenesis

in Fakultät Wissenschaftszentrum Weihenstephan für Ernährung, Landnutzung und Umwelt

Fakultät, Institut, Lehrstuhl, Klinik, Krankenhaus, Abteilung

unter der Anleitung und Betreuung durch: Prof. Dr. Siveke / Prof. Dr Klingespor ohne sonstige Hilfe erstellt und bei der Abfassung nur die gemäß § 6 Ab. 6 und 7 Satz 2 angebotenen Hilfsmittel benutzt habe.

☒ Ich habe keine Organisation eingeschaltet, die gegen Entgelt Betreuerinnen und Betreuer für die Anfertigung von Dissertationen sucht, oder die mir obliegenden Pflichten hinsichtlich der Prüfungsleistungen für mich ganz oder teilweise erledigt.

☒ Ich habe die Dissertation in dieser oder ähnlicher Form in keinem anderen Prüfungsverfahren als Prüfungsleistung vorgelegt.

☒ Die vollständige Dissertation wurde in _____ veröffentlicht. Die promotionsführende Einrichtung

hat der Veröffentlichung zugestimmt.

☒ Ich habe den angestrebten Doktorgrad noch nicht erworben und bin nicht in einem früheren Promotionsverfahren für den angestrebten Doktorgrad endgültig gescheitert.

☐ Ich habe bereits am _____ bei der Fakultät für _____ der Hochschule _____ unter Vorlage einer Dissertation mit dem Thema _____ die Zulassung zur Promotion beantragt mit dem Ergebnis: _____

Die öffentlich zugängliche Promotionsordnung der TUM ist mir bekannt, insbesondere habe ich die Bedeutung von § 28 (Nichtigkeit der Promotion) und § 29 (Entzug des Doktorgrades) zur Kenntnis genommen. Ich bin mir der Konsequenzen einer falschen Eidesstattlichen Erklärung bewusst.

Mit der Aufnahme meiner personenbezogenen Daten in die Alumni-Datei bei der TUM bin ich

☒ einverstanden, ☐ nicht einverstanden.

Ort, Datum, Unterschrift

Danksagungen

Mein besonderer Dank gilt Prof. Martin Klingespor für die bereitwillige und hilfreiche Betreuung der Doktorarbeit am Wissenschaftszentrum Weihenstephan. Bei Prof. Jens Siveke möchte ich mich sehr für die Möglichkeit zu dieser Arbeit bedanken. Außerdem möchte ich mich besonders herzlich für die sehr gute und motivierende Betreuung bedanken. Am meisten ist ihm für seine verständnisvolle Unterstützung, seine Geduld und sein Vertrauen zu danken.

Herzlichen Dank schulde ich außerdem Dr. Ana Hidalgo-Sastre, die mit ihrem Einsatz entscheidend zur Publikation der Ergebnisse meiner Doktorarbeit beigetragen hat.Ein großer Dank gilt auch meiner Arbeitsgruppe, die immer für wissenschaftliche Diskussionen, Rat und Tat, Hilfsbereitschaft und den ein oder anderen Spaß zu haben waren. Danke: Barbara, Pawel, Irina, Vicky, Marija, Nicole, Katharina, Clara, Florian, Tobias, Thomas, Mathilde, Silke, Aayush, Alexander und Marcel.

Mein größter Dank gilt meiner Familie. Meiner Mutter, die mir Alles gegeben hat und mich Geduld, Zuversicht, Ehrgeiz, Selbstvertrauen, Lebensfreude und Güte gelehrt hat und deren Weisheit und Liebe ich jeden Tag vermisse. Meinem Vater, der mich auch ohne große Worte versteht und mein Fels ist. Meinen Freunden, die mich motivieren und mir immer wieder zeigen, was im Leben wichtig ist und Moritz, ohne den ich diesen Abschnitt meines Lebens nur halb so gut gemeistert hätte.